12-12-2012 12:00 AM

The role of non-canonical Wnt/planar cell polarity signalling in breast cancer progression

Connor D. MacMillan
The University of Western Ontario

Supervisor
Dr. Ann Chambers
The University of Western Ontario Joint Supervisor
Dr. Alan Tuck
The University of Western Ontario

Graduate Program in Pathology
A thesis submitted in partial fulfillment of the requirements for the degree in Master of Science

THE ROLE OF NON-CANONICAL WNT/PLANAR CELL POLARITY SIGNALLING IN BREAST CANCER PROGRESSION

(Spine title: Non-canonical Wnt Signalling in Breast Cancer)

(Thesis format: Monograph)

by

Connor D. MacMillan

Graduate Program in Pathology

A thesis submitted in partial fulfillment
of the requirements for the degree of
Master of Science

The School of Graduate and Postdoctoral Studies
The University of Western Ontario
London, Ontario, Canada

THE UNIVERSITY OF WESTERN ONTARIO
School of Graduate and Postdoctoral Studies

CERTIFICATE OF EXAMINATION

Joint-Supervisor

Dr. Ann Chambers

Joint-Supervisor

Dr. Alan Tuck

Supervisory Committee

Dr. Eva Turley

Examiners

Dr. Chadan Chakraborty

Dr. Mark Darling

Dr. Lynn-Marie Postovit

The thesis by

Connor David MacMillan

entitled:

The role of non-canonical Wnt/planar cell polarity signalling in breast cancer progression

is accepted in partial fulfillment of the
requirements for the degree of
Master of Science

Date

Chair of the Thesis Examination Board

Abstract

The role of planar cell polarity (PCP) signalling in breast cancer is unclear, as evidence shows that activation of this pathway with WNT5A can either promote or inhibit progression. Using the 21T cells, which represent distinct stages of breast cancer progression when grown in a mouse xenograft model (21PT, atypical ductal hyperplasia; 21NT ductal carcinoma in situ; 21MT-1, invasive mammary carcinoma), I hypothesized that WNT5A will promote progression only when VANGL1, another component of PCP signalling, is elevated.

Each 21T cell line showed distinct stage-specific morphologies when grown in a Matrigel "on-top" assay. WNT5A overexpression promoted progression to an invasive phenotype in 21NT (ductal carcinoma in situ-like) cells that was partially dependent on RHOA, but not in 21PT (atypical ductal hyperplasia-like) cells. VANGL1 overexpression alone or with recombinant Wnt5a increased migration but had no effect on invasion in 21PT cells. Finally, knockdown of WNT5A and VANGL1 separately did not change morphology of 21MT-1 (invasive, metastatic) cells; however, WNT5A knockdown was incomplete.

PCP signalling likely plays a role in promoting progression to an invasive phenotype but this may be independent of high VANGL1 expression.

Keywords

breast cancer progression, invasion, non-canonical Wnt, planar cell polarity, VANGL1, WNT5A

Co-Authorship Statement

A part of the introduction was adapted from a published book chapter entitled "Progression of early breast cancer to an invasive phenotype", by C. D. MacMillan, A. F. Chambers, and A.B. Tuck in *Breast Cancer Metastasis and Drug Resistance: Progress and Prospects*, Ahmad A. (ed). Springer, 2012. I wrote this book chapter with assistance from A. F. Chambers and A. B. Tuck. The VANGL1-myc expression vector was constructed by L. H. Souter and H. S. Leong. The viral supernatant for shRNAs against RHOA and Luciferase was produced by A. E. Robertson and H. S. Leong.

Epigraph

“Answers are a luxury enjoyed every now and then. So early on, learn to love the questions themselves”

- Neil deGrasse Tyson

Acknowledgments

Firstly, I would like to thank my supervisors, Drs. Ann Chambers and Alan Tuck, for their support and guidance. They challenged my ideas and provided me with advice while allowing me the independence to develop as a researcher. Thank you for supporting my desire to attend medical school, and the not so small amount of letter-writing you did for me! I would also like to thank my advisory committee members, Drs. Eva Turley and John Lewis, for their valuable feedback and direction.

I would like to say a special thank you to the members of the Chambers' lab – you became more than colleagues and I truly value your friendship. Hon Leong provided invaluable assistance throughout my graduate experience. Hon is a supportive friend and a dedicated researcher whose future work is sure to impact the lives of many. Allen Clifford has been a great listener and provided much needed comedic relief when things didn't turn out exactly as expected the first time around (or the second!). I would also like to thank David Dales for his technical support and Joe Andrews for his help with statistics.

I would also like to thank Karla Williams and Dr. Marc Coppolino for encouraging me to attend graduate school and for teaching me the foundations of research in cell biology.

Lastly, I would like to thank my wife Jen; you share my dreams, and support me as I strive to reach my goals. You are always there to listen to me with compassion and understanding, and speak to me with encouragement. You know when to help me when I need it, and know when to step aside when I don't. You've helped me accomplish more than I could on my own!

Table of Contents

List of Tables

List of Figures

List of Abbreviations

αHE/10F	Supplemented alpha modification of Eagle's media
α-MEM	Alpha modification of Eagle's medium
ADH	Atypical ductal hyperplasia
ALH	Atypical lobular hyperplasia
ANOVA	Analysis of variance
AP-1	Activator protein 1
Arp2/3	Actin-related protein 2/3
ATP	Adenosine triphosphate
BSA	Bovine serum albumin
CD82	Cluster of differentiation 82
Cdc42	Cell division cycle 42 (GTP binding protein, 25kDa)
cDNA	Complementary DNA
CE	Convergent extension
CGH	Comparative genomic hybridization
CIP	Calf intestinal phosphatase
c-Src	Cellular-Src
CXCR4	Chemokine (C-X-C motif) receptor type 4
Daam1	Dishevelled associated activator of morphogenesis 1
DCIS	Ductal carcinoma in situ
DMEM	Dulbecco's modified Eagle media
DNA	Deoxyribonucleic acid
dNTPs	Deoxynucleotide triphosphates

DOC	Deoxycholate
Dvl	Dishevelled
E-cadherin	Epithelial cadherin
ECL	Enhanced chemoluminescence
ECM	Extracellular matrix
EDTA	Ethylenediaminetetraacetic acid
EGF	Epidermal growth factor
EGTA	Ethylene glycol tetraacetic acid
ER	Estrogen receptor
ERK	Extracellular signal-regulated kinase
EV	Empty vector
FBS	Fetal bovine serum
FEA	Flat epithelial atypia
Fzd	Frizzled receptor
GAP	GTPase activating protein
GAPDH	Glyceraldehyde 3-phosphate dehydrogenase
GDP	Guanosine diphosphate
GEF	Guanine exchange factor
GTP	Guanosine triphosphate
HEPES	4-(2-hydroxyethyl)-1-piperazineethanesulfonic acid
HRP	Horseradish peroxidase
IDC	Invasive ductal carcinoma
ILC	Invasive lobular carcinoma
JNK	c-Jun N-terminal kinase

KAI1	Kangai 1
LB	Luria Bertani
LCIS	Lobular carcinoma in situ
LOH	Loss of heterozygosity
LRP5/6	Low-density lipoprotein receptor-related protein 5/6
LUC	Luciferase
MAP2K	Mitogen-activated protein kinase kinase
MAP3K	Mitogen-activated protein kinase kinase kinase
MAPK	Mitogen-activated protein kinase
MEKK	MAP/ERK kinase kinase
MMP	Matrix metalloproteinase
mRNA	Messenger RNA
NLK	Nemo-like kinase
NOS1AP	Nitric oxide synthase 1 (neuronal) adaptor protein
NSCLC	Non-small cell lung cancer
PBS	Phosphate buffered saline
pCMV	Cytomegalovirus promoter
PCP	Planar cell polarity
PCR	Polymerase chain reaction
PKC	Protein kinase C
PVDF	Polyvinylidene fluoride
qRT-PCR	Quantitative real-time polymerase chain reaction
Rac1	Ras-related C3 botulinum toxin substrate 1
RHOA	Ras homolog gene family, member A

RIPA	Radioimmunoprecipitation assay buffer
RNA	Ribonucleic acid
ROCK	RHO-associated protein kinase
ROR1/2	Receptor tyrosine kinase-like orphan receptor 1/2
RORα	Retinoic acid receptor-related orphan receptor alpha
SCID	Severe combined immunodeficiency
SCRIB	Scribbled homolog (Drosophila)
SDF-1	Stromal cell-derived factor 1
SDS-PAGE	Sodium dodecyl sulfate polyacrylamide gel electrophoresis
SE	Standard error
shRNA	short hairpin ribonucleic acid
siRNA	Small interfering ribonucleic acid
T4 PNK	T4 polynucleotide kinase
TAK	TGF-β-activated kinase
TBST	Tris-buffered saline Tween-20
TDLU	Terminal duct lobular unit
TGF-β	Transforming growth factor β
Tpl2	Tumor progression locus 2
Tris-HCl	Tris(hydroxymethyl)aminomethane hydrochloride
UDH	Usual ductal hyperplasia
VANGL1	Vang-like 1 (van gogh, Drosophila)
VEGF	Vascular endothelial growth factor
WNT5A	Wingless-type mouse mammary tumor virus integration site family, member 5A

Chapter 1

1 Introduction

Breast cancer continues to be a major health concern among women worldwide. In North America, there has been a decreasing trend in the mortality rate of breast cancer over the last several decades (American Cancer Society 2012; Canadian Cancer Society's Steering Committee on Cancer Statistics 2012). This is likely due to increased screening and improved diagnostic recognition of early curable stages. However, there will still be approximately 45 000 deaths due to metastatic breast cancer in North America in 2012 (American Cancer Society 2012; Canadian Cancer Society's Steering Committee on Cancer Statistics 2012); therefore, there continues to be a need to understand what drives the progression of breast cancer. An important event in the progression of breast cancer is the transition from earlier non-invasive lesions to an invasive phenotype.

1.1 Breast cancer progression

1.1.1 Definition of breast cancer progression

Evidence has led to a histological model of breast cancer progression in which cells from the terminal duct lobular unit give rise to atypical ductal hyperplasia (ADH) or atypical lobular hyperplasia (ALH), which can progress to ductal carcinoma in situ (DCIS) or lobular carcinoma in situ (LCIS), and eventually to invasive ductal carcinoma (IDC) or lobular carcinoma (ILC) respectively (Figure 1.1) (Page et al. 1985; Page and Dupont 1993; Lakhani et al. 1995; Allred et al. 2001; Arpino et al. 2005; Allred et al. 2008). This model of breast cancer progression will be discussed from histomorphological and epidemiological perspectives.

1.1.2 A histopathological overview of the pre-invasive stages of breast cancer progression

The human breast is composed of thousands of small glands lined by epithelial cells that produce milk. These glands are composed of a single terminal duct with multiple end acini (terminal ductules in the non-functioning state) and are referred to as the terminal duct lobular unit (TDLU). Once milk is excreted from cells of the TDLU, it is propagated outward through a series of interconnecting and increasingly larger ducts. The TDLU is composed of two cell layers: (a) an inner luminal epithelial layer composed of low columnar cells in the terminal duct and cuboidal cells in the acini/terminal ductules, and (b) an outer myoepithelial layer directly adjacent to the basement membrane. Pre-invasive epithelial lesions are characterized by a neoplastic epithelial cell proliferation which remains confined to the ductal-lobular network and does not penetrate the basement membrane or invade into the surrounding stroma.

The two most common types of invasive breast cancer are known as invasive lobular carcinoma and invasive ductal ("no special type, NOS") carcinoma. These are preceded by pre-invasive lobular and ductal neoplasias respectively. Both types of breast cancers arise in the TDLU and the distinction between the two is based on morphological differences of the cells (Wellings and Jensen 1973; Wellings et al. 1975). Specifically, the lobular morphology consists of small, non-polarized cells that are discohesive, with vacuolated cytoplasm and a high nuclear to cytoplasmic ratio, resembling cuboidal cells of breast acini/terminal ductules. In contrast, the ductal morphology consists of larger, polarized cells, in cohesive groups that resemble columnar cells of terminal ducts. The pre-invasive lobular lesions include atypical lobular hyperplasia (ALH) and lobular carcinoma in situ (LCIS). Pre-invasive ductal lesions are thought to progress from flat

epithelial atypia (FEA), to atypical ductal hyperplasia (ADH), to ductal carcinoma in situ (DCIS). In addition, although more controversial, there is some evidence that usual ductal hyperplasia (UDH) and an entity known as “unfolded lobules” may in some instances also be considered early stages of breast cancer progression (Arpino et al. 2005; Sgroi 2010).

FEA, ADH, and DCIS are considered non-obligate precursors of invasive ductal carcinoma (IDC). FEA is characterized by a proliferation and replacement of luminal cells of the TDLU by one or more layers of columnar epithelial cells that exhibit low-grade cytological atypia (Schnitt 2003). The cells of FEA do not fill the TDLU but grow as either a single cell layer or multiple cell layers (Lerwill 2008). FEA by present definition is comprised of both columnar cell change with atypia and columnar cell hyperplasia with atypia. Columnar cell change with atypia is characterized by TDLUs that display dilated acini/ductules lined by one or two layers of columnar epithelial cells. Columnar cell hyperplasia with atypia is used to describe TDLUs that display dilated acini/ductules lined by more than two cell layers of atypical columnar cells. Like FEA, ADH is also characterized by low-grade cytological atypia, but differs from FEA in that it exhibits architectural abnormalities such as solid patterns with even cell placement, punched-out secondary lumina, rigid bridging, and cribriform or micropapillary morphologies. The differences between ADH and DCIS are based upon the nature of the atypia and the extent of epithelial proliferation (Tavassoli and Norris 1990; Page and Rogers 1992). DCIS is classified based on cytomorphological (low, intermediate, or high nuclear grade) and architectural features, as well as the presence or absence of luminal necrosis, all of which have been associated with outcome. Comedo-type DCIS consists of

cells that appear cytologically malignant and are associated with abundant central luminal necrosis. Comedo-type DCIS is generally more aggressive and is associated with high or (according to some authors) intermediate nuclear grade DCIS. Lastly, important distinguishing factors between DCIS and IDC are the complete loss of the outer myoepithelial layer in the latter, with extension of neoplastic cells into the surrounding stromal compartment, beyond the basement membrane (Pinder and Ellis 2003).

The spectrum of lobular neoplasias includes ALH and LCIS, both of which are considered non-obligate precursors of invasive lobular carcinoma (ILC) (Marshall et al. 1997; Venkitaraman 2010). The main histological distinction between ALH and LCIS is based on the amount that the TDLU is filled by neoplastic cells and the amount the lobular unit becomes distended as a result (Page et al. 1985). In ALH, the TDLU is colonized by a homogenous cell population of small, round, non-polarized, loosely cohesive cells that have a high nuclear to cytoplasmic ratio. The proliferation of ALH is limited and leaves the acinar/ductular lumina somewhat intact. Conversely, cells of classical LCIS are cytomorphologically similar to ALH, but proliferation is extensive enough to completely fill and distend the TDLU. Variants of LCIS have been described, including a pleomorphic variant, which consists of medium- to large-sized cells, with pleomorphic nuclei, and LCIS with zonal ("comedo type") necrosis (Eusebi et al. 1992; Weidner and Semple 1992).

1.1.3 Epidemiological evidence of breast cancer progression

Epidemiological studies have provided support for a linear model of breast cancer progression. Through long term cohort studies it has been shown that having a previous ADH or DCIS diagnosis greatly increases the risk of developing invasive mammary

carcinoma, up to 4-5 times for ADH and up to 8-10 times for DCIS compared to the general population (Page et al. 1985; Page and Dupont 1993; Fitzgibbons et al. 1998). In addition, the relative risk positively correlates with grade, extent, and presence of zonal necrosis. Similarity, the risk of invasive disease in women diagnosed with LCIS (classic type) is estimated at 8-10 times greater than women in the general population (Fitzgibbons et al. 1998). The relative risk associated with a finding of FEA is not yet well-established, but studies to date suggest that the risk for developing DCIS or invasive mammary carcinoma varies from a slightly increased risk to an increase in risk similar to ADH (Schnitt 2003; Martel et al. 2007; Kunju and Kleer 2007; Lerwill 2008). Although epidemiologic data would suggest possible precursor status of usual ductal epithelial hyperplasia as well (1.5-2 fold increased risk for mammary carcinoma), molecular (loss of heterozygosity) studies indicate that this is likely a rare event (Ellis 2010).

1.1.4 Molecular evidence of ductal and lobular carcinoma progression

The histological patterns observed during breast cancer progression are likely rough phenotypic indications of underlying molecular changes. There is interest in identifying the cellular and molecular events involved to determine which lesions are more likely to progress. An important barrier in understanding these changes has been the inability to accurately assess the molecular events as they relate to progression. Highly specific tissue-microdissection technologies and rapidly evolving high-throughput genomic and transcriptomic analyses have combined to identify a number of genomic and gene-expression correlates between different stages of breast cancer.

DCIS forms a spectrum of neoplastic lesions, with some lesions behaving more aggressively than others. These different behaviours are to some degree associated with

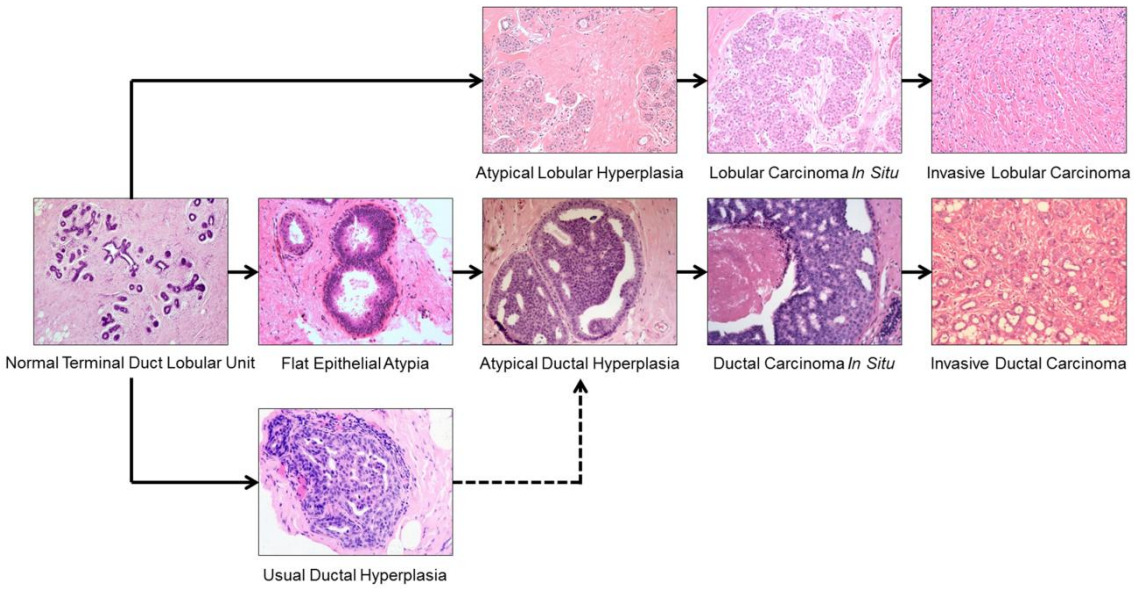

Figure 1.1 Traditional linear model of breast cancer progression. Multiple lines of evidence (histomorphological, immunohistochemical, and molecular) support this model. Molecular alterations occurring in the normal terminal duct lobular unit (TDLU) can result in flat epithelial atypia (FEA). FEA may lead to additional changes that give rise to atypical ductal hyperplasia and ductal carcinoma in situ, upon which subsequent alterations in turn give rise to invasive ductal carcinoma (middle). Likewise, molecular alterations occurring in the normal TDLU result in atypical lobular hyperplasia, which can give rise to lobular carcinoma in situ, upon which subsequent alterations gives rise to invasive lobular carcinoma (top). There is some evidence that usual ductal hyperplasia may in some instances also be considered as an early stage of breast cancer progression (bottom) (from MacMillan et al. 2012).

morphologic characteristics, as described above; however, it has been further revealed that different morphological subtypes of DCIS reflect distinct genomic alterations (Figure 1.2). For example, comparative genomic hybridization (CGH)-based studies of DCIS revealed frequent loss of 16q in low- and intermediate-grade DCIS and gain of 1q and loss of 11q in intermediate-grade DCIS (Buerger et al. 1999; Simpson et al. 2005). Additionally, high-grade DCIS was characterized by frequent loss of 8p, 11q, 13q, and 14q; gains of 1q, 5p, 8q, and 17q; and amplifications of 17q12 and 11q13 (Buerger et al. 1999). Further CGH analysis comparing DCIS and IDC revealed an almost identical pattern of genetic variations (Buerger et al. 1999; Buerger et al. 2001) and there is also a correlation between copy number variations and progression (Yao et al. 2006). Together, these data support the view that DCIS is a direct precursor to IDC and that distinct genetic abnormalities are reflected by nuclear grade within the morphological spectrum of DCIS.

A number of loss of heterozygosity (LOH)-based and CGH-based studies support the hypothesis that ADH is a precursor to low grade-DCIS. For example, LOH in regions 16q and 17p in ADH is similar to the variations observed in low grade-DCIS (Lakhani et al. 1995; O'Connell et al. 1998; Amari et al. 1999). Given that ADH and low-grade DCIS share many architectural and cytological features (Tavassoli and Norris 1990; Page and Rogers 1992), it makes sense that they share common chromosomal abnormalities. This supports the presumed sequence of progression of ADH to low-grade DCIS; however, the progression to high-grade DCIS is less clear. In terms of histological presentations and genetic aberrations, high-grade DCIS is more heterogeneous than low- and intermediate-grade DCIS. Despite the greater intricacy of the pattern of genetic aberrations found in

high-grade DCIS (those with 17q12 amplifications), deletions of 16q are less frequent, suggesting that the majority of high-grade DCIS lesions arise de novo.

There is also molecular evidence suggesting that FEA is a precursor to ADH and/or low-grade DCIS. It has been shown that FEA has similar genetic alterations compared to ADH and both low-grade DCIS and low-grade invasive carcinoma (Moinfar et al. 2000). There is commonly a LOH at chromosome 16q in FEA, low-grade DCIS, and low-grade IDC (Moinfar et al. 2000) and there are comparable chromosomal copy number gains and losses present in FEA, ADH, and low-grade DCIS (Simpson et al. 2005). A number of immunohistochemical approaches have also linked FEA, ADH, and low-grade DCIS. For example, the atypical/neoplastic cells of all three of these pre-invasive lesions show the same high-level expression of estrogen receptors, progesterone receptors and cytokeratin 19 (Oyama et al. 2000; Simpson et al. 2005), an increase in expression of cyclin D1 (Oyama et al. 2000), as well as identical negativity for cytokeratin 5/6 (Simpson et al. 2005) and Human Epidermal Growth Factor Receptor 2 (HER2) (Kusama et al. 2000; Simpson et al. 2005). These data support the view that FEA may be a precursor to ADH and low-grade DCIS.

Much of the research on understanding the gene-expression alterations that occur during the early pre-invasive stages of breast cancer have focused on the neoplastic epithelial cells of ADH and DCIS (Ma et al. 2003; Ma et al. 2009). For example, a patient-matched microdissection and microarray-based study showed that marked transcriptional alterations occur between normal TDLUs and ADH, which are sustained in DCIS and IDC (Ma et al. 2003). However, in several studies, there were no major transcriptional profile changes between the pre-invasive and invasive stages (Ma et al.

2003; Porter et al. 2003; Ma et al. 2009). This has led these authors to suggest that both pre-invasive and invasive stages of progression are clonal in origin and that genes expressed during ADH and DCIS may be responsible for progression. A number of studies have linked gene expression patterns during early stages of progression to the risk of developing IDC and metastasis (van de Vijver et al. 2002; Paik et al. 2004; Goetz et al. 2006; Jerevall et al. 2008); however, there is a need clinically to further identify and characterize reliable markers of risk for progression.

Distinct differences in gene expression are also associated with grade (Ma et al. 2003; Desmedt and Sotiriou 2006; Sotiriou et al. 2006). For example, distinct gene-expression patterns are present in low- and high nuclear-grade DCIS (Ma et al. 2003) similar to what is observed in IDC. Additionally, ADH and low-grade DCIS share gene-expression patterns associated with ER expression, whereas high-grade DCIS have a gene-expression pattern more associated with the cell-cycle and mitosis (Ma et al. 2003). In a similar respect, gene expression analysis of intermediate-grade DCIS show a combination of low- and high-grade characteristics (Ma et al. 2003; Sotiriou et al. 2006). These gene expression analyses support the view that low- and high-grade breast cancers arise from normal TDLUs through distinct molecular pathways (Figure 1.2). Defining distinct molecular pathways and breast cancer subtypes continues to be an evolving field as stratification of breast cancer into distinct subgroups and their molecular drivers involves an integrated view of the both the genome and transcriptome (Curtis et al. 2012).

CGH-based analyses of ALH and classic LCIS has revealed a similar pattern of chromosomal variation – loss of 16p, 16q, 17p, and 22q (Lu et al. 1998) in both. Further studies have identified a common loss in 16q in ALH, LCIS, and classic ILC (Mastracci

et al. 2006; Morandi et al. 2006). This supports the view that ALH and LCIS are closely related lesions and that all three (ALH, LCIS, and classic ILC) represent a progression continuum. Additionally, gene expression analysis of LCIS and classic ILC shows a pattern that is correlated with low-grade DCIS and IDC (Cao et al. 2008). Taken together, these studies support a common –16q, low-grade molecular pathway that includes ALH, LCIS, and classic ILC, as well as FEA, ADH, low-grade DCIS and low-grade IDC.

A small subset of ILCs shows a more aggressive clinical course, and consists of neoplastic lobular cells with more marked nuclear atypia (pleomorphic ILC). These cancers share common genetic variations with classic ILC – e.g. loss of 16q and gain of 1q; as well as common features of high grade IDC – e.g. amplification of 17q12 (Middleton et al. 2000; Simpson et al. 2008). However, a CGH-based study revealed that overall genetic variations of pleomorphic ILC are more closely correlated to those observed in classic ILC compared to IDC (Simpson et al. 2008). This suggests that pleomorphic ILC has a common molecular pathway of progression to that of classic ILC, that later accumulates alterations more characteristic of a high grade lesion (Figure 1.2). Similarly, there is CGH evidence that variant LCIS (pleomorphic LCIS, LCIS with necrosis) is of a common molecular background to classic LCIS (loss of 16q, gain of 1q), but that it is also associated with numerous further genetic aberrations that are more characteristic of a high grade lesion (Boldt et al. 2010).

1.1.5 The transition from pre-invasive to invasive breast cancer

The transition from a pre-invasive to an invasive phenotype occurs when cells of DCIS (or LCIS) invade through the basement membrane and into the surrounding stromal tissue, thus representing a key event in the progression of breast cancer. There is evidence

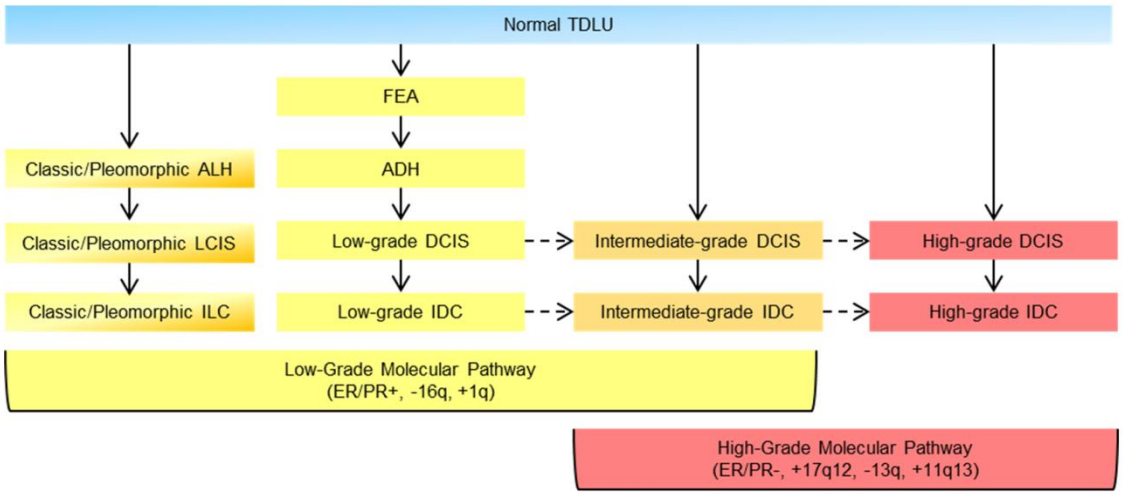

Figure 1.2 A multistep model of human breast cancer progression based on immunohistochemical and gene-expression data. Molecular events that occur in the normal terminal duct lobular unit (TDLU—blue rectangle) give rise to two distinct molecular pathways (low- and high-grade molecular pathways). Linear pathological progression occurs from normal TDLUs to invasive breast cancer (solid arrows) and intrastage progression occurs within ductal carcinoma in situ (DCIS) and invasive ductal carcinoma (IDC) (dotted arrows). The low-grade molecular pathway is characterized by loss of 16q, gain of 1q, and estrogen receptor (ER) and progesterone receptor (PR) positivity and is observed during pre-invasive and invasive stages of both ductal and lobular lesions (yellow rectangles). The high-grade molecular pathway is characterized by amplification of 17q12 and 11q13, loss of 13q, and ER/PR negativity (red rectangles). Pleomorphic lobular lesions [atypical lobular hyperplasia (ALH), lobular carcinoma in situ (LCIS), and invasive lobular carcinoma (ILC)] resemble high-grade tumors; however, immunohistochemical and genetic analyses support an association with the low-grade molecular pathway. Abbreviations: ADH, atypical ductal hyperplasia; FEA, flat epithelial atypia (modified from MacMillan et al. 2012).

that the tumor microenvironment is important during progression and that molecular changes in non-neoplastic cells (Allinen et al. 2004; Hu et al. 2005; Ma et al. 2009), in addition to neoplastic epithelial cells, have the potential to drive progression (Orimo et al. 2005; Karnoub et al. 2007; Hu et al. 2008; Sung et al. 2011). For example, in a cell line model for DCIS (Hu et al. 2008), the transition from DCIS to IDC did not require additional molecular alterations within the neoplastic epithelial cells, but rather progression to IDC was promoted by fibroblasts and suppressed by myoepithelial cells that make up the stromal and periductal microenvironment of DCIS. Molecular profiling of isolated epithelial and myoepithelial cells identified a signalling interaction network involving transforming growth factor β (TGF-β), hedgehog, cell adhesion molecules and p63, which was required for the differentiation of myoepithelial cells. Elimination of this signalling network resulted in loss of the myoepithelial cells and progression to an invasive phenotype (Hu et al. 2008). Similarly, the establishment of the self-sustaining TGF-β and stromal cell-derived factor 1 (SDF-1) autocrine signalling loops in resident mammary myofibroblasts can give rise to carcinoma-associated myofibroblasts that promote progression to invasive mammary carcinoma (Kojima et al. 2010). In addition, carcinoma-associated fibroblasts may mediate tumor growth and angiogenesis through the secretion of SDF-1 by acting directly on neoplastic epithelial cells via the chemokine (C-X-C motif) receptor 4 (CXCR4) and by recruiting endothelial progenitor cells, respectively (Orimo et al. 2005). In addition, tumor-associated macrophages can have progression-promoting effects through the secretion of immunosuppressive cytokines, the release of free radicals such as nitric oxide and hydrogen peroxide, and the secretion of angiogenic factors. It has been suggested that these signalling mechanisms may be useful

as therapeutic targets to block the development of tumor-promoting stromal cells (Malmberg 2004).

Studies such as these have changed our view of breast cancer progression as solely an epithelial/tumor cell-driven process. Two possible models of the DCIS-to-IDC transition ("escape" vs. "release") have been suggested (Polyak and Hu 2005). The "escape" model proposes that genetic alterations accumulate in a subpopulation of neoplastic epithelial cells which provides them with the ability to disrupt the myoepithelial layer and invade through the basement membrane into the surrounding stromal compartment. In contrast, the "release" model proposes that degradation of the basement membrane and subsequent invasion is due to alterations in the tumor microenvironment, particularly in the myoepithelial cells, myofibroblasts, fibroblasts, and tumor infiltrating inflammatory cells. What is actually occurring is most likely a combination of both models whereby changes in neoplastic epithelial cells and non-neoplastic cells of the tumor microenvironment both contribute to the transition from pre-invasive to invasive disease.

1.2 Cell migration and metastasis

1.2.1 Cell migration

Cell migration is an important mechanism in a number of biological processes. For example, in the event that the immune system is required to respond to a pathogen, the body relies on the ability of immune cells, such as natural killer cells, to migrate to the site of infection (Walzer and Vivier 2011). Endothelial cell migration, mediated by endothelial growth factor (VEGF) and mitochondrial reactive oxygen species, is required during the repair of damaged blood vessels that have become injured from atherosclerosis

(Wang et al. 2011). During spermatogenesis, germ cells migrate across the seminiferous epithelium and use important mediators such as matrix metalloproteases (MMPs) in order to invade through this dense tissue (Chen et al. 2011). A number of processes during development also require cell migration. For example, the disrupted function of the planar cell polarity (PCP) pathway, which is important for polarized cell movements, is implicated in neural tube defects (Wu et al. 2011). Cell migration is also important in ductal morphogenesis in the breast. For example, cells in elongating mammary ducts reorganize into a multilayered epithelial cell layer and migrate collectively. Initiation of the duct required important effectors of migration including Rac and myosin light-chain kinase whereas polarization to a bilayer depended on RHO-associated protein kinase (ROCK) (Ewald et al. 2008). It is evident that cell migration is an important underlying mechanism during a number of normal physiological processes. However, these same mechanisms can also be used by cancerous cells to migrate and invade during metastasis.

1.2.2 Cell migration and cancer metastasis

Metastasis is the spread of cancer from the primary tumor to a secondary site and consists of several consecutive, potentially rate-limiting steps (Talmadge and Fidler 2010). First, cancer cells migrate and invade from the primary tumor into surrounding stromal compartment. Next, they undergo intravasation into the blood or lymphatic vessels. Once they are in the circulation, cancer cells extravasate out of vessels at the secondary site using migration and invasion mechanisms. Finally, the cancer cells colonize and grow at the secondary site (Talmadge and Fidler 2010). Inhibiting the migration and invasion into the stroma and away from the primary tumor, one of the earliest steps in metastasis, can prevent the rest of the metastatic cascade (Zijlstra et al.

2008), supporting the idea that tumor cell migration is required for metastasis (Palmer et al. 2011; Shieh et al. 1999).

1.2.3 RHO family of GTPases

As noted above, cell migration is a key process in the metastasis of cancer. The RHO-family GTPases (Ras-homology-family of guanosine triphosphates) regulate many proteins involved in cell migration and are important downstream effectors in the PCP pathway (see *section 1.4.2*). The prototypical RHO-family GTPases are: Cdc42, Rac1, and RHOA. These proteins are themselves regulated by RHO-GEFs (guanine exchange factors) and RHO-GAPs (GTPase activating proteins). RHO-GEFs exchange a GDP for a GTP, which places the RHO-GTPase in its active state. Conversely, RHO-GAPs inactivate RHO-GTPases by removing a phosphate group from GTP making it a GDP (Tomar and Schlaepfer 2009). RHO-GTPases can be activated upon adhesion of the cells to the extracellular matrix (ECM), which initiates cell migration (Tomar and Schlaepfer 2009).

After contact with the extracellular matrix, Cdc42 activates actin polymerization, which in turn produces actin-rich filopodia (Olson and Sahai 2009). Filopodia are used for directional cell migration and the presence of filopodia is associated with increased invasion (Olson and Sahai 2009; Pan et al. 2011). Cdc42 also mediates lamellipodia formation in 2D environments (Olson and Sahai 2009). Lamellipodia formation may correspond to invadopodia formation that is seen in 3D environment since both rely on similar actin-related protein 2/3 (Arp2/3)-mediated actin polymerization (Olson and Sahai 2009).

Similar to Cdc42, Rac1 is also activated upon cell adhesion to extracellular matrix components and can induce formation of lamellipodia in migrating cells through Arp2/3 (Olson and Sahai 2009). RHOA has two functions during cell migration. It is involved in forming stress fibres to facilitate cell adhesion during the initial phase of migration and it induces cell contractility during later phases (Tomar and Schlaepfer 2009), both of which are mediated by a downstream effector protein ROCK.

ROCK inhibits the depolymerisation of actin filaments by activating LIM kinase, which in turn phosphorylates cofilin thereby inactivating its actin-depolymerization activity. This results in an increase in the number of stable actin stress fibres that are required during cell adhesion (Riento and Ridley 2003; Maekawa et al. 1999). ROCK also regulates cell migration through the promotion of cellular contraction by increasing the activity of the motor protein myosin II, using one of two different mechanisms. Firstly, ROCK can phosphorylate myosin light chain which increases the myosin II ATPase activity, resulting in the net shortening of actin fibres. Secondly, ROCK can inactivate myosin light chain phosphatase, leading to increased levels of phosphorylated myosin light chain (Riento and Ridley 2003).

The expression of Rac1 is increased in human gastric cancer and expression is correlated with tumor grade (Walch et al. 2008). In addition, active Rac1 expression is associated with increased grade in upper urinary tract cancers and is involved in lymph node metastasis (Kamai et al. 2010). Immunohistochemical analysis of hepatocellular carcinoma tissue samples established an association between RHOA expression and poor differentiation. It was also shown that RHOA was required for cell migration of hepatocellular carcinoma cell lines (Gou et al. 2011). Recently, RHOA was found to be a

downstream effector of PCP mediated migration of the MDA-MB-231 breast cancer cell line (Zhu et al. 2012). The above implicates a role for RHO-family GTPases in cancer cell migration and metastasis.

1.3 Models and methods used to study breast cancer progression

1.3.1 In vitro breast cancer progression models

In order to study the pre-invasive stages of breast cancer progression, several in vitro models have been developed. Most take advantage of established human breast epithelial cell lines which have been altered with activated oncogenes that drive production of these pre-invasive phenotypes (Weaver et al. 1995; Miller et al. 2000; Stampfer and Yaswen 2000; Briand and Lykkesfeldt 2001).

One in vitro model of breast cancer progression is the HMT-3522 series cell lines (Weaver et al. 1995; Briand and Lykkesfeldt 2001), which consists of three cell lines derived from a single patient presenting with fibrocystic change. The HMT-3522/S1 cell line was produced during in vitro culture of the explant and was shown to be non-tumorigenic in a mouse xenograft model; whereas the HMT-3522/S2 cell line was established after an epidermal growth factor (EGF)-independent growth selection of the HMT-3522/S1 cell line and was shown to be tumorigenic. The third cell line, HMT-3522/T4-2, was derived from a HMT-3522/S2 tumor and is considered to be the most tumorigenic of the three cell lines. The HMT-3522 cell lines have undergone malignant transformation in vitro without being exposed to known carcinogenic agents and this transformation resembles some aspects of progression during pre-invasive breast disease (Briand and Lykkesfeldt 2001). Similarly, the MCF10AT series cell lines represent a

range of pre-invasive breast lesions (Miller et al. 2000; Stampfer and Yaswen 2000). The MCF10A cells, also derived from a patient with fibrocystic change, are benign, immortalized breast epithelial cells. The MCF10AT cell line was derived from these cells by ras transformation. Subclones of the MCF10AT cells have generated a number of pre-invasive lesions including ADH and DCIS (Miller et al. 2000; Stampfer and Yaswen 2000). Both the HMT-3522 and the MCF10AT cell lines have proven useful; however, both model systems suffer from disadvantages. Both show mixed phenotypes and lack of stability of the phenotypes after culture. Additionally, the HMT-3522 cell lines lack a pre-DCIS stage, while the MCF10AT series is ras-transformation dependent, an uncommon event in spontaneous human breast cancers.

The 21T series cell lines, which were all derived from a single patient with metastatic breast cancer, represent a human breast cancer progression series (Band et al. 1990; Souter et al. 2010). When grown in the mammary fat pad of nude mice, each cell line can reproduce a distinct stage of progression. For example, 21PT cells are non-tumorigenic and generate lesions of ADH, 21NT cells form lesions with the morphology of DCIS, and 21MT-1 cells generate IDC and are both tumorigenic and metastatic (Souter et al. 2010).

1.3.2 Matrigel and 3D in vitro culture

In vitro systems are very useful for high throughput studies. However, it has been shown that when grown in 2D in vitro culture, cell lines can have distinctly different morphology and genetic profiles compared to in vivo growth (Shaw et al. 2004; Fournier and Martin 2006; Kenny et al. 2007; Lee et al. 2007; Hebner et al. 2008; Martin et al. 2008). Also, important signals released by the extracellular matrix, which control normal

homeostasis and tissue phenotypes, are lost when cells are cultured in 2D. When cells are cultured in a laminin-rich extracellular matrix, these signals remain intact (Lee et al. 2007). By allowing cells to grow in a 3D conformation in contact with extracellular matrix proteins, certain characteristics of cell morphogenesis, proliferation, apoptosis, and invasiveness may be studied in a highly controlled 3D environment. In fact, there have been many studies using 3D systems to examine molecular controls of morphogenesis in normal and neoplastic breast epithelial cells (Fauquette et al. 1997; Weaver et al. 1997; Wang et al. 1998; Debnath et al. 2002; Hebner et al. 2008). There has been limited use of 3D in vitro systems to directly study the progression through the pre-invasive to invasive stages of breast cancer; however, use of the HMT-3522 cell lines (Rizki et al. 2008) and the 21T cell lines (Souter et al. 2010) in 3D systems has proven useful in identifying potential regulators of progression.

1.3.3 The human 21T breast epithelial cell lines represent a progression series

As mentioned above, the 21T cell lines, which were derived from a single patient with metastatic breast cancer, represent a human breast cancer progression series (Band et al. 1990; Souter et al. 2010). For example, the 21PT cell line was found to be consistently non-tumorigenic and non-metastatic when injected into the mammary fat pads of nude mice and, upon further histological examination, there were some lesions mimicking ADH. When 21PT cells were grown embedded in 3D Matrigel, they developed in colonies capable of forming well-defined acinar structures, while maintaining cell polarity. Many of these colonies showed a mixture of cells with normal-appearing and atypical nuclei (Souter et al. 2010).

In contrast, the 21NT cells were found to be tumorigenic and non-metastatic when injected into the mammary fat pad of nude mice and the lesions that formed had a histology representative of DCIS. The involved ducts showed a uniform neoplastic cell population, with intermediate and high grade nuclei, solid and cribriform architectural patterns, with zonal necrosis. When 21NT cells were grown embedded in 3D Matrigel, the colonies that formed showed features consistent with DCIS, including nuclear atypia in all of the constituent cells and a spherical, non-infiltrative behaviour (Souter et al. 2010).

The 21MT-1 cells, when injected into the mammary fat pad of nude mice, were found to form tumors showing invasive mammary carcinoma, most with associated DCIS (intermediate and high nuclear grade). When 21MT-1 cells were grown embedded in 3D Matrigel, they formed highly disorganized, non-spherical colonies, with almost no lumen formation within the colonies themselves, which is consistent with the behaviour observed in the nude mouse xenografts (Souter et al. 2010).

1.3.4 The 21T cell lines show stage-specific gene expression patterns

Microarray analysis was used to identify unique differential gene expression patterns between the three 21T cell lines (Souter et al. 2010). Interestingly, differences in Wnt pathway components, such as changes in WNT5A and VANGL1 expression, were found between the 21PT and 21NT cell lines, which represent ADH and DCIS respectively. This is consistent with a number of recent studies implicating Wnt signalling pathways in breast cancer progression (Mohinta et al. 2007). One particular (non-canonical) Wnt pathway, the planar cell polarity (PCP) pathway, which involves the Wnt ligand WNT5A, has been shown to have both inhibitory and promoting effects in

cancer, depending on the context (Kikuchi and Yamamoto 2008). It has been suggested that the PCP pathway has a predominately inhibitory role early in progression by inhibiting canonical Wnt signalling and β-catenin stabilization. However, during later stages of progression, the PCP pathway may itself drive progression by stimulating cell migration through the downstream effectors RHOA and Rac1 (Wang 2009). In the 21T series cell lines, WNT5A expression was found to be decreased from the 21PT cells to the 21NT cells (ADH to DCIS transition), and was found to be increased from the 21NT cells to the 21MT-1 cells (DCIS to IMC transition). VANGL1 expression was found to be increased from the 21PT cells to the 21NT cells and remained relatively high in the 21MT-1 cell line (Souter et al. 2010).

1.4 Non-canonical Wnt/PCP signaling

1.4.1 An overview of Wnt signaling

Wnt signalling comprises a number of highly conserved cell signalling pathways that control cellular processes that are fundamental to embryogenesis such as proliferation, differentiation, polarity, and migration. However, aberrant Wnt signalling has been implicated in a number of different pathologies including cancer (Logan and Nusse 2004).

There are two distinct patterns of Wnt pathway signalling: the canonical Wnt/β-catenin-dependent pathway and non-canonical Wnt/β-catenin independent pathways. Both make use of a large family of cysteine-rich secreted ligands with at least 19 members in humans. The Wnt ligands themselves have been divided into two groups based on whether they induce transformation in a mouse mammary epithelial cell line; this Wnt-induced transformation is associated with the ligand's ability to activate specific

pathways (Wong et al. 1994). Highly transforming Wnt ligands include Wnt1, Wnt3, Wnt3a, and Wnt7a and these have been shown to activate the canonical Wnt/β-catenin-dependent pathway. Activation of the canonical Wnt/β-catenin-dependent pathway mediates β-catenin localization to the nucleus where it activates various transcription factors affecting gene expression (Kikuchi et al. 2009; MacDonald et al. 2009). Non-transforming or partially-transforming Wnt ligands include Wnt2, Wnt4, Wnt5a, Wnt5b, Wnt6, Wnt7b, and Wnt11 and these have been shown to activate non-canonical Wnt/β-catenin independent pathways.

Non-canonical Wnt signalling itself is made up of a number of different signalling pathways (Semenov et al. 2007), the most characterized being the Wnt/Ca^{2+} pathway and the Wnt/planar cell polarity (PCP) pathway. During Wnt/Ca^{2+} signalling, Wnt ligand binding to the Frizzled (Fzd) receptor activates phospholipase C, which leads to an increase in intracellular Ca^{2+} levels and activation of protein kinase C (PKC). This signalling pathway is involved during development but has also been implicated in cancer (Kohn and Moon 2005). For example, WNT5A induces an epithelial to mesenchymal transition through PKC/Ca^{2+} signalling, which in turn promotes melanoma metastasis (Dissanayake et al. 2007).

Among the non-canonical Wnt pathways, the Wnt/PCP pathway was the first described and the most widely studied (Simons and Mlodzik 2008; Zallen 2007). *Drosophila* has served as a useful model for PCP signalling because planar cell polarity occurs in a number of visible structures. The term “planar cell polarity” was derived from the tissue polarity necessary to generate polarization within the plane of the epithelium (Nubler-Jung et al. 1987). An analogous planar cell polarity signalling pathway was also

observed in vertebrates, involved in processes such as convergent extension (CE) movements of mesenchymal cells during gastrulation, ordered arrangement of hairs of mammalian skin and cilia of the respiratory tract, and orientation of axon extension (Goodrich 2008).

1.4.2 PCP signaling

The PCP pathway is highly conserved and is made up of consecutive steps that establish polarity in individual cells, ultimately giving whole tissues direction and polarity (Tree et al. 2002). Firstly, upstream PCP components, such as WNT5A, provide long range signals that establish overall polarity within the developing tissue (Strutt and Strutt 2005). Secondly, core PCP components, such as Fzd, Dishevelled (Dvl), Clsr, VANGL1, and Prickle, interpret these long range singles and establish planar polarity within single cells. Finally, downstream effectors, such as Daam1, RHOA, Rac1, ROCK, and c-Jun N-terminal kinase (JNK), use the signals mediated by the upstream and core PCP components to regulate cell polarity and migration by acting directly on the cytoskeleton (Figure 1.3). The RHO-family GTPases RHO and Rac are particularly important in mediating downstream PCP signalling (Schlessinger et al. 2009). Taken together, PCP pathway components induce intracellular cytoskeleton rearrangements and affect cell behaviours by transducing extracellular polarity signals and integrating both extracellular and intracellular proteins.

1.4.3 PCP signaling and cancer

The role of non-canonical Wnt signalling is critical in the formation of a number of embryonic tissues and organs (Wang and Steinbeisser 2009; Karner et al. 2006; Barrow 2006). These embryonic processes may, however, be co-opted in the course of

tumor progression. Many conserved signalling pathways that are important during development, including Wnt, Hedgehog, and Notch, often become aberrant during cancer development which supports the theory that tumorigenesis and development share similar signalling processes (Kho et al. 2004). Even though canonical Wnt/β-catenin signalling has been shown to be a critical player during tumorigenesis/cancer progression (Takemaru et al. 2008), there has been accumulating evidence that PCP signalling may also play a role (Katoh 2005; Kikuchi and Yamamoto 2008).

1.4.4 PCP signaling and metastasis

Breast cancer metastasis accounted for approximately 45 000 deaths in North American in 2012 (American Cancer Society 2012; Canadian Cancer Society's Steering Committee on Cancer Statistics 2012). As breast cancer progresses, from in situ to invasive disease, cells may develop the ability to invade through the basement membrane and into the surrounding stromal compartment, eventually forming secondary tumors at distant sites. Therefore, there continues to be a need to understand what drives progression of breast cancer, especially throughout earlier non-invasive stages and from non-invasive to invasive stages. Given PCP signalling has a central role in mediating cell motility during development; it seems likely that aberrant PCP signalling may play a role in progression to an invasive phenotype capable of metastasis.

Different PCP components have been shown to be involved in modulating cancer progression. For example, WNT5A, the prototypical non-canonical Wnt ligand, has been shown to promote metastasis of breast cancer by activating Rac and JNK (Pukrop et al. 2006). WNT5A has also been implicated in metastasis of melanoma and gastric cancer (Weeraratna et al. 2002; Kurayoshi et al. 2006).

The Fzd family of receptors, a core component of PCP signalling, consists of 10 members. One such member, Fzd7, has been shown to act in both canonical and non-canonical Wnt signalling pathways (Medina et al. 2000). Looking specifically at non-canonical Wnt signalling, Fzd7-mediated PCP signalling regulates cell movements by activating JNK and RHO in Xenopus (Medina et al. 2000; Kinoshita et al. 2003; Tanegashima et al. 2008). In humans, Fzd7 promotes invasion through PCP signalling in colon cancer cell lines (Vincan et al. 2007; Ueno et al. 2008) and migration in hepatocellular carcinoma (Merle et al. 2004).

There have been three members of Dvl, a cytoplasmic phosphoprotein that acts directly downstream of the Fzd receptor, identified in humans (Dvl1, Dvl2, and Dvl3). It has been shown that the expression of Dvl1 and Dvl3 is higher in nodal metastases of non-small cell lung cancer (NSCLC) compared to primary tumors. Specifically, Dvl1 expression was correlated with β-catenin expression in metastatic tissues, but there was no correlation between Dvl3 and β-catenin expression in primary tumors or metastases. Additionally, overexpression of Dvl1 and Dvl3 promoted invasion in A549 and QG56 lung cancer cell lines but there were differing effects on β-catenin stabilization (Wei et al. 2008), suggesting that progression of NSCLC to an invasive phenotype may be mediated by Dvl1 through the canonical Wnt pathway, but also by Dvl3 independent of β-catenin.

VANGL1 has been implicated in various cancers. Downregulation of VANGL1 expression inhibits growth of hepatocellular carcinoma cells (Yagyu et al. 2002). VANGL1 has also been shown to bind to the metastasis suppressor Kangai 1/Cluster of differentiation 82 (KAI1/CD82) and subsequent overexpression of VANGL1 in the mouse colon cancer cell line CT-26 increased invasiveness and adhesion to fibronectin in

vitro and increased tumorigenicity and metastasis in vivo (Lee et al. 2004). VANGL1 overexpression also increased invasion and migration of squamous cancer cells in vitro and promoted metastasis in a mouse squamous tumor model in vivo (Lee et al. 2009). Additionally, suppression of VANGL1 via small interfering RNA (siRNA) decreased colon cancer metastasis in mice, thereby supporting VANGL1's role as a metastasis promoter (Lee et al. 2005). VANGL1 was also implicated in colorectal cancer by promoting cell migration and invasion through the formation of a functional complex with Dvl and PKCδ (Kho et al. 2009). This suggests that overexpression of VANGL1 can promote invasion and metastasis through PCP signalling. Recently, VANGL1 was found to form a complex with scribbled homolog (SCRIB) and Nitric oxide synthase 1 (neuronal) adaptor protein (NOS1AP) along cellular protrusions resembling lamellipodia in metastatic breast cancer cells, but not in normal breast cells. Subsequent knockdown of VANGL1 with shRNA reduced cell migration, implicating a role for VANGL1 and PCP signalling in breast cancer metastasis (Anastas et al. 2012).

1.4.5 Complex role for PCP signaling in cancer progression

Despite the large body of evidence that implicates PCP signalling in promoting invasion and metastasis, just exactly how PCP signalling is involved in cancer progression is still uncertain. Additionally, because of the critical involvement of β-catenin signalling during tumor development and the antagonism between the different Wnt pathways, it is possible that PCP signalling may in some instances/cellular contexts inhibit cancer progression (Veeman et al. 2003).

WNT5A, the prototypical Wnt ligand which activates non-canonical Wnt signalling, can act as both an oncogene or tumor suppressor depending on the context. A

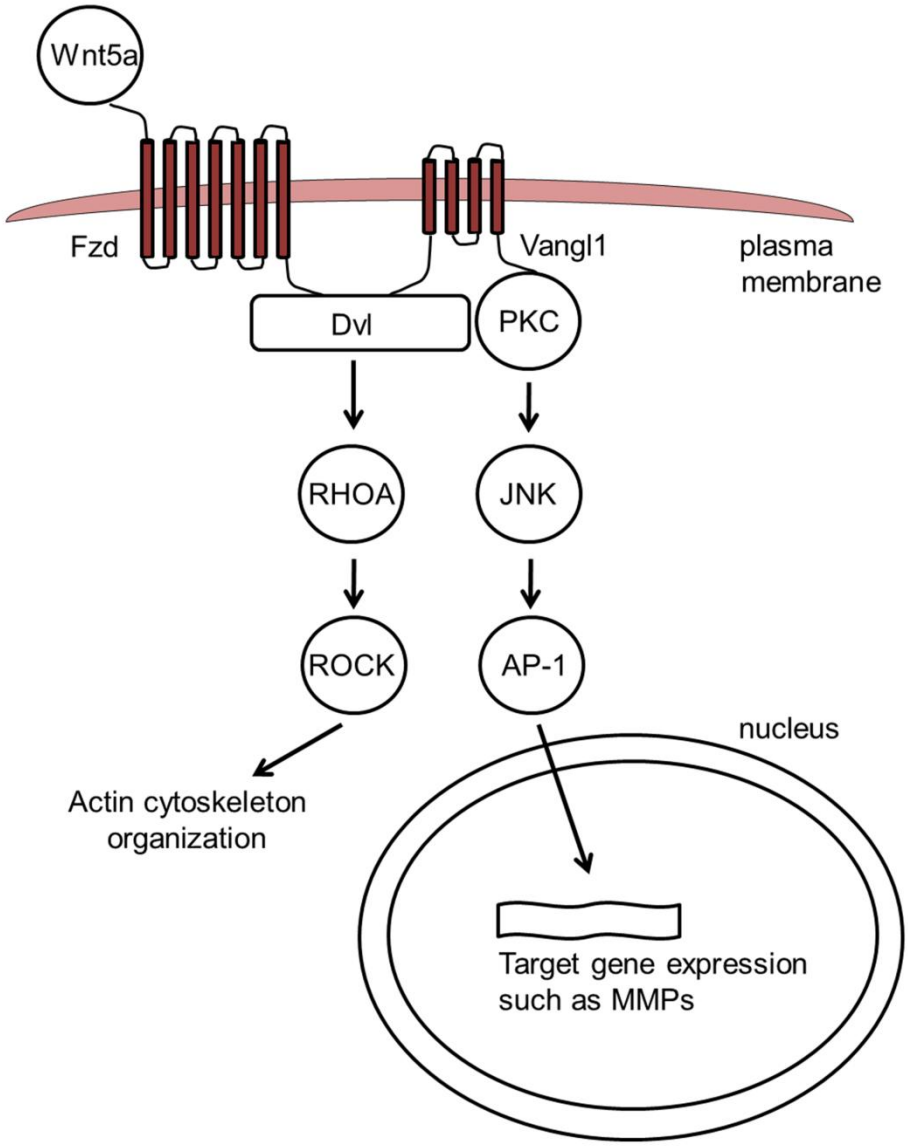

Figure 1.3 Simplified overview of non-canonincal Wnt/PCP signalling. Upstream PCP components, such as WNT5A, provide long range signals that establish overall polarity within the developing tissue. Core PCP components, such as Fzd, Dishevelled (Dvl), Clsr, VANGL1, and Prickle, interpret these long range singles and establish planar polarity within single cells. Downstream effectors, such as Daam1, RHO, Rac, ROCK, and JNK, use the signals mediated by the upstream and core PCP components to regulate cell polarity and migration by acting directly on the cytoskeleton. VANGL1 promotes cell migration and invasion through the formation of a functional complex with Dvl and PKC.

number of studies suggest that WNT5A acts as a tumor suppressor by antagonizing the Wnt/β-catenin pathway. For example, disruption of WNT5A expression with a WNT5A antisense expression vector mimicked transformation caused by Wnt1 in the mouse mammary epithelial cell line C57MG, suggesting that WNT5A is an important regulator of cell growth and differentiation (Olson and Gibo 1998). Additionally, there is evidence that in hematopoietic malignancies, thyroid carcinoma, colorectal cancer, hepatocellular carcinoma, and breast cancer, WNT5A is downregulated and in some cases there is an inverse correlation between WNT5A and β-catenin expression (Liang et al. 2003; Kremenevskaja et al. 2005; Leris et al. 2005; Ying et al. 2007; Ying et al. 2008; Liu et al. 2008). As discussed above, however, in more advanced stages of cancer progression, WNT5A has been shown to be upregulated and to promote invasion and metastasis in melanoma, gastric cancer, and breast cancer (Pukrop et al. 2006; Weeraratna et al. 2002; Kurayoshi et al. 2006). Therefore, it appears that the PCP pathway may have a dual role in breast cancer progression by behaving as an inhibitor of progression during earlier stages and as a promoter of cancer progression during later stages. Thus, it is important to fully characterize the PCP pathway to better understand the specific context that allows WNT5A to act as either a tumor suppressor or an oncogene.

1.5 Thesis rationale and hypothesis

1.5.1 Rationale

The 21T cell lines, derived from the same patient with metastatic breast cancer (Band et al. 1990), represent a mammary tumor progression series and mimic specific stages of breast cancer (21PT, ADH; 21NT, DCIS; 21MT-1, IDC) (Souter et al. 2010). Expression profiling of these cell lines has revealed significant differences in the non-canonical Wnt/PCP pathway members VANGL1 and WNT5A (Souter et al. 2010). Specifically, VANGL1 expression is relatively high in the 21NT cell line compared to the 21PT cell line and remains relatively high in 21MT-1 cells; whereas WNT5A expression is moderate in the 21PT cell line, relatively low in the 21NT cell line, and relatively high in the 21MT-1 cell line compared to the 21PT and 21NT cell lines (Souter et al. 2010).

WNT5A has been shown to promote differentiation early in progression. However, in later stages it has been shown to promote progression. This dual effect of WNT5A may be due to the presence or absence of other Wnt pathway components such as VANGL1. Hence, it is important to further characterize the role of this pathway in inhibiting or promoting breast cancer progression by addressing whether the cellular context (such as VANGL1 expression) can alter the response to WNT5A.

1.5.2 Thesis hypothesis

WNT5A promotes breast cancer progression in the 21T cells in the presence of VANGL1.

1.5.3 Project Objectives

Objective 1. Improve the in vitro breast cancer progression model to assess 3D morphology with the 21T cell lines.

Objective 2. Test molecular controls of breast cancer progression, specifically the roles of WNT5A and VANGL1.

Specific aim 1: Determine the role of WNT5A overexpression using the 21T cell lines via stable transfection.

Specific aim 2: Determine the role of VANGL1 overexpression using the 21T cell lines via stable transfection.

Specific aim 3: Determine the role of WNT5A and VANGL1 on breast cancer progression via shRNA knockdown using the 21T cell lines.

Chapter 2

2 Methods

2.1 Cell lines and culture conditions

The 21T parental cell lines (21PT, 21NT, and 21MT-1) were a kind gift from Dr. Vimla Band (Dana Farber Cancer Institute, Boston, MA) (Band et al. 1990) and were cultured in alpha modification of Eagle's medium (α-MEM) supplemented with 2mM L-glutamine, insulin (1mg/mL), epidermal growth factor (12.5ng/mL), hydrocortisone (2.8mM), 10mM 4-(2-hydroxyethyl)-1-piperazineethanesulfonic acid (HEPES), 1mM sodium pyruvate, 0.1mM non-essential amino acids, and 50mg/mL gentamycin reagent (now called αHE – all supplements from Wisent Bioproducts, Montreal, QC) as previously described (Band et al. 1990). For regular culture conditions, the αHE media was further supplemented with 10% fetal bovine serum (FBS; Sigma) and named αHE10F. The 21T stable clones were cultured in the above supplemented growth media with the addition of 500μg/mL G418 (Wisent Bioproducts) or 0.8μg/mL puromycin (Sigma-Aldrich, St. Louis, MO) as selection markers.

2.2 Generation of WNT5A expression vector

An expression vector containing WNT5A was constructed in order to overexpress Wnt5a protein in 21PT and 21NT cells. To construct the expression vector, WNT5A cDNA was PCR-amplified using a pCMV-Sport expression vector containing WNT5A (Genbank accession number: NM_003392), provided by the Centre for Applied Genomics at The Hospital for Sick Children (University of Toronto, Toronto, ON) as the cDNA template. PCR amplification was performed using Phusion High-Fidelity DNA Taq Polymerase (New England BioLabs, Pickering, ON) at the following conditions:

98^{o}C for 30 seconds, followed by 40 cycles of 98^{o}C for 7 seconds, 62^{o}C for 15 seconds and 72^{o}C for 45 seconds and finally a 72^{o}C hold for 8 minutes. The primers for PCR amplification can be found in Table 2.1. Five separate PCR reactions were completed and run on a 1% agarose gel. Bands at the appropriate size (~1500 kb) were gel extracted, using an EZ-10 Spin Column DNA Gel Extraction Kit (Bio Basic, Markham, ON) and pooled. Next, the WNT5A PCR product was incubated with T4 polynucleotide kinase (T4 PNK; New England BioLabs) to phosphorylate the insert. Finally, the WNT5A PCR product was purified using a QIAquick PCR purification kit (Qiagen, Mississauga, ON), following the manufacturer's protocol and the concentration was determined by spectrophotometry, using a NanoDrop 1000 Spectrophotometer (Thermo Scientific, Mississauga, ON).

WNT5A was inserted into a pcDNA3.1/myc-His B plasmid (Invitrogen Life Technologies, Mississauga, ON), such that the myc-His tag would be fused to the C-terminus of WNT5A. The plasmid was digested with EcoRV (New England BioLabs) so that the WNT5A sequence would be inserted downstream of the pCMV promoter into the multiple cloning site. The plasmid was subsequently incubated with calf intestinal phosphatase (CIP; New England BioLabs) to dephosphorylate the plasmid. The plasmid was then electrophoresed on a 1% agarose gel and extracted using an EZ-10 Spin Column DNA Gel Extraction Kit (Bio Basic).

The prepared plasmid and WNT5A PCR product were incubated overnight with ATP (adenosine triphosphate) and T4 DNA ligase (both from New England BioLabs) at 16°C to complete the ligation. Competent bacteria (DH5alpha, made in-house) were then transformed with the ligated plasmid and streaked on Luria Bertani (LB) agar (Invitrogen

Life Technologies) plates with 50µg/mL ampicillin (Gibco Life Technologies, Grand Island, NY). Twenty bacteria colonies were picked and expanded in LB + ampicillin media, and DNA was isolated using an EZ-10 Spin Column Plasmid DNA Miniprep Kit (Bio Basic). The DNA was digested with Xhol and BsrGl (both from New England BioLabs) and run on a 1% agarose gel to see which ligation resulted in correct insertion. Four of the 20 clones were sent to the DNA Sequencing Facility at Robarts Research Institute (London, ON) for sequencing. Clones with the proper sequence were used for stable transfections.

2.3 Site directed mutagenesis

A pcDNA3.1/myc-His B expression vector containing VANGL1 (previously constructed by L. H. Souter and H. S. Leong in a manner similar to WNT5A) underwent site directed mutagenesis in order to introduce a stop codon at the end of full length VANGL1 (VANGL1-stop) using QuikChange Site-Directed Mutagenesis Kit (Agilent Technologies, Wilmington, DE) according to the manufacturer's protocol. VANGL1-myc DNA template (50ng), primers designed specially to introduce a stop codon (125ng each – see Table 2.1), dNTPs, and PfuTurbo DNA polymerase were mixed in PCR tubes. PCR amplification was performed using the following parameters 95^{o}C for 30 seconds, followed by 18 cycles of 95^{o}C for 30 seconds, 55^{o}C for 60 seconds, and 68^{o}C for 14 minutes. Five separate PCR reactions were completed. DpnI restriction enzyme was added to each amplification reaction for 1 hour at 37°C in order to digest the non-mutated parental DNA strand. Competent bacteria (DH5alpha) were then transformed with the digested reaction mixture and streaked on LB agar (Invitrogen Life Technologies) plates with 50µg/mL ampicillin (Gibco Life Technologies). Twenty bacteria colonies were

picked and expanded in LB + ampicillin media, and DNA was isolated using an EZ-10 Spin Column Plasmid DNA Miniprep Kit (Bio Basic). Clones were sent to the DNA Sequencing Facility at Robarts Research Institute for sequencing. Clones with the proper sequence were used for stable transfections.

2.4 Stable transfections

Stably transfected cell lines were generated to overexpress WNT5A in the 21PT and 21NT cells and VANGL1 in the 21PT cells using PolyJet DNA In Vitro Transfection Reagent (SignaGen Laboratories, Rockville, MD). Plasmids lacking the gene of interest were also transfected into each cell line as an empty vector control. The day before transfection, 21PT or 21NT cells were seeded in 10cm dishes at a density that would result in 70-80% confluency the next day. Cells were transfected with 5μg of the appropriate expression vector following the manufacturer's protocol. PolyJet/DNA complex-containing medium was replaced 18 hours post-transfection with αHE10F. Forty-eight hours post-transfection, the media was replaced with αHE10F containing 500μg/mL G418. Approximately two weeks post-transfection, G418 resistant clones were pooled, expanded, and frozen down in vials for later use.

2.5 Generation of lentivirus particles and transduction

To generate shRNA containing lentivirus particles against WNT5A, VANGL1, and RHOA, HEK293T cells were plated in 2mL of high glucose Dulbecco's Modified Eagle Media (DMEM) + 10% FBS in 6 well plates and incubated for 24 hours prior to transfection. Co-transfection of a three plasmid system was carried out using hairpin-pLKO.1 vector (1ug), envelope plasmid (VSVG/pMD2.G; 100ng) and packaging plasmid (pCMV-R8.74psPAX2; 900ng) as previously described (Moffat et al. 2006). SuperFect

Transfection Reagent (Qiagen) was used according to the manufacturer's protocol. Cells were incubated for 18 hours post transfection and the media containing the transfection reagent was replaced with 2mL high glucose DMEM + 10% FBS. Approximately 48 hours post-transfection, the viral supernatant (2mL) was collected, passed through a 0.2μm filter, and stored at 4°C. Media (2mL) was replenished, and viral harvesting was repeated a second time 24 hours later, pooled with previous harvest, aliquoted, and stored at -80°C until further use. HEK293T cells, pLKO.1-shRNA clones (WNT5A, VANGL1, RHOA, LUC – Table 2.2), pMD2.G and pCMV-R8.74psPAX2 plasmids were all gifts from Dr. Jason Moffat (University of Toronto). Generation of viral supernatant for RHOA and LUC shRNAs were previously prepared by A. E. Robertson and H. S. Leong.

2.6 Quantitative real-time polymerase chain reaction (qRT-PCR)

Total RNA was extracted from 3 biological replicates of each cell line grown in 10cm dishes using TRIZOL (Invitrogen Life Technologies) following the manufacturer's protocol. RNA concentration was determined using a NanoDrop spectrophotometer (Thermo Scientific) (and 5ug of RNA for each sample was DNase I (Invitrogen Life Technologies) treated prior to reverse transcription to cDNA using SuperScript III Reverse Transcriptase with random hexamers (both from Invitrogen Life Technologies). qRT-PCR was performed on cDNA samples and water-primer set only controls using RT2 SYBR-Green qPCR Master Mix (SuperArray Biosciences Corporation, Frederick, MD). Reactions were carried out in a 96-well plate and were spun for 2500RPM for 30 seconds prior to placing the plate in the Thermo Cycler. Samples amplified with either WNT5A, VANGL1, of RHOA specific primers were reported relative to GAPDH as fold

expression normalized to control cell lines. For a list of primers used for qRT-PCR see Table 2.1.

2.7 Preparation of 21T cell lysates

The 21T cells were grown on 10cm dishes. Subconfluent monolayers were washed once with ice cold PBS. RIPA buffer (10nM Tris-HCl pH 7.5, 1mM EDTA, 0.5mM EGTA, 150nM NaCl, 1% Triton-X 100, 0.5% DOC, and 1% SDS) containing one protease inhibitor tablet per 10mL (cOmplete, Mini, EDTA-free Protease Inhibitor Cocktail, Roche; Mannheim, Germany) was applied directly to the plate to lyse the cells (400uL per 10cm dish). The cells were removed with a cell scraper, collected in a clean microcentrifuge tube, and placed on a rotator for 20 minutes at 4°C. Tubes were spun at 13000 RPM for 10 minutes at 4°C and the resulting supernatant was collected and transferred to a clean microcentrifuge tube. The concentrations of the protein samples were determined using a BioRad Bradford Assay (Mississauga, ON) by comparing to BSA standards.

2.8 Electrophoresis and Western blotting

Protein was separated via SDS-PAGE on 8% polyacrylamide gels. Separated proteins were transferred onto PVDF membrane and probed for proteins of interest by Western blot. Membranes were blocked with 5% skim-milk in TBST (Tris-buffered saline with 0.1% Tween-20) overnight at 4°C. After washing membranes once with TBST, they were incubated with required primary antibodies for 1.5 hours at room temperature. Rat anti-Wnt5a antibody was purchased from R&D Systems (Burlington, ON, catalogue no. MAB645) and mouse the anti-myc antibody was a kind gift from Dr. Joe Mymryk (London Regional Cancer Program, London, ON). Membranes were washed

Table 2.1 Primer sequences for WNT5A cloning, VANGL1 site-directed mutagenesis, and qRT-PCR

Primer Name	Sequence (5' to 3')
WNT5A Cloning Primers	
Forward	GCCACCATGAAGAAGTCCATTGGAATATTAA
Reverse	GGAGATCGTGGACCAGTTTGTGTGCAAG
VANGL1 Mutagenesis Primers	
Forward	GCTTACAGTCTGAGACATCCGTTTAAATCCAGCACAGTGGCGG
Reverse	CGAGCGGCCGCCACTGTGCTGGATTTAAACGGATGTCTCAGAC
WNT5A qRT-PCR Primers	
Forward	GATGCAGATAGGCAGCCGCG
Reverse	GGAGCCCTTGGCGTGGATGC
VANGL1 qRT-PCR Primers	
Forward	ACCTGAGTATCCAGCGAGCAG
Reverse	CGCCGTTCATGTTCGGCCTCT
RHOA qRT-PCR Primers	
Forward	GGGACACAGCTGGGCAGGAGGA
Reverse	GGTTTCACCGGCTCCTGCTTCA
GAPDH qRT-PCR Primers	
Forward	AGGCTGGGGCTCATTTGCAG
Reverse	CCATCCACAGTCTTCTGGGTG

Table 2.2 shRNA target sequences used to knockdown WNT5A, VANGL1, RHOA and Luciferase

Gene (Identifier)	shRNA Target Sequence
RHOA (46)	GTTGGGAATAAGAAGGATCTT
RHOA (48)	TGGAAAGACATGCTTGCTCAT
RHOA (49)	GAAAGCAGGTAGAGTTGGCTT
WNT5A (B1)	CAAAGAATGCCAGTATCAATT
WNT5A (B2)	CCAGGTTGTAATTGAAGCCAA
WNT5A (B3)	CCTGTTCAGATGTCAGAAGTA
VANGL1 (A6)	AGTCTGAGACATCCGTTTAAA
VANGL1 (A8)	GCTCTTTATCTCCATGGCATT
VANGL1 (A10)	CTCGTAGTCAATGTGAAGAAA
Luciferase	ACGCTGAGTACTTCGAAATGT

with TBST 3 times for 5 minutes each and incubated with horseradish peroxidase (HRP)-conjugated anti-mouse secondary antibody (Amersham GE Healthcare, catalogue no. NXA931 - diluted 1:10000 in 5% skim milk TBST) or HRP-conjugated goat anti-rat secondary antibody (R&D Systems catalogue no. HAF005 1:1000 in 5% skim milk TBST) for 1 hour at room temperature. Membranes were washed 5 times for 3 minutes each. Detection was performed using the ECL Plus Western Blotting Detection Reagents (Amersham GE Healthcare, Piscataway, NJ) and then exposed to film in a dark room. Densitometric quantification was performed using ImageJ (Open source software, National Institutes of Health, USA).

2.9 Three-dimensional Matrigel culture and immunofluorescence

Subconfluent monolayers were trypsinized, washed, resuspended in αHE media containing 2% growth factor reduced Matrigel (BD Biosciences, Mississauga, ON) and 2% FBS, and plated as single cell suspensions on 100% Matrigel in 8-well chambers slides as previously described (Debnath et al. 2003; Lee et al. 2007). αHE media containing 2% Matrigel and 2% FBS was changed every 3 days. Following the indicated time points, the cell colonies were fixed with 10% (w/v) formalin in phosphate buffered saline (PBS) for 20 minutes at room temperature. Cells were then permeabilized with 0.5% Triton X-100 in PBS for 20 minutes at 4°C and blocked with 10% normal goat serum (Invitrogen Life Technologies) for 45 minutes at room temperature. Cell colonies were probed using a purified mouse anti-E-cadherin primary antibody (BD Biosciences, catalogue no. 61081) for 1.5 hours in 10% normal goat serum at room temperature. Following primary antibody incubation, the cell colonies were washed 3 times with PBS

for 5 minutes per wash. Cell colonies were then probed with Alexa Fluor 488 Goat anti-mouse secondary antibody (Invitrogen Life Technologies) and Alexa Fluor 546 conjugated phalloidin (Invitrogen Life Technologies) to stain for F-actin in 10% normal goat serum for 1 hour at room temperature. Following secondary antibody and phalloidin incubation, the cell colonies were washed 5 times with PBS for 3 minutes each. Finally, cell colonies were incubated for 15 minutes at room temperature with 3μg/mL Hoechst 33342, trihydrochloride, trihydrate (Invitrogen Life Technologies) to stain for the nuclei. Chamber slide gaskets were removed prior to mounting with Vectashield mounting medium (Vector Laboratories, Burlington, ON). Images were captured with an Olympus Confocal Imaging System (FluoView FV1000 coupled to the IX81 Motorized Inverted System Microscope) at the Victoria Research Laboratory Confocal Microscope Core Facility (London, ON) and processed using Volocity software (PerkinElmer, Woodbridge, ON).

2.10 Transwell migration assay

The migration of the 21PT and 21NT cells overexpressing WNT5A was tested using a Boyden chamber system (Corning Life Sciences; Lowell, MA). The day before the assay, 6.5mm transwell inserts (8.0μm pores) were each coated with 6μg of gelatin (diluted in 60μL of sterile Milli-Q water). Plates were allowed to dry overnight at room temperature. On the day of the assay, the gelatin coated transwell inserts were reconstituted by adding 0.1mL of αHE media supplemented with 0.1% BSA to the upper chamber for 90 minutes at room temperature. Subconfluent cells were washed twice with PBS, and resuspended in serum free media containing 0.1% BSA at a concentration of $5x10^5$ cells/mL. Media containing chemoattractant (0.8mL of αHE10F) was added to the

bottom chambers and 0.1mL of the cell suspension ($5.0x10^4$ cells per well) was immediately added to the upper chambers in triplicate. The Boyden chambers were incubated at 37°C and 5% CO_2 for 5 hours. During recombinant Wnt5a treatment, recombinant Wnt5a (R&D Systems) was added at the upper and lower chambers at the beginning of the assay.

After the assay was complete, the inner chamber inserts were removed and fixed/stained/washed using the Diff-Quick staining system (modified Wright Giemsa stain, Sigma-Aldrich) according to manufacturer's protocol. The cells that did not migrate to the underside of the membrane were removed using a cotton swab. The insert wells were allowed to dry overnight and images of 5 non-overlapping fields of view were acquired using Image-Pro Analysis Software (Media Cybernetics, Acton, MA) coupled to an inverted microscope. Images were captured at 10X objective. Cells were counted from these pictures using ImageJ (Open source software).

2.11 Transwell invasion assay

The invasion of the 21PT and 21NT cells overexpressing WNT5A and VANGL1 was tested using a Boyden chamber system precoated with Matrigel (reconstituted basement membrane proteins - BD Biosciences). Two hours prior to plating, the Matrigel precoated transwells (6.5mm inserts and 8.0μm pores) were reconstituted by adding 0.5mL of αHE media supplemented with 0.1% BSA to the upper and lower chambers at 37°C and 5% CO_2. Cells were washed twice with PBS, and resuspended in serum free media containing 0.1% BSA at a concentration of $1x10^5$ cells/mL. The media used for reconstitution of the Matrigel in the lower and upper chambers was removed. Media containing chemoattractant (0.75mL of αHE10F) was added to the bottom chambers and

0.5mL of the cell suspension ($5x10^4$ cells) was immediately added to the upper chambers in triplicate. The Boyden chambers were incubated at 37°C and 5% CO_2 for 22 hours. During recombinant Wnt5a treatment, recombinant Wnt5a (R&D Systems) was added at the appropriate concentration to the upper and lower chambers at the beginning of the assay.

After the assay was complete, the inner chamber inserts were removed and fixed/stained/washed using the Diff-Quick staining system (Sigma-Aldrich) according to manufacturer's protocol. The cells that did not invade to the underside of the membrane were removed using a cotton swab. The insert wells were allowed to dry overnight and images of 5 non-overlapping fields of view were acquired using Image-Pro Analysis Software (Media Cybernetics) coupled to an inverted microscope. Images were captured at 10X objective. Cells were counted from these pictures using ImageJ (Open source software).

2.12 Statistical analysis

Statistical analyses were done using GraphPad Prism 5.0 software (La Jolla, CA). Colony morphology experiments, migration and invasion assays, and mRNA and protein levels were analyzed using ANOVA followed by Tukey's post hoc test (for comparison between more than two groups) or Student's *t*-test (for comparison between two groups). *P*-values less than 0.05 were considered statistically significant.

Chapter 3

3 Results

3.1 Objective 1: Improve the in vitro breast cancer progression model to assess 3D morphology with the 21T cell lines

The use of the 21T cell lines in a 3D in vitro system has proven useful in identifying potential regulators of progression (Souter et al. 2010); however, the method of embedding the 21T cell lines in Matrigel in order to assess 3D morphology is costly, time consuming, and the thickness of the Matrigel layer does not allow for easy visualization of the embedded cells in situ. Here, the 21T cell lines were characterized using a modified 3D in vitro system in which cells are seeded on top of Matrigel, as opposed to embedded within (Lee et al. 2007; Debnath et al. 2003), and 3D morphology was analyzed using confocal microscopy. First, each parental cell line was characterized over time (section *3.1.1* to *3.1.3*) and finally, all three cell lines were compared in order to choose a suitable endpoint to the 3D morphology assay (section *3.1.4*).

3.1.1 Characterization of the 21PT (ADH) cell line

In order to characterize the 21PT cell line, cells were grown on top of 100% Matrigel in a 2% FBS, 2% Matrigel solution for 3, 6, 9, and 12 days; after the specified time point the cells were fixed, permeabilized, stained, and imaged using a confocal microscope. The percentage of 21PT colonies (a group of 2 or more cells) that exhibited lumen formation at day 3 was 7.19% (SE 2.34), at day 6 was 20.35% (SE 5.30), at day 9 was 47.49% (SE 2.20), and at day 12 was 57.88% (SE 2.59) (*Figure 3.1A*, *3.1B*). These differences were significant between day 3 and day 9 ($p<0.001$), day 3 and day 12

(p<0.001), day 6 and day 9 (p<0.01), and day 6 and day 12 (p<0.001). The percentage of 21PT colonies that were polarized (unequal distribution of actin and E-cadherin) at day 3 was 43.35% (SE 5.26), at day 6 was 56.85% (SE 4.17), at day 9 was 62.69% (SE 3.67), and at day 12 was 69.28% (SE 2.33) (*Figure 3.1A, 3.1B*). These differences were significant between day 3 and day 9 (p<0.05) and day 3 and day 12 (p<0.01). In the colonies that were considered polarized, actin was localized to the apical region of the colony (inside the colony located near the lumen) and E-cadherin was localized to the cell to cell junctions and the basal region of the colony. The percentage of 21PT colonies that were spherical (round, smooth edged colony) vs. non-spherical at day 3 was 39.60% (SE 9.93), at day 6 was 66.99% (SE 4.24), at day 9 was 72.41% (SE 5.68), and at day 12 was 71.45% (SE 0.51) (*Figure 3.1A, 3.1B*). These differences were significant between day 3 and day 9 (p<0.05) and day 3 and day 12 (p<0.05). The number of nuclei per colony in the 21PT cell line at day 3 was 3.25 (SE 0.53), at day 6 it was 6.96 (SE 0.50), at day 9 it was 8.09 (SE 0.74), and at day 12 it was 12.92 (SE 1.65) (*Figure 3.1C*).

3.1.2 Characterization of the 21NT (DCIS) cell line

In order to characterize the 21NT cell line, cells were grown on top of 100% Matrigel in a 2% FBS, 2% Matrigel solution for 3, 6, 9, and 12 days; after the specified time point cells were fixed, permeabilized, stained, and imaged using a confocal microscope. The percentage of 21NT colonies that exhibited lumen formation at day 3 was 9.56% (SE 0.89), at day 6 was 15.37% (SE 0.65), at day 9 was 13.48% (SE 2.40), and at day 12 was 29.21% (SE 5.29) (*Figure 3.2A, 3.2B*). These differences were significant between day 3 and day 12 (p<0.01), day 6 and day 12 (p<0.05), and day 9 and day 12 (p<0.01). The percentage of 21NT colonies that were polarized at day 3 was

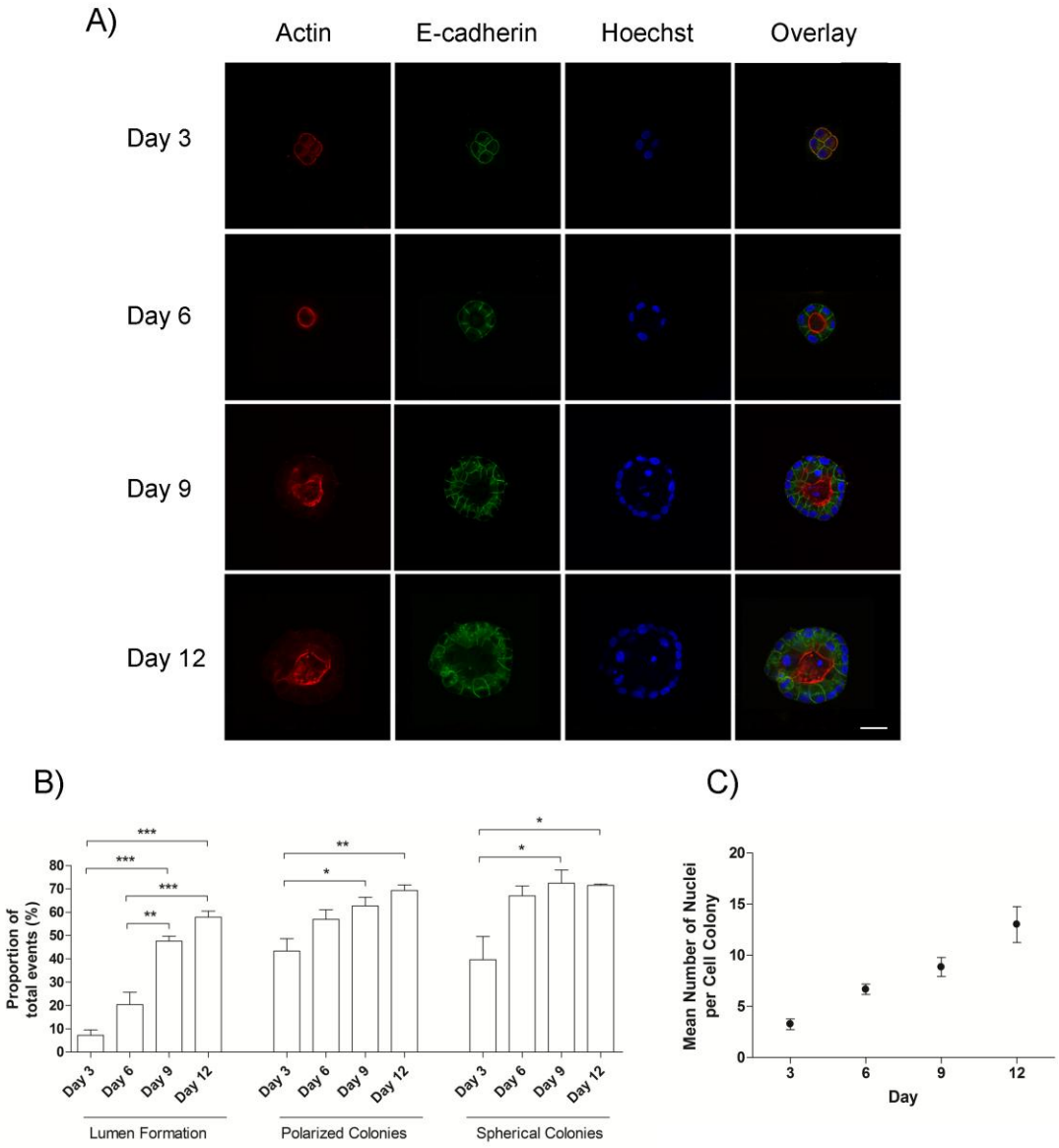

Figure 3.1 Characterization of the 21PT cell line grown in 3D Matrigel. The 21PT cells were grown on top of 100% Matrigel in αHE + 2% FBS and 2% Matrigel for 3, 6, 9, and 12 days. Cell colonies were fixed, permeabilized, stained, and imaged using confocal microscopy. A) Representative cell colonies are shown at each day. Actin is shown in red, E-cadherin is shown in green, and the nuclear stain Hoechst is shown in blue. An overlay of all three channels is shown in the final set of panels. B) The proportion of colonies exhibiting lumen formation is increased from day 3 to day 9, from day 3 to day 12, from day 6 to day 9, and from day 6 to day 12. The proportion of polarized colonies is increased from day 3 to day 6 and from day 3 to day 12. The proportion of spherical colonies (vs. non-spherical colonies) is increased from day 3 to day 9 and from day 3 to day 12. C) The number of nuclei per colony increased over time. Colony morphology was analyzed using one-way ANOVA followed by Tukey's post hoc test. * $p<0.05$, ** $p< 0.01$, *** $p<0.001$. Scale bar represent 30μm.

54.59% (SE 11.31), at day 6 was 49.06% (SE 3.77), at day 9 was 38.25% (SE 3.10), and at day 12 was 45.94% (SE 8.78) (*Figure 3.2A, 3.2B*). These differences were not significant. In the colonies that were considered polarized, actin was localized to the center of the colony (inside the colony, apical aspect of the cells) and E-cadherin was localized to the cell to cell junctions. The percentage of 21NT colonies that were spherical (vs. non-spherical) at day 3 was 51.14% (SE 2.59), at day 6 was 61.10% (SE 2.81), at day 9 was 44.12% (SE 4.80), and at day 12 was 50.99% (SE 3.10) (*Figure 3.2A, 3.2B*). These differences were not significant. The number of nuclei per colony in the 21NT cell line at day 3 was 6.44 (SE 0.93), at day 6 it was 12.42 (SE 1.38), at day 9 it was 20.00 (SE 2.95), and at day 12 it was 29.25 (SE 5.82) (*Figure 3.2C*).

3.1.3 Characterization of the 21MT-1 (IDC) cell line

In order to characterize the 21MT-1 cell line, cells were grown on top of 100% Matrigel in a 2% FBS, 2% Matrigel solution for 3, 6, 9, and 12 days; after the specified time point cells were fixed, permeabilized, stained, and imaged using a confocal microscope. The percentage of 21MT-1 colonies that exhibited lumen formation at day 3 was 0% (SE 0), at day 6 was 0.89% (SE 0.45), at day 9 was 4.78% (SE 1.75), and at day 12 was 1.67% (SE 0.67) (*Figure 3.3A, 3.3B*). These differences were not significant. The percentage of 21MT-1 colonies that were polarized at day 3 was 12.80% (SE 1.26), at day 6 was 16.31% (SE 7.38), at day 9 was 19.96% (SE 1.78), and at day 12 was 6.67% (SE 5.44) (*Figure 3.3A, 3.3B*). These differences were not significant. Actin was localized to the cell periphery (not apically oriented) and E-cadherin was localized to the cytoplasmic region of cell (not to the cell to cell junctions). The percentage of 21MT-1 colonies that were spherical (vs. non-spherical) at day 3 was 4.91% (SE 0.22), at day 6

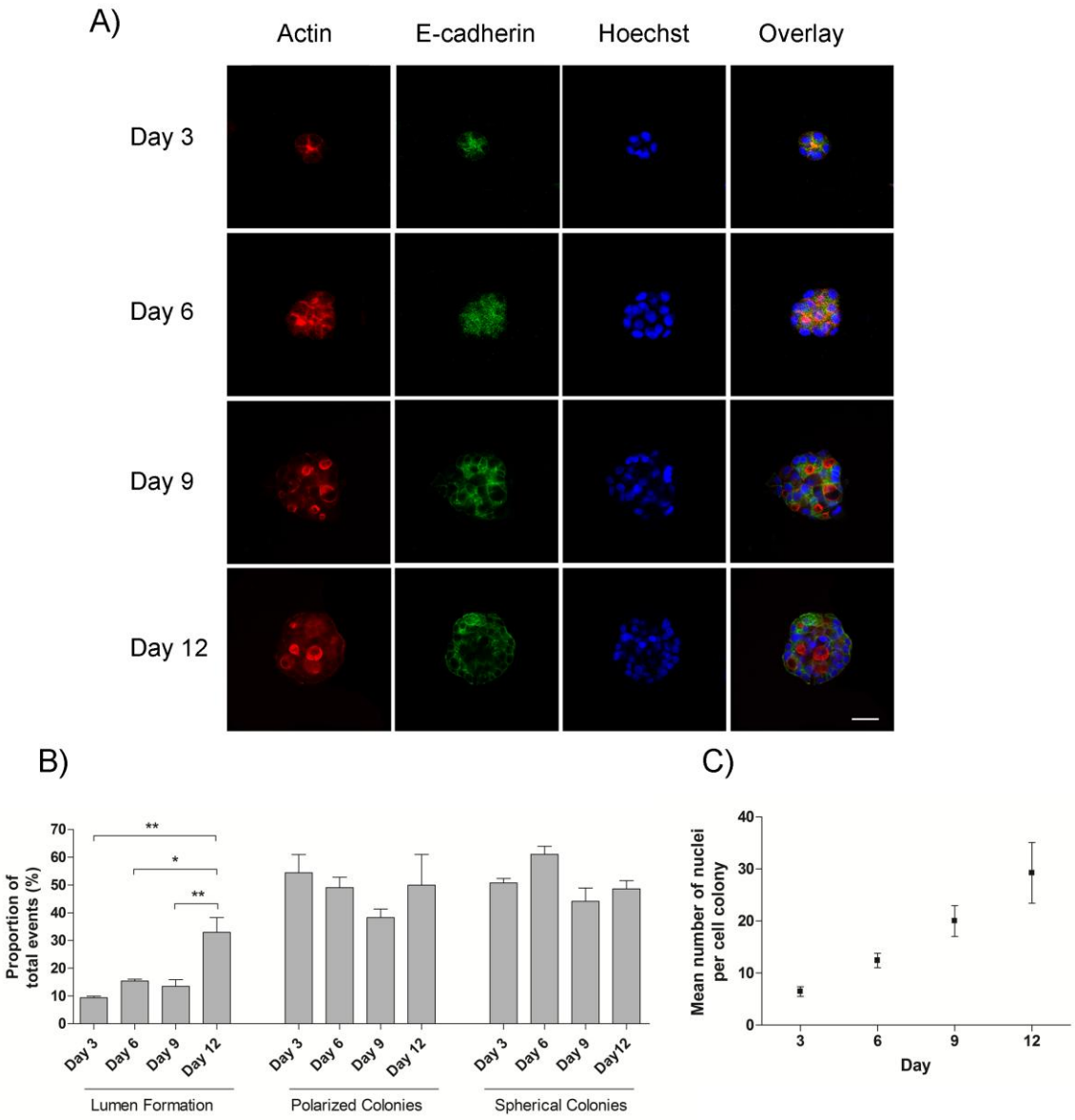

Figure 3.2 Characterization of the 21NT cell line grown in 3D Matrigel. The 21NT cells were grown on top of 100% Matrigel in αHE + 2% FBS and 2% Matrigel for 3, 6, 9, and 12 days. Cell colonies were fixed, permeabilized, stained, and imaged using confocal microscopy. A) Representative cell colonies are shown at each day. Actin is shown in red, E-cadherin is shown in green, and the nuclear stain Hoechst is shown in blue. An overlay of all three channels is shown in the final set of panels. B) The proportion of colonies exhibiting lumen formation is increased from day 3 to day 12, from day 6 to day 12, and from day 9 to day 12. The proportion of polarized colonies and spherical colonies is not different among the days. C) The number of nuclei per colony increased over time. Colony morphology was analyzed using one-way ANOVA followed by Tukey's post hoc test. * $p<0.05$, ** $p< 0.01$. Scale bar represent 30μm.

was 6.67% (SE 4.04), at day 9 was 15.61% (SE 2.57), and at day 12 was 17.08% (SE 3.06) (*Figure 3.3A, 3.3B*). These differences were not significant. The number of nuclei per colony in the 21MT-1 cell line at day 3 was 4.69 (SE 0.42), at day 6 it was 11.39 (SE 1.52), at day 9 it was 27.06 (SE 4.20), and at day 12 it was 56.17 (SE 9.86) (*Figure 3.3C*).

3.1.4 Comparison of each 21T cell line and selecting a suitable endpoint

In order to choose a suitable endpoint for the 3D morphology assay data from sections *3.1.1* to *3.1.3* were reanalyzed with respect to each cell line instead of time. At day 9 (data not shown) and day 12 (*Figure 3.4A*, *3.4B*) each cell line displayed a characteristic morphology with respect to lumen formation, polarized colonies, and spherical colonies. Between the three cell lines, there was an overall decrease in lumen formation, polarized colonies, and spherical colonies from 21PT to 21NT to 21MT-1. There was also an increase in the number of nuclei per cell colony from 21PT to 21NT to 21MT-1 (*Figure 3.4C*). Thus, using the 21T cells in an on-top Matrigel assay to measure 3D morphology yielded comparable results to the embedded method that was previously used in our lab (Souter et al. 2010), but in a quicker, more efficient fashion.

3.2 Objective 2: Test molecular controls of breast cancer progression. Specific aim 1: Determine the role of WNT5A overexpression using the 21T cells lines via stable transfection

WNT5A expression was found to be moderate in 21PT (ADH), low in 21NT (DCIS), and high in 21MT-1 (IDC) (Souter et al. 2010). To determine the functional role

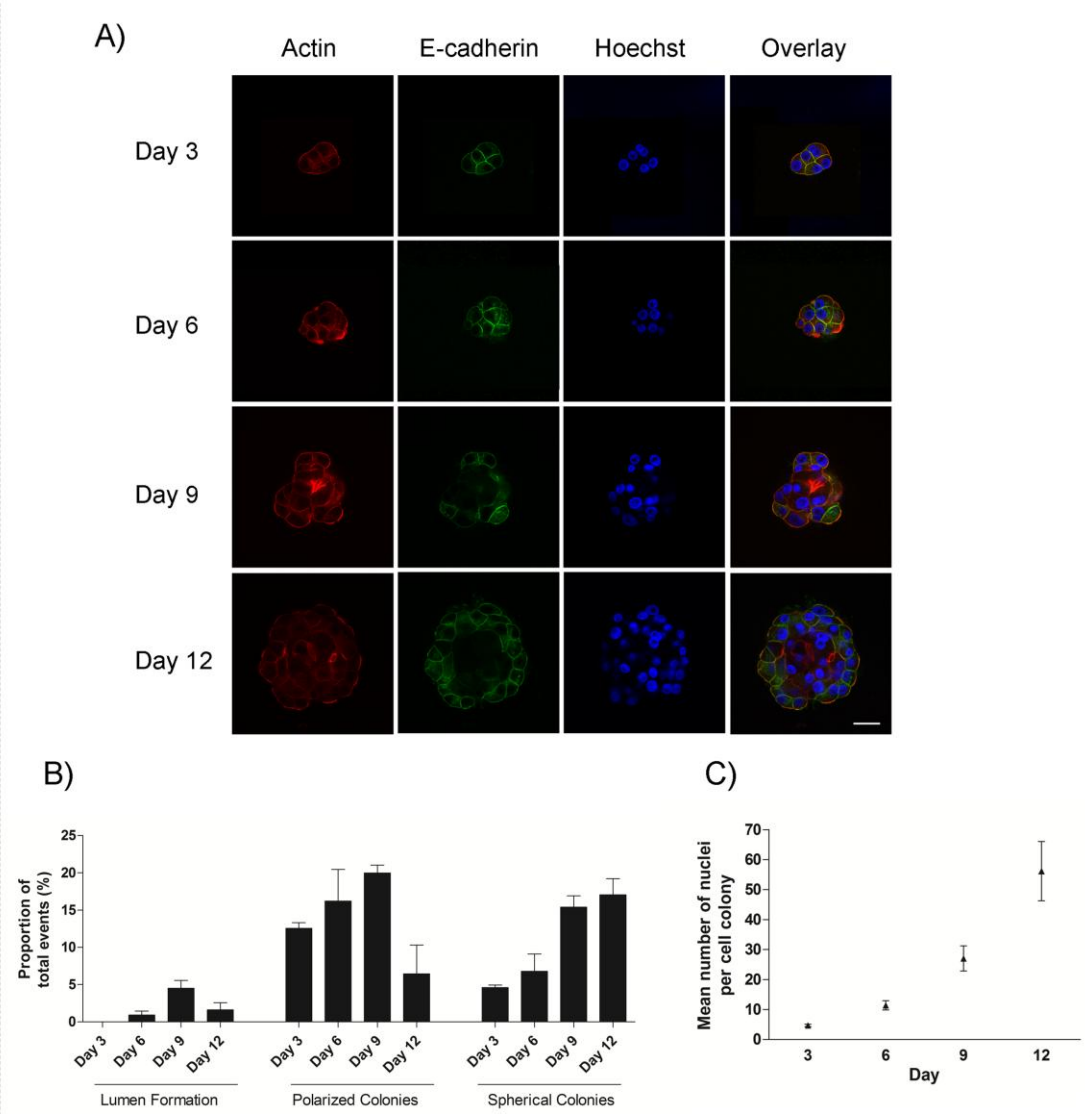

Figure 3.3 Characterization of the 21MT-1 cell line grown in 3D Matrigel. The 21MT cells were grown on top of 100% Matrigel in αHE + 2% FBS and 2% Matrigel for 3, 6, 9, and 12 days. Cell colonies were fixed, permeabilized, stained, and imaged using confocal microscopy. A) Representative cell colonies are shown at each day. Actin is shown in red, E-cadherin is shown in green, and the nuclear stain Hoechst is shown in blue. An overlay of all three channels is shown in the final set of panels. B) The proportion of colonies exhibiting lumen formation, polarization, and sphericalness did not change between any of the days. C) The number of nuclei per colony increased over time. Colony morphology was analyzed using a one-way ANOVA followed by Tukey's post hoc test and $p<0.05$ was considered significant. Scale bar represent 30μm.

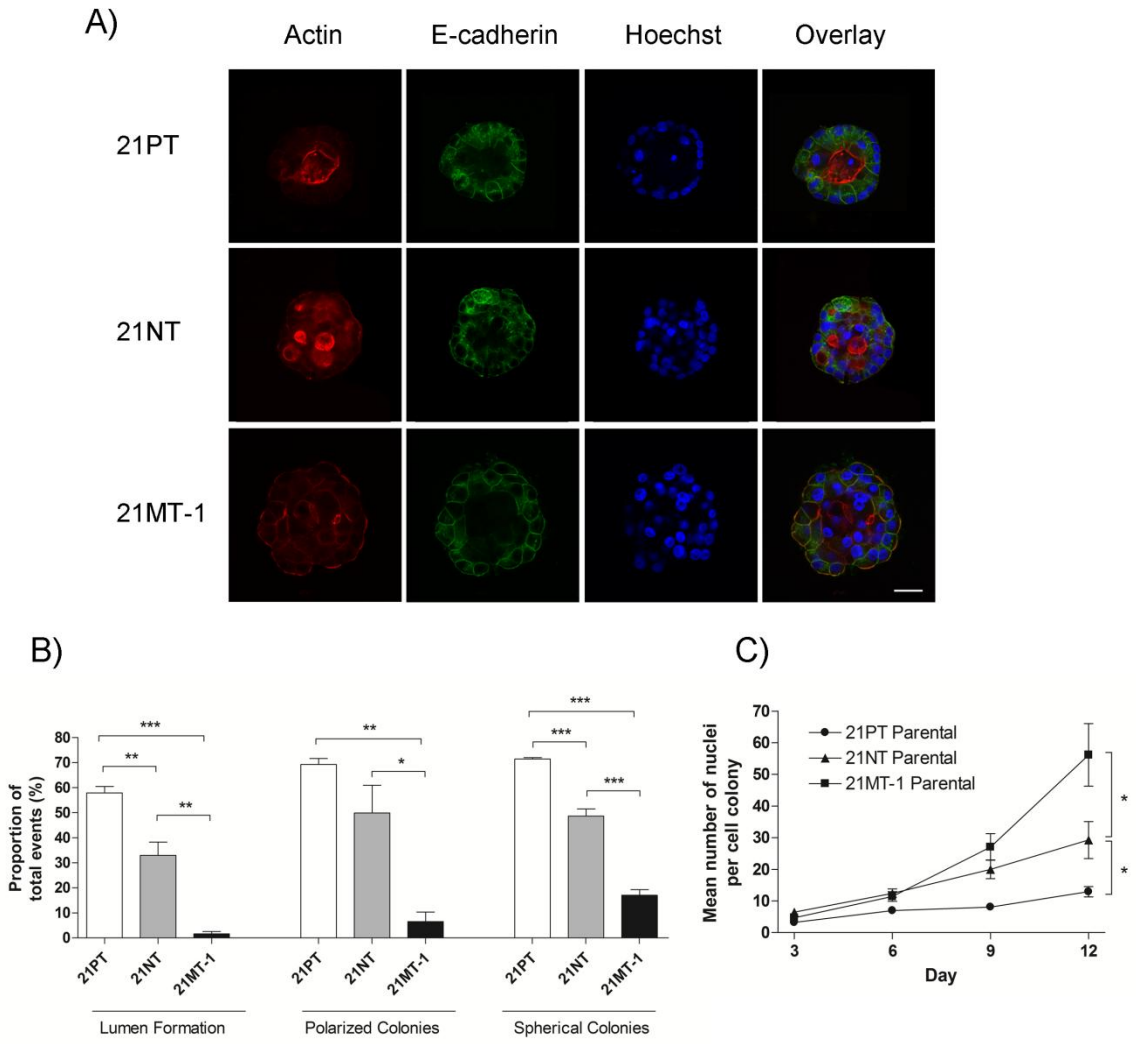

Figure 3.4 21T cell lines form distinct growth patterns in 3D Matrigel after 12 days. The 21MT cells were grown on top of 100% Matrigel in αHE + 2% FBS and 2% Matrigel for 12 days. Cell colonies were fixed, permeabilized, stained, and imaged using confocal microscopy. A) Representative cell colonies are shown at each day. Actin is shown in red; E-cadherin is shown in green; and the nuclear stain Hoechst is shown in blue. An overlay of all three channels is shown in the final set of panels. B) The proportion of colonies exhibiting lumen formation decreased from 21PT to 21NT to 21MT-1, the proportion of polarized colonies decreased from 21NT to 21MT-1, and the proportion of spherical colonies (vs. non-spherical colonies) decreased from 21PT to 21NT to 21MT-1. C) The number of nuclei per colony increased from 21PT to 21NT to 21MT-1. Means were analyzed using one-way ANOVA followed by Tukey's post hoc test and $p<0.05$ was considered statistically significant. *$p<0.05$, ** $p<0.01$, *** $p<0.001$. Scale bar represent 30μm.

of WNT5A in the transition between different stages of breast cancer progression, WNT5A was overexpressed in 21PT and 21NT cells. The 3D morphology and invasive potential of these cell lines were examined.

3.2.1 WNT5A is differentially expressed in the 21T cell lines

WNT5A expression was examined at the mRNA and protein levels in the 21T cell lines. Total RNA was extracted from the 21PT, 21NT and 21MT-1 cell lines and subsequently reverse transcribed into cDNA. Primers specific to WNT5A were used in a qRT-PCR to examine relative levels of WNT5A among the three cell lines. WNT5A mRNA expression is higher in the 21MT-1 cell line compared to both the 21PT and 21NT cell lines by 43.7-fold ($p<0.01$) and 109.1-fold ($p<0.01$) respectively; however, WNT5A mRNA levels were not significantly different between the 21PT and 21NT parental cell lines (*Figure 3.5A*). Protein was extracted from the 21T parental cell lines and analyzed by Western blot with an antibody specific to Wnt5a protein. Wnt5a expression was higher in the 21MT-1 cell line compared to the 21PT and 21NT cell lines. Wnt5a expression levels were higher in the 21MT-1 cell line compared to the 21PT and 21NT cell line by 5.02-fold ($p<0.01$) and 3.78-fold ($p<0.01$) respectively; however, the difference between the expression levels of Wnt5a between 21PT and 21NT was not significant (*Figure 3.5B, 3.5C*).

3.2.2 WNT5A expression is increased in 21PT and 21NT cells after transfection

A WNT5A expression vector containing a myc-His epitope was constructed and transfected into 21PT cells (21PT + WNT5A) and 21NT cells (21NT + WNT5A). The expression vector alone (without WNT5A) was also transfected into 21PT cells (21PT +

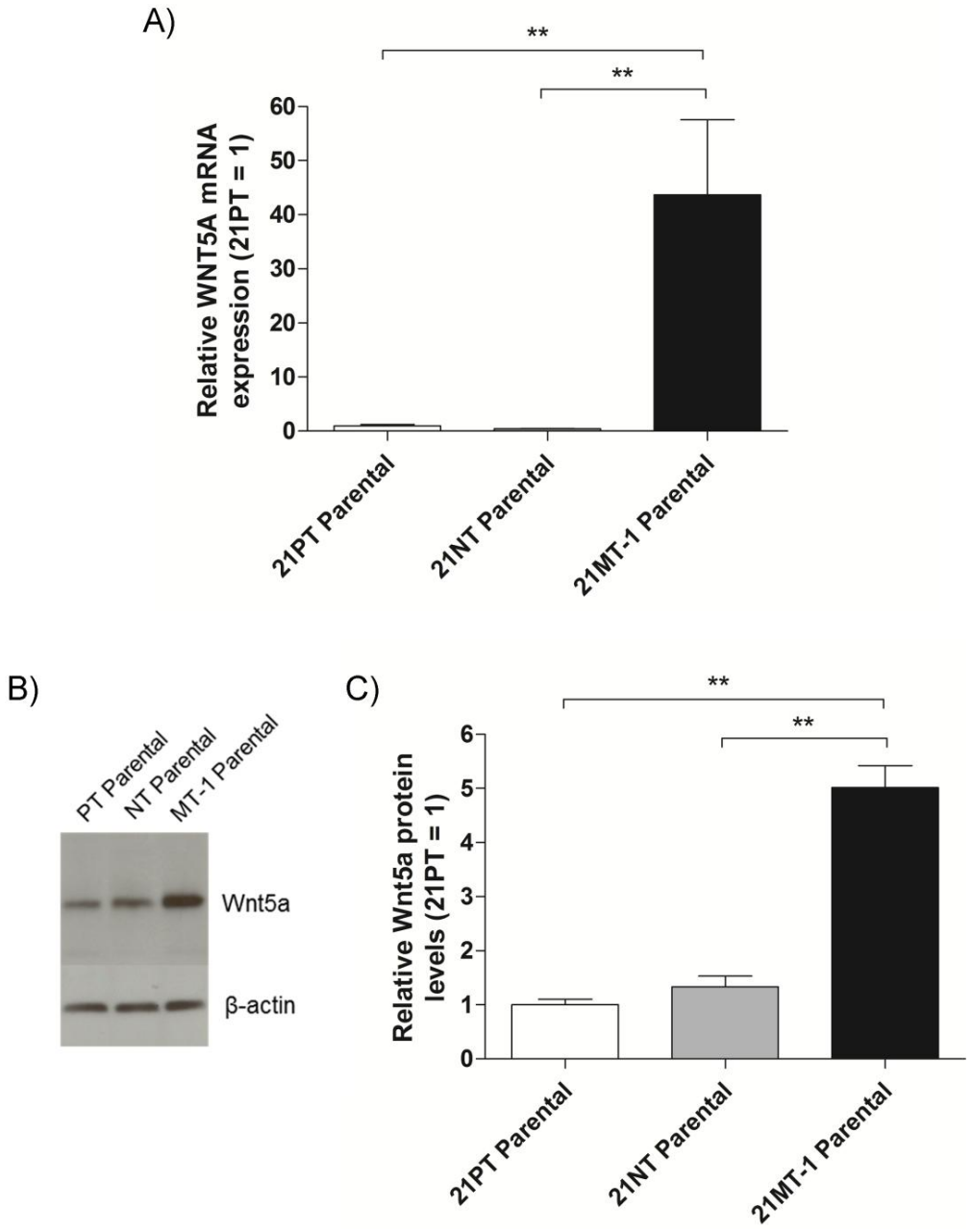

Figure 3.5 WNT5A mRNA and protein levels in the 21T parental cell lines. For ease of comparison, the expression levels for 21PT parental cells were set to 1. A) WNT5A mRNA expression is higher in the 21MT-1 cell line compared to both the 21PT and 21NT cell lines.WNT5A expression was similar in both 21PT and 21NT parental cell lines. mRNA expression levels were calculated as a ratio to the housekeeping gene GAPDH. B, C) Wnt5a protein expression was higher in the 21MT-1 cell line compared to the 21PT and 21NT cell. Wnt5a protein levels were similar in both 21PT and 21NT parental cell lines. Protein levels were calculated as a ratio with β-actin. An ANOVA was performed with Tukey's post hoc test and $p<0.05$ was considered statistically significant. **$p<0.01$.

EV) and 21NT cells (21NT + EV). Both qRT-PCR and Western blot were used to determine if levels of WNT5A were increased in 21PT + WNT5A cells and 21NT + WNT5A cells compared to empty vector controls.

WNT5A mRNA was increased in both the 21PT + WNT5A cells and 21NT + WNT5A cells compared to their respective empty vector controls. WNT5A mRNA was increased in the 21PT + WNT5A cell line by 675-fold compared to 21PT + EV ($p<0.001$). WNT5A mRNA was increased in the 21NT + WNT5A cell line by 272-fold compared to the 21NT + EV cell line ($p<0.001$) (*Figure 3.6A, 3.6B*). Likewise, Wnt5a protein was increased in both the 21PT + WNT5A cells and 21NT + WNT5A cells compared to their respective empty vector controls. In the 21PT + WNT5A cell line, Wnt5a protein was increased 6.02-fold compared to the 21PT + EV cells ($p<0.001$). In the 21NT + WNT5A cell line, Wnt5a protein was increased 6.67-fold compared to the 21NT + EV cells ($p<0.001$) (*Figure 3.6E, 3.6F, 3.6G*). In order to show that the increase in Wnt5a was due to transfection of a WNT5A-myc construct, an anti-myc antibody was used to detect myc epitope expression. The 21PT + WNT5A and 21NT + WNT5A cell lines had myc positivity shown by Western blot at the predicted molecular weight of Wnt5a-myc (*Figure 3.6C, 3.6D*).

3.2.3 WNT5A overexpression increased migration of both 21PT and 21NT cells

To first assess the migratory ability of WNT5A overexpression in the 21T cell lines, the 21PT + WNT5A and 21NT + WNT5A cells were used in a transwell migration assay. 21PT + EV, 21PT + WNT5A, 21NT + EV and 21NT + WNT5A cells were placed in the upper chamber of a transwell migration system (membranes with 8.0μm pores coated with 6μg of gelatin) and allowed to migrate through the pores in order to reach

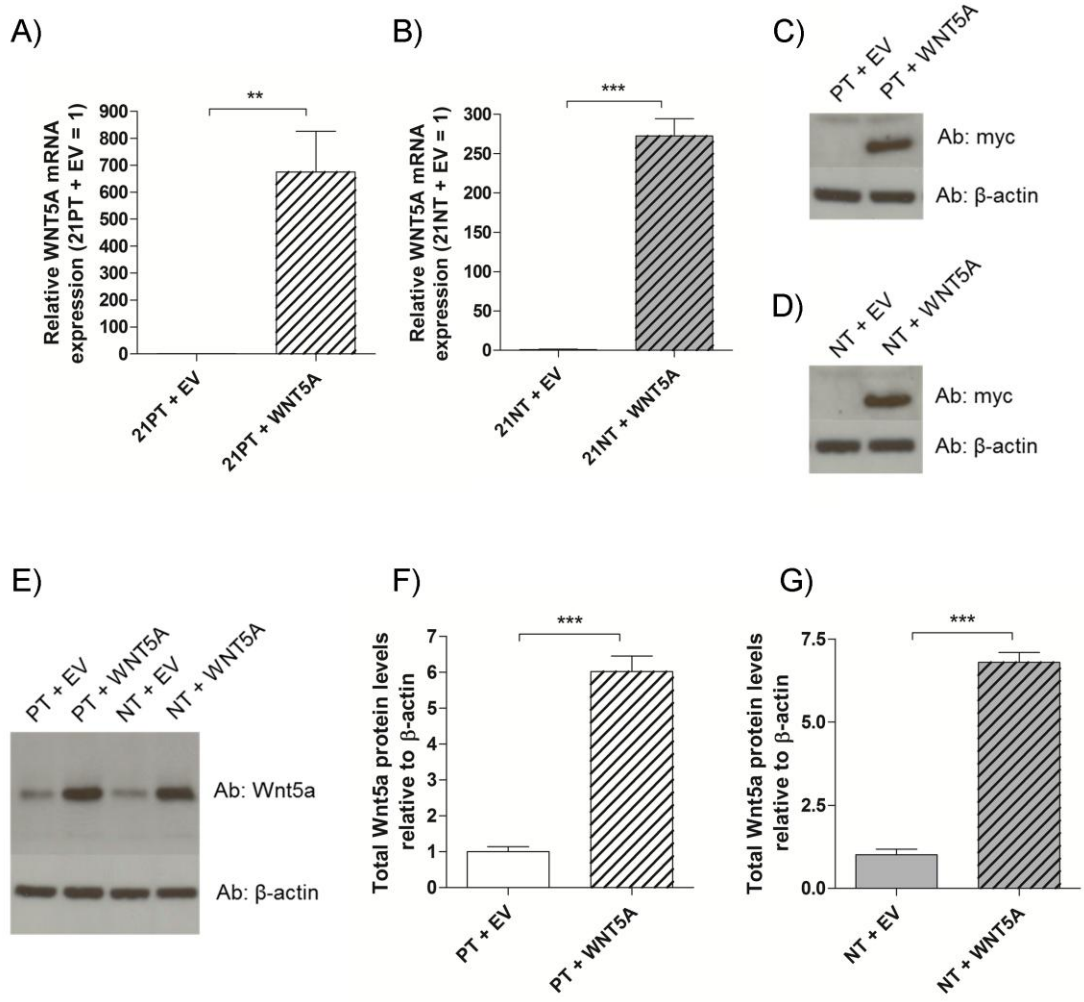

Figure 3.6 WNT5A mRNA and protein levels in the 21T cell lines after transfection with WNT5A-myc. For ease of comparison, the expression levels for 21PT parental cells were set to 1. A, B) WNT5A mRNA expression is increased in the 21PT + WNT5A and 21NT + WNT5A cell lines compared to the respective empty vector controls. mRNA expression levels were calculated as a ratio to the housekeeping gene GAPDH. C, D) Both 21PT + WNT5A and 21NT + WNT5A cell lines are positive for myc protein expression at the predicted molecular weight for a Wnt5a-myc fusion protein. E, F, G) Wnt5a protein expression was increased in the 21PT + WNT5A and the 21NT + WNT5A cell lines compared to the respective empty vector controls. Protein levels were calculated as a ratio to β-actin. To analyze mRNA and protein levels a Student's *t*-test was performed and $p<0.05$ was considered statistically significant. $^{**}p<0.01$, $^{***}p<0.001$.

FBS (chemoattractant) that was present in the lower chamber. WNT5A overexpression increased migration in both 21PT and 21NT cell lines. WNT5A overexpression increased the 21PT cell's ability to migrate from 24.67 (SE 11.84) cells per field of view for the 21PT + EV cell line to 71.00 (SE 2.66) cells per field of view for the 21PT + WNT5A cell line ($p<0.01$) (*Figure 3.7A, 3.7B*). WNT5A overexpression increased the 21NT cells' ability to migrate from 18.47 (SE 0.267) cells per field of view for the 21NT + EV cell line to 147.8 (SE 4.40) cells per field of view for the 21NT + WNT5A cell line ($p<0.001$) (*Figure 3.7A, 3.7B*).

3.2.4 WNT5A overexpression increased invasion of 21NT cells but not of 21PT cells

To assess the invasive ability of WNT5A overexpression in the 21T cell lines, the 21PT + WNT5A and 21NT + WNT5A cells were used in a transwell invasion assay. 21PT + EV, 21PT + WNT5A, 21NT + EV and 21NT + WNT5A cells were placed in the upper chamber of a transwell system (membranes with 8.0μm pores precoated with Matrigel) and allowed to invade through the pores in order to reach FBS (chemoattractant) that was present in the lower chamber. WNT5A overexpression increased invasion in 21NT cell line only. WNT5A overexpression increased the 21NT cell's ability to invade from 31.67 (SE 4.04) cells per field of view in the 21NT + EV cell line to 104.7 (SE 20.13) cells per field of view in the 21NT + WNT5A ($p<0.01$) cell line (*Figure 3.8A, 3.8B*).

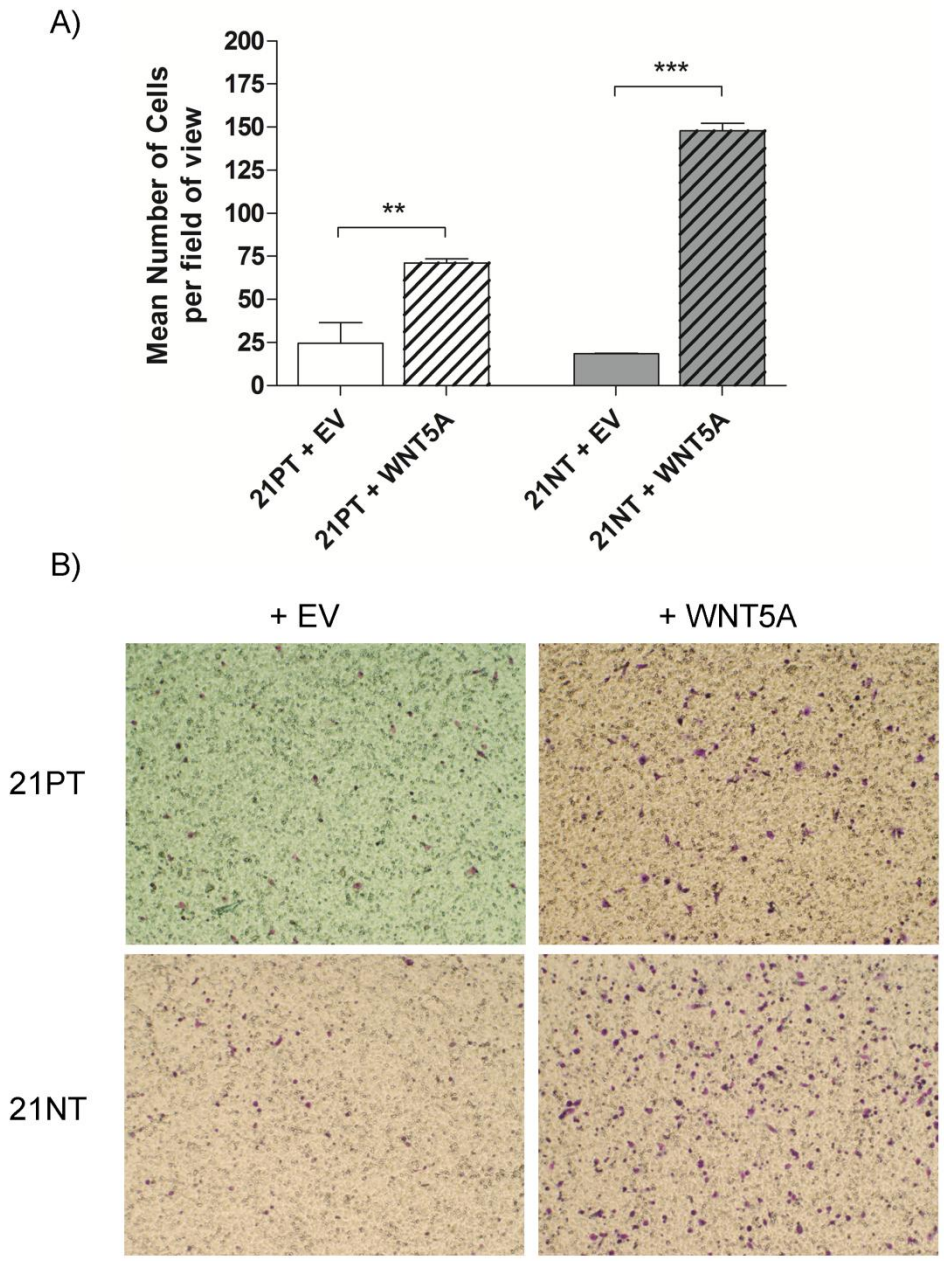

Figure 3.7 WNT5A overexpression increased migration of 21PT and 21NT cells. A) Transwell migration assay using 21PT + EV, 21PT + WNT5A, 21NT + EV, and 21NT + WNT5A cells towards FBS for 5 hours. 21PT + WNT5A cells showed an increase in the number of cell the migrated to the underside of the transwell membranes compared to the empty vector control. Likewise, 21NT + WNT5A cells exhibited an increase in the number of cells that migrated to the underside of the transwell membrane compared to the empty vector control. B) Representative images used for counting the number of cells per field of view. To analyze migration a one-way ANOVA was performed with Tukey's post hoc test and $p<0.05$ was considered statistically significant. **$p<0.01$, ***$p<0.001$.

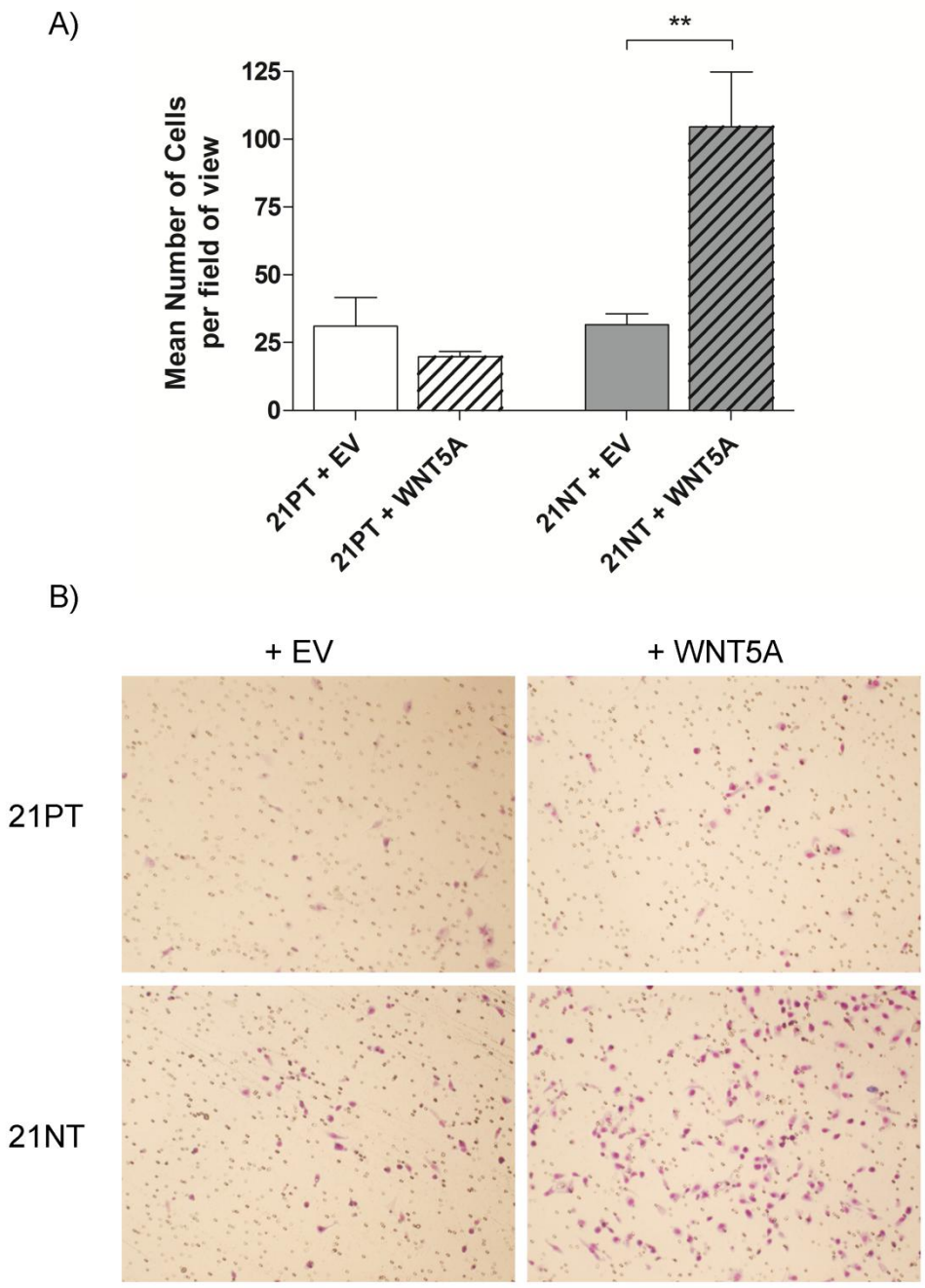

Figure 3.8 WNT5A overexpression increased invasion of 21NT cells but not of 21PT cells. A) Transwell invasion assay using 21PT + EV, 21PT + WNT5A, 21NT + EV, and 21NT + WNT5A cells towards FBS for 20 hours. 21NT + WNT5A cells showed an increase in the number of cells that invaded to the underside of the transwell membrane compared to the empty vector control. However, WNT5A overexpression did not increase invasion of 21PT cells. B) Representative images used for counting the number of cells per field of view. To analyze invasion a one-way ANOVA was performed with Tukey's post hoc test and $p<0.05$ was considered statistically significant. **$p<0.01$, ***$p<0.001$.

3.2.5 WNT5A overexpression decreased the percentage of spherical colonies formed by 21NT cells but had no effect on 3D morphology of 21PT cells

The 3D morphology of the 21PT and 21NT transfectants was assessed using the modified 3D morphology assay described in *Section 3.1*. The 21PT + EV, 21PT + WNT5A, 21NT + EV, and 21NT + WNT5A were grown on top of 100% Matrigel in a αHE media containing 2% Matrigel and 2% FBS for 12 days. WNT5A overexpression had no effect on 3D morphology with respect to lumen formation and polarized colonies in either cell line. However, WNT5A overexpression decreased the percentage of colonies that were spherical in 21NT cells only. The percentage of spherical colonies decreased from 37.37% (SE 5.00) in 21NT + EV cells to 22.26% (SE 1.46) in 21NT + WNT5A cells ($p<0.05$) (*Figure 3.9A, 3.9B*). There was no effect on the number of nuclei per cell colony after WNT5A overexpression (*Figure 3.9C*).

3.2.6 WNT5A overexpression increased total RHOA expression and shRNA targeting RHOA reduced its expression in 21PT cells

To investigate the functional response of WNT5A overexpression in 21PT cells, the downstream effector RHOA was examined. Overexpression of WNT5A in 21PT cells increased the expression of RHOA at the mRNA level. RHOA expression was increased by 1.75-fold ($p<0.01$) (*Figure 3.10*). To determine if WNT5A-induced RHOA expression plays a functional role in 21PT cell migration or invasion, RHOA expression was knocked down using a panel of three short hairpin RNAs (Table 2.2). RHOA mRNA knockdown was achieved for one of the three shRNAs in 21PT + WNT5A cells. RHOA expression was decreased to a level similar to 21PT + EV cells, compared to an off target knockdown control (21PT + WNT5A + Luciferase shRNA) (*Figure 3.10*).

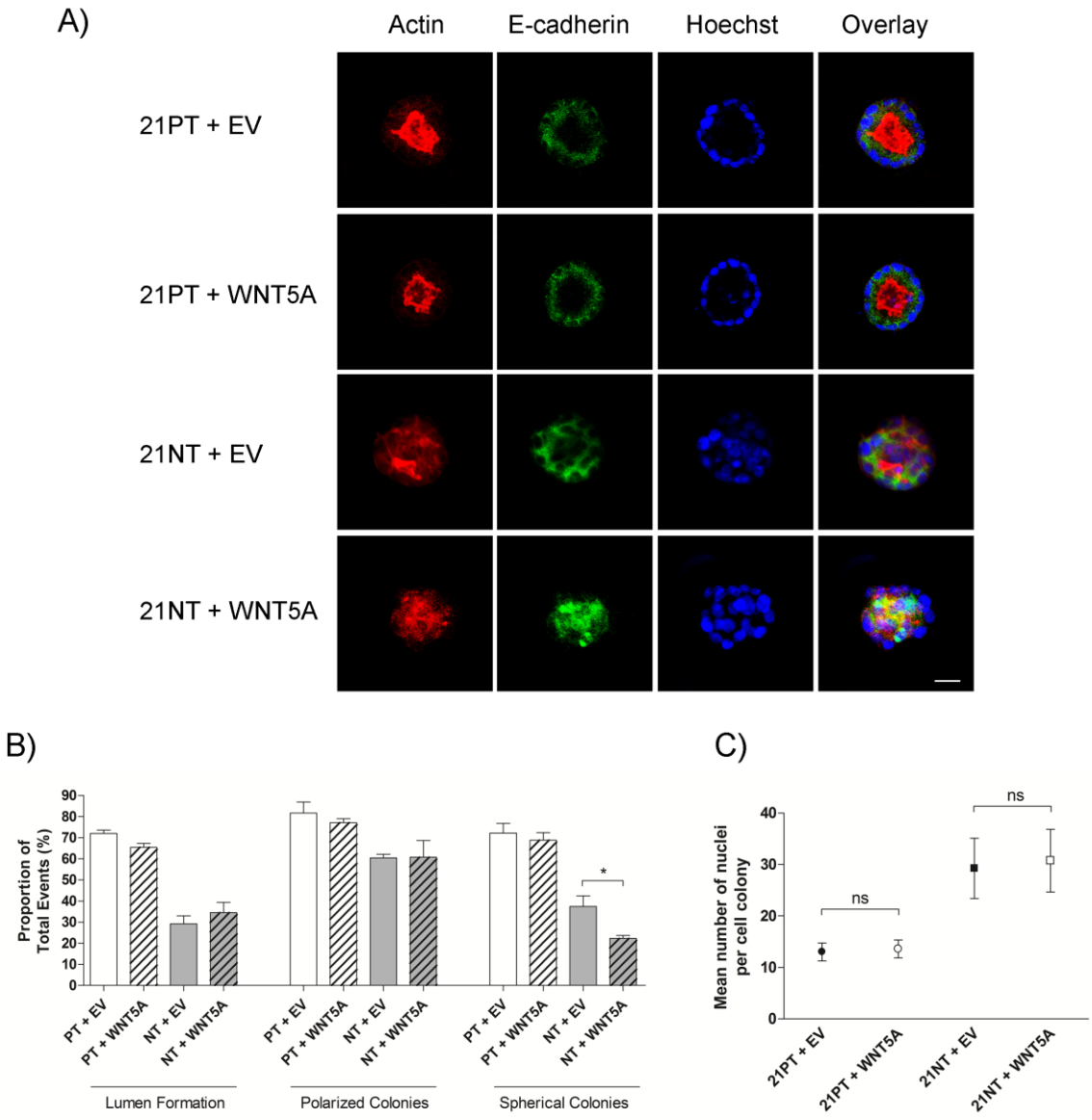

Figure 3.9 WNT5A overexpression decreased the proportion of spherical colonies formed by 21NT cells and had no effect on colony morphology of 21PT cells. The 21PT + EV, 21PT + WNT5A, 21NT + EV, and 21NT + WNT5A cells were grown on top of 100% Matrigel in a αHE + 2% FBS and 2% Matrigel 12 days. Cell colonies were fixed, permeabilized, stained, and imaged using confocal microscopy. A) Representative cell colonies are shown at each day. Actin is shown in red, E-cadherin is shown in green, and the nuclear stain Hoechst is shown in blue. An overlay of all three channels is shown in the final set of panels. B) There was a decrease in the proportion of spherical colonies formed by 21NT cells when overexpressing WNT5A. C) WNT5A overexpression had no effect on the number of nuclei per cell colony. Data regarding colony morphology and nuclei were analyzed using one-way ANOVA followed by Tukey's post hoc test and $p<0.05$ was considered statistically significant. *$p<0.05$. Scale bar represents 30μm.

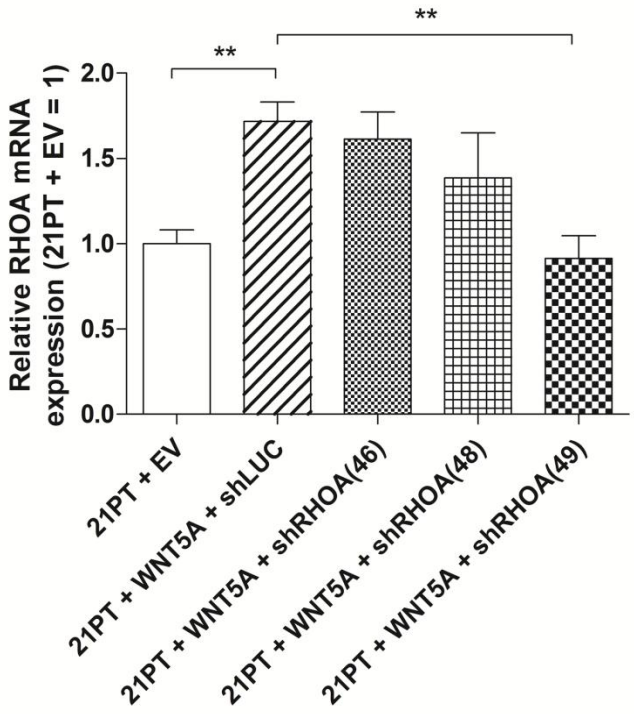

Figure 3.10 WNT5A overexpression increases total RHOA expression and shRNA targeting RHOA reduces its expression in the 21PT cell line. After overexpression of WNT5A in the 21PT cell line that was an increase in the expression of total RHOA at the mRNA level. RHOA expression was knocked down using a panel of three shRNAs. RHOA mRNA knockdown was achieved in one of the three shRNAs in the 21PT + WNT5A cell line to a level similar to 21PT + EV compared to an off target knockdown control (21PT + WNT5A + Luciferase shRNA). mRNA expression was analyzed using one-way ANOVA followed by Tukey's post hoc test and $p<0.05$ was considered statistically significant. **$p<0.01$.

3.2.7 RHOA knockdown reduced WNT5A-induced migration but had no effect on invasion of 21PT cells

To assess the change in migration due to RHOA knockdown in 21PT + WNT5A cells, transwell migration assays were used. 21PT + EV, 21PT + WNT5A + shRHOA, and 21PT + WNT5A + shLUC cells were placed in the upper chamber of a transwell migration system and allowed to migrate through the pores in order to reach FBS (chemoattractant) that was present in the lower chamber. RHOA knockdown decreased migration of 21PT + WNT5A cells from 59.33 (SE 9.53) cells per field of view to 15.00 (SE 0.58) cells per field of view ($p<0.01$), a level similar to that of 21PT + EV (*Figure 3.11A, 3.11C*). To assess the change in invasion due to RHOA knockdown in 21PT + WNT5A cells, transwell invasion assays were again used. 21PT + EV, 21PT + WNT5A + shRHOA, and 21PT + WNT5A + shLUC cells were placed in the upper chamber of the transwell invasion system (membranes precoated with Matrigel) and allowed to invade through the pores in order to reach FBS (chemoattractant) that was present in the lower chamber. There was no difference in invasion between these three cell lines (*Figure 3.11B, 3.11C*).

3.2.8 WNT5A overexpression increased RHOA expression and shRNA targeting RHOA reduced its expression in 21NT cells

To similarly investigate the functional response to WNT5A overexpression in 21NT cells, the downstream effector RHOA was again examined in these cells. Overexpression of WNT5A in the 21NT cell line increased the expression of RHOA at the mRNA level by 1.77-fold ($p<0.01$) (*Figure 3.12*). To determine if WNT5A induced RHOA expression plays a functional role in 21NT cell migration or invasion, RHOA expression was knocked down using the same panel of three short hairpin RNAs used in

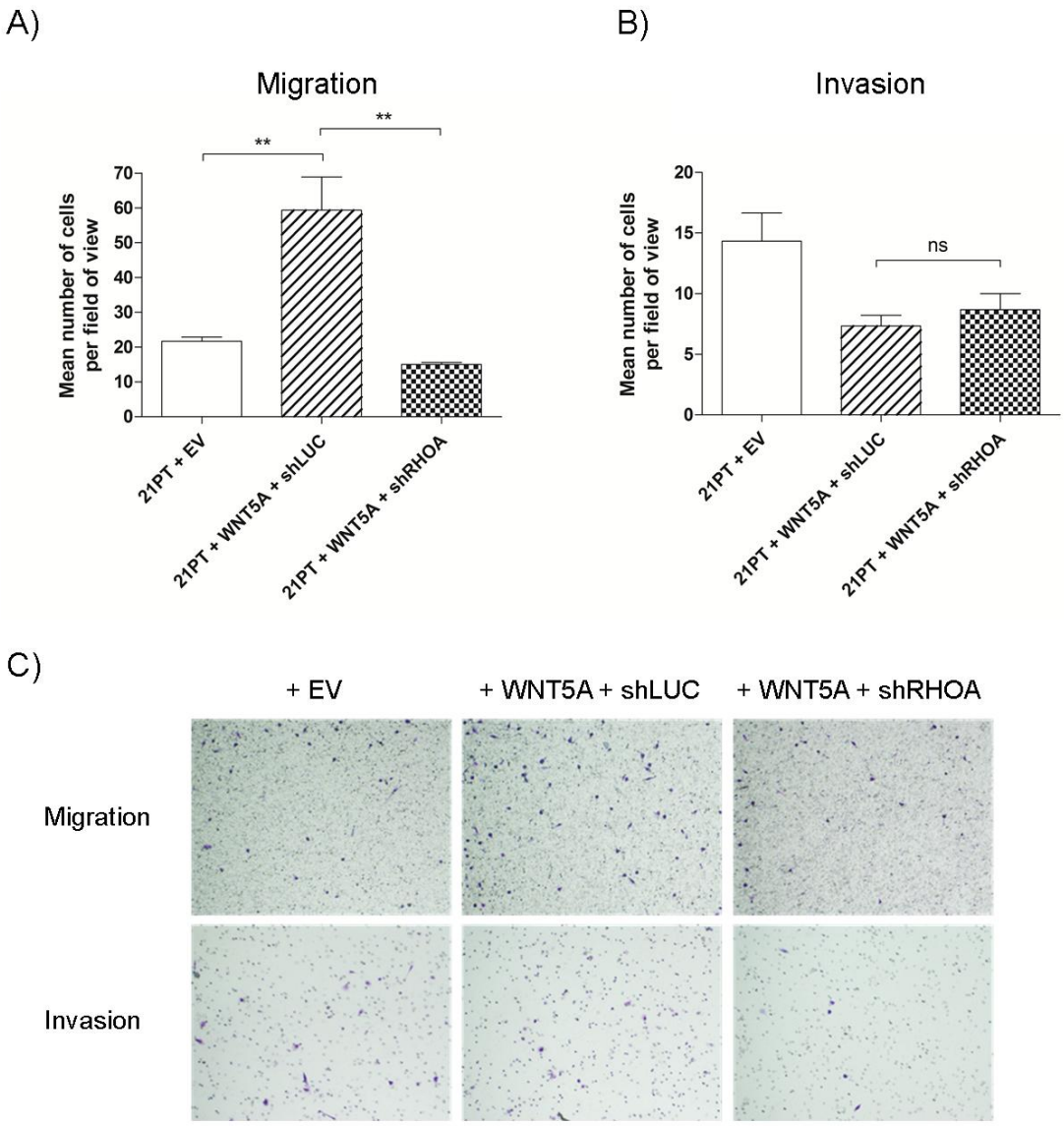

Figure 3.11 RHOA knockdown reduced the WNT5A induced increase in migration but had no effect on invasion of 21PT cells. A) Transwell migration assay using 21PT + EV, 21PT + WNT5A + shLUC, and 21PT + WNT5A + shRHOA cells towards FBS for 5 hours. Knockdown of RHOA in 21PT + WNT5A cells decreased migration to levels similar to 21PT + EV. Such an effect was not seen using an off target knockdown. B) Transwell invasion assay using 21PT + EV, 21PT + WNT5A + shLUC, and 21PT + WNT5A + shRHOA cells towards FBS for 20 hours. Knockdown of RHOA in 21PT + WNT5A cells had no effect on invasion. C) Representative images used for counting the number of cells per field of view. To analyze the number of cells per field of view a one-way ANOVA was performed with Tukey's post hoc test and $p<0.05$ was considered statistically significant. **$p<0.01$.

21PT cells (Table 2.2). RHOA mRNA knockdown was achieved using two of the three shRNAs in 21NT + WNT5A cells. In the most effective knockdown, RHOA expression was decreased to a level lower than the 21NT + EV compared to an off target knockdown control (21NT + WNT5A + Luciferase shRNA) (*Figure 3.12*).

3.2.9 RHOA knockdown reduced WNT5A-induced migration and invasion of 21NT cells

To assess the change in migration due to RHOA knockdown in 21NT cells overexpressing WNT5A, transwell migration assays were used. 21NT + EV, 21NT + WNT5A + shRHOA, and 21NT + WNT5A + shLUC cells were placed in the upper chamber of a transwell migration system and allowed to migrate through the pores in order to reach FBS (chemoattractant) that was present in the lower chamber. RHOA knockdown decreased migration of 21NT + WNT5A cells from 240.0 (SE 41.63) cells per field of view to 106.7 (SE 6.88) cells per field of view ($p<0.05$), a level similar to 21NT + EV (*Figure 3.13A, 3.13C*). To assess the change in invasion due to RHOA knockdown in 21NT cells overexpressing WNT5A, transwell invasion assays were again used. 21NT + EV, 21NT + WNT5A + shRHOA, and 21NT + WNT5A + shLUC cells were placed in the upper chamber of a transwell invasion system and allowed to invade through the pores in order to reach FBS (chemoattractant) that was present in the lower chamber. RHOA knockdown decreased invasion of 21NT + WNT5A cells from 152.7 (SE 9.49) cells per field of view to 102.3 (SE 13.68) cells per field of view ($p<0.05$), to a level that was still higher than 21NT + EV ($p<0.01$) (*Figure 3.13B, 3.13C*).

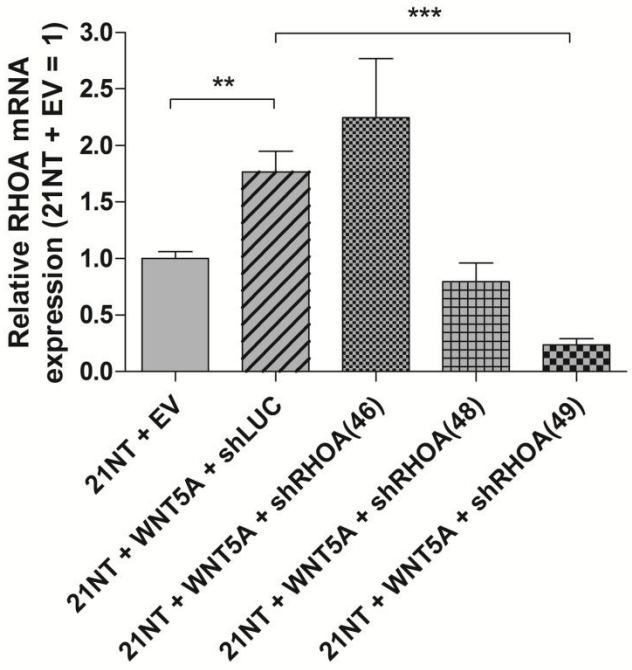

Figure 3.12 WNT5A overexpression increased RHOA expression and shRNA targeting RHOA reduced its expression in 21NT cells. After overexpression of WNT5A in 21NT cells there was an increase in the expression of RHOA at the mRNA level. RHOA expression was knocked down using a panel of three shRNAs. RHOA mRNA knockdown was achieved in 21NT + WNT5A cells using two of the three shRNAs to a level similar to or less than 21NT + EV. No significant effect was seen using an off target knockdown control (21NT + WNT5A + Luciferase shRNA). mRNA expression was analyzed using one-way ANOVA followed by Tukey's post hoc test and $p<0.05$ was considered statistically significant. **$p<0.01$, ***$p<0.001$.

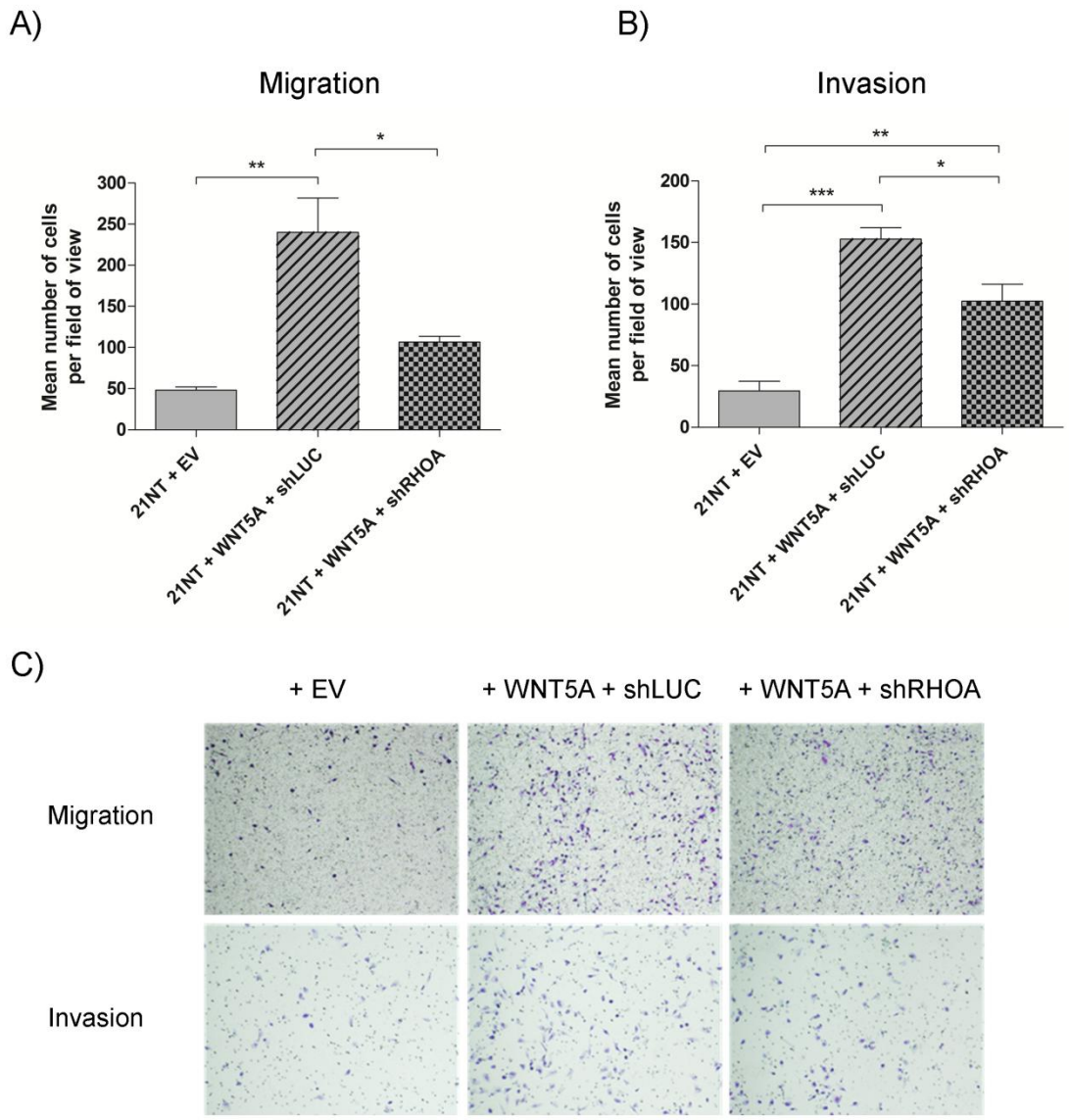

Figure 3.13 RHOA knockdown reduced the WNT5A-induced increase in migration and partially reduced WNT5A-induced invasion of 21NT cells. A) Transwell migration assay using 21NT + EV, 21NT + WNT5A + shLUC, and 21NT + WNT5A + shRHOA cells towards FBS for 5 hours. Knockdown of RHOA in 21NT + WNT5A cells decreased migration to a level similar to 21NT + EV. In contrast, no significant effect was seen using the off target knockdown control. B) Transwell invasion assay using 21NT + EV, 21NT + WNT5A + shLUC, and 21NT + WNT5A + shRHOA cells towards FBS for 20 hours. Knockdown of RHOA in 21NT + WNT5A cells partially decreased WNT5A-induced invasion, whereas no significant effect was seen using the off target knockdown control. C) Representative images used for counting the number of cells per field of view. To analyze the number of cells per field of view a one-way ANOVA was performed with Tukey's post hoc test and $p<0.05$ was considered statistically significant. *$p<0.05$, **$p<0.01$, ***$p<0.001$.

3.3 Objective 2: Test molecular controls of breast cancer progression. Specific aim 2: Determine the role of VANGL1 overexpression using the 21T cell lines via stable transfection

VANGL1 expression was previously found to be low in 21PT (ADH) and significantly higher in both 21NT (DCIS) and 21MT-1 (IDC) (Souter et al. 2010). To determine if VANGL1 plays a functional role in early breast cancer progression, VANGL1 was overexpressed in 21PT cells. The 3D morphology and invasive and migratory abilities of these cell lines were examined.

3.3.1 VANGL1 is differentially expressed in the 21T cell lines

VANGL1 mRNA expression was examined in the 21T cell lines. Total RNA was extracted from the 21PT, 21NT and 21MT-1 cell lines and subsequently reverse transcribed into cDNA. Primers specific to VANGL1 were used in a qRT-PCR to examine relative levels of VANGL1 among the three cell lines. VANGL1 mRNA expression was higher in the 21MT-1 cell line compared to both the 21PT and 21NT cell lines by 2.27-fold ($p<0.001$) and 2.48-fold ($p<0.001$) respectively; however, VANGL1 mRNA levels were not found to be significantly different between the 21PT and 21NT parental cell lines (*Figure 3.14*).

3.3.2 VANGL1 mRNA expression was increased in 21PT cells after transfection

A VANGL1 expression vector containing a myc-His epitope was constructed and transfected into 21PT cells (21PT + VANGL1-myc). An expression vector containing only the full length version of VANGL1 (without the myc-His epitope) was also

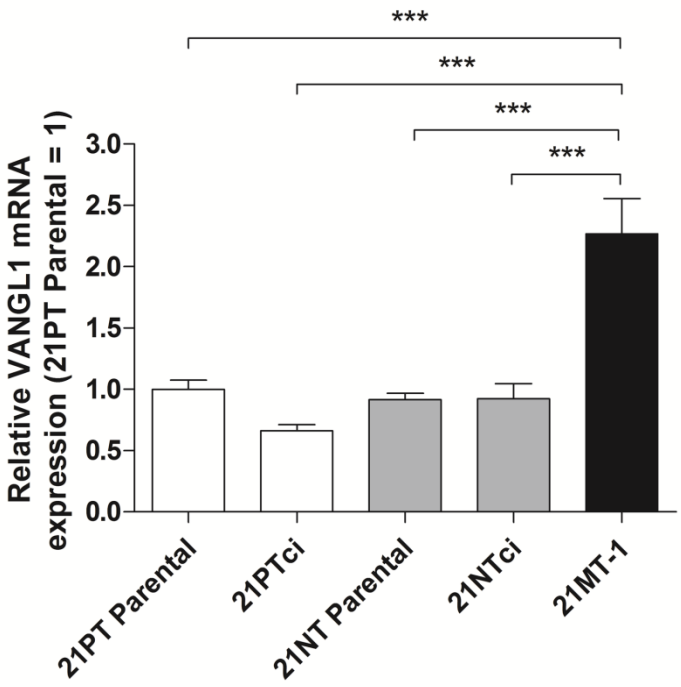

Figure 3.14 VANGL1 mRNA levels in the 21T parental and derivative cell lines. For ease of comparison, the expression level for 21PT parental cells was set to 1. VANGL1 mRNA expression is increased in the 21MT-1 parental cell line compared to both the 21PT and 21NT cell lines as well as the 21PTci and 21NTci cells. VANGL1 expression was similar in the 21PT and 21NT parental cell lines and the 21PTci and 21NTci cells. mRNA expression levels were calculated as a ratio to the housekeeping gene GAPDH. To analyze mRNA expression a one-way ANOVA was performed with Tukey's post hoc test and $p<0.05$ was considered statistically significant. ***$p<0.001$.

constructed and transfected into 21PT cells (21PT + VANGL1-stop). The expression vector alone (without VANGL1) was also transfected into 21PT cells (21PT + EV). qRT-PCR was used to determine if levels of VANGL1 were increased in 21PT + VANGL1-myc and 21PT + VANGL1-stop cells compared to empty vector controls. VANGL1 mRNA was increased in the 21PT + VANGL1-myc cells by 8.12-fold (SE 0.92) compared to 21PT + EV ($p<0.001$) and increased in the 21PT + VANGL1-stop by 8.46-fold (SE 0.87) compared to 21PT + EV ($p<0.001$) (*Figure 3.15A*). The 21PT + VANGL1-myc cell line had myc positivity shown by Western blot (*Figure 3.15B*). Additionally, VANGL1 mRNA expression was not increased in 21PT + WNT5A cells compared to the empty vector control (i.e. overexpression of transfected WNT5A did not increase expression of endogenous VANGL1, *Figure 3.15A*).

3.3.3 VANGL1 overexpression increased migration but had no effect on invasion in 21PT cells

To first assess the migratory ability of VANGL1 overexpression in 21PT cells, transwell migration assays were used. 21PT + EV, 21PT + VANGL1-myc, and 21PT + VANGL1-stop cells were placed in the upper chamber of a transwell migration system and allowed to migrate through the pores in order to reach FBS that was present in the lower chamber. VANGL1 overexpression increased 21PT cells' ability to migrate from 19.37 (SE 1.76) cells per field of view in 21PT + EV cells to 62.27 (SE 10.16) cells per field of view for 21PT + VANGL1-myc cells ($p<0.05$) and to 87.53 (SE 6.58) cell per field of view for 21PT + VANGL1-stop ($p<0.01$) (*Figure 3.16A, 3.16C*). To assess the invasive ability of VANGL1 overexpression in 21PT cells, 21PT + VANGL1 cell lines were used in a transwell invasion assay. 21PT + EV, 21PT + VANGL1-myc, and 21PT + VANGL1-stop cells were placed in the upper chamber of a transwell system and allowed

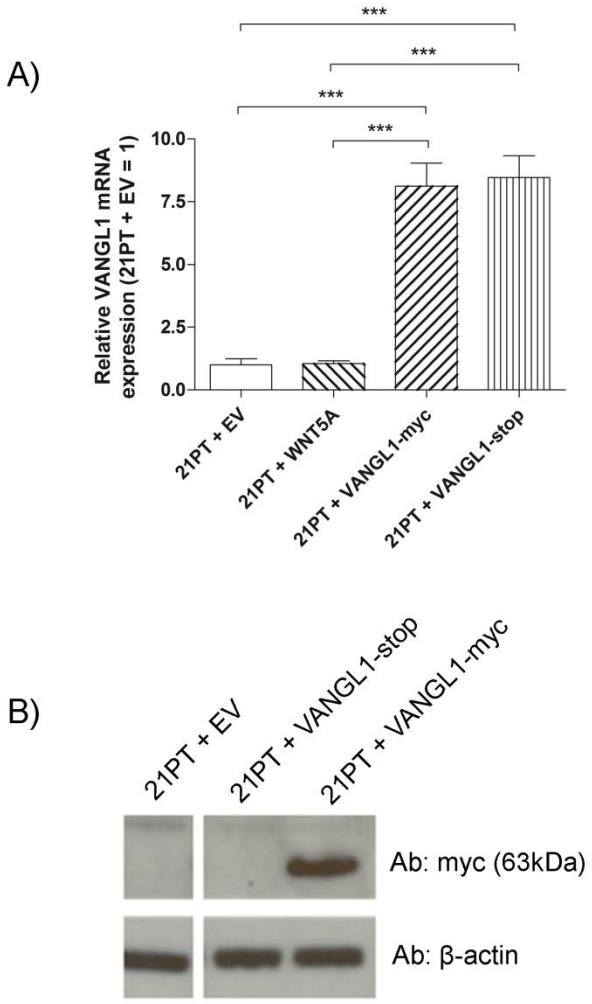

Figure 3.15 VANGL1 levels in 21PT cells after transfection with VANGL1-myc and VANGL1-stop. For ease of comparison, the expression level for 21PT + EV cells was set to 1. A) VANGL1 mRNA expression was increased in the 21PT + VANGL1-myc and 21NT + VANGL1-stop cells compared to an empty vector control and 21PT + WNT5A. mRNA expression levels were calculated as a ratio to the housekeeping gene GAPDH. B) 21PT + VANGL1-myc cells were positive for myc protein by Western blotting for myc protein expression at the predicted molecular weight for a Vangl1-myc fusion protein. To analyze mRNA expression a one-way ANOVA was performed with Tukey's post hoc test and $p<0.05$ was considered statistically significant. ***$p<0.001$.

to invade through the pores in order to reach FBS that was present in the lower chamber. VANGL1 overexpression did not change the number of cells that invaded through the membrane (*Figure 3.16B, 3.16C*).

3.3.4 VANGL1 overexpression did not change 3D morphology or growth of 21PT cells

The 3D morphology of the 21PT transfectants was assessed using the modified 3D morphology assay described in section 3.1. The 21PT + VANGL1-myc, 21PT + VANGL1-stop, and 21PT + EV cells were grown on top of 100% Matrigel in αHE media containing 2% Matrigel and 2% FBS for 12 days. VANGL1 overexpression had no effect on 3D morphology with respect to lumen formation, polarized colonies, and spherical colonies in either cell line compared to the empty vector control (*Figure 3.17A, 3.17B*). Overexpression of VANGL1 in 21PT cells did not have an effect on the number of nuclei per cell colony (*Figure 3.17C).*

3.3.5 Recombinant Wnt5a protein increased migration but did not increase invasion of 21PT + EV and 21PT + VANGL1 cells

To test the effect of both VANGL1 and WNT5A on breast cancer progression, recombinant Wnt5a protein was used as a treatment on 21PT cells that already overexpress VANGL1. To first assess treatment of recombinant Wnt5a on VANGL1 overexpressing cells, the 21PT + EV and 21PT + VANGL1 cells were placed in the upper chamber of a transwell migration system (membranes with 8.0μm pores coated with 6μg of gelatin) and allowed to migrate through the pores in order to reach FBS (chemoattractant) that was present in the lower chamber. Each cell line was treated with 0, 150, 300, and 600ng/mL recombinant Wnt5a. There was an increase in migration in both cell lines only when 600ng/mL recombinant Wnt5a was used (data not shown). Thus

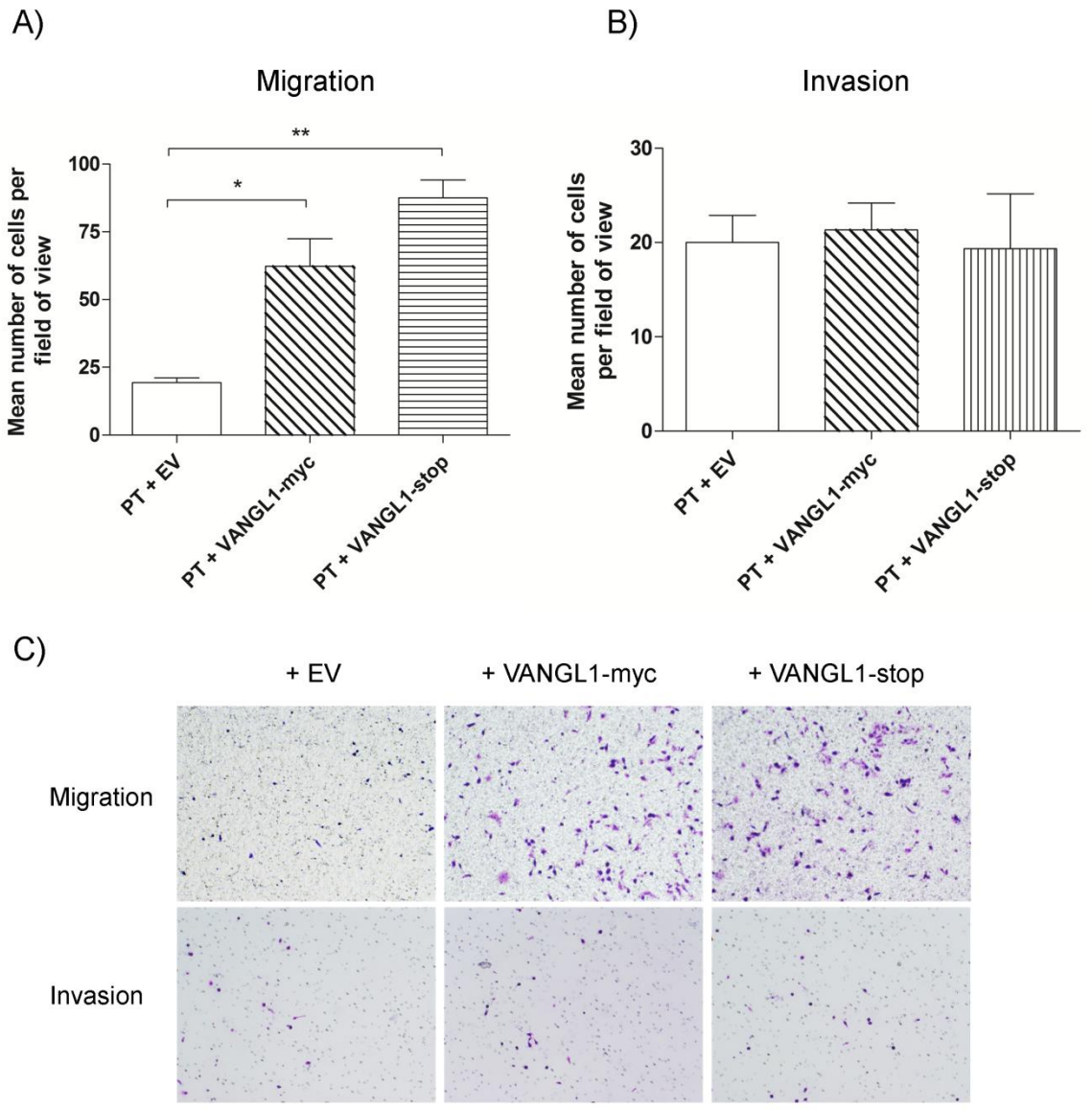

Figure 3.16 VANGL1 overexpression increased migration but not invasion of 21PT cells. A) Transwell migration assay using 21PT + EV, 21PT + VANGL1-myc, and 21PT + VANGL1-stop cells towards FBS for 5 hours. Both 21PT + VANGL1-myc and 21PT + VANGL1-stop cell lines exhibited an increase in the number of cells that migrated to the underside of the transwell membranes compared to 21PT + EV. C) Transwell invasion assay using 21PT + EV, 21PT + VANGL1-myc, and 21PT + VANGL1-stop cells towards FBS for 20 hours. Overexpression of VANGL1 had no effect on invasion of 21PT cells C) Representative images used for counting the number of cells per field of view. To analyze the number of cells per field of view a one-way ANOVA was performed with Tukey's post hoc test and $p<0.05$ was considered statistically significant. *$p<0.05$, **$p<0.01$.

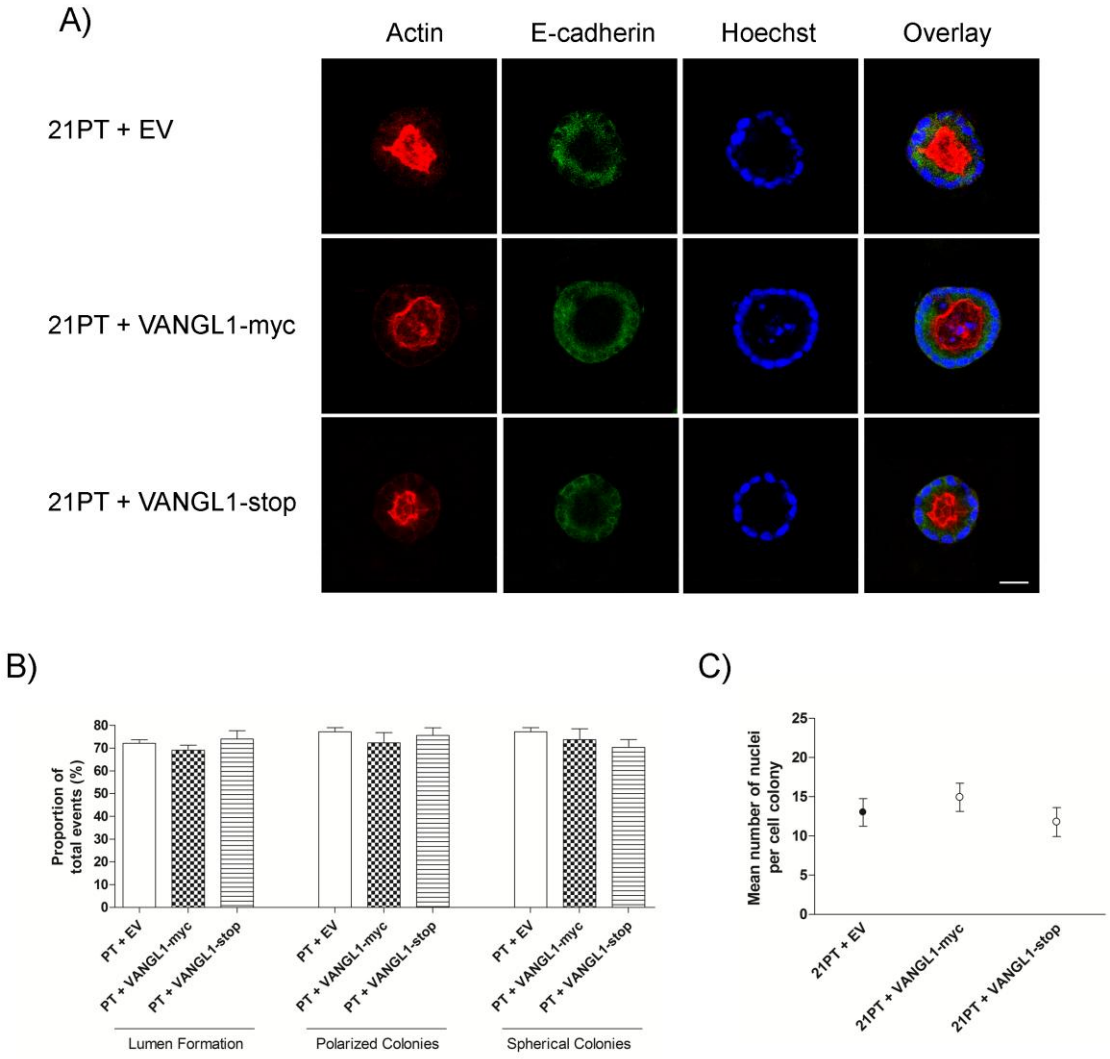

Figure 3.17 VANGL1 overexpression had no effect on the 3D morphology or growth of 21PT cells. The 21PT + EV, 21PT + VANGL1-myc, and 21PT + VANGL1-stop cells were grown on top of 100% Matrigel in αHE + 2% FBS and 2% Matrigel for 12 days. Cell colonies were fixed, permeabilized, stained, and imaged using confocal microscopy. A) Representative cell colonies are shown at each day. Actin is shown in red, E-cadherin is shown in green, and the nuclear stain Hoechst is shown in blue. An overlay of all three channels is shown in the final set of panels. B) There was no effect from VANGL1 overexpression on 3D morphology of 21PT cells. C) There was no effect of VANGL1 overexpression on the number of nuclei per cell colony. Colony morphology was analyzed using one-way ANOVA followed by Tukey's post hoc test and $p<0.05$ was considered statistically significant. Scale bar represent 30μm.

for following migration and invasion assays, only 600ng/mL was used. Recombinant Wnt5a treatment increased migration from 19.37 (SE 1.76) cell per field of view to 32.10 (SE 1.99) cells per field of view in the 21PT + EV cell line ($p<0.05$) (*Figure3.18A, 3.18B*). Likewise, recombinant Wnt5a treatment increased migration from 62.27 (SE 10.16) cells per field of view to 108.5 (SE 8.26) cells per field of view in the 21PT + VANGL1-myc cell line ($p<0.05$) (*Figure 3.18A, 3.18B*).

Next, to test the effect of both VANGL1 and WNT5A on breast cancer progression, recombinant Wnt5a protein was used as a treatment on 21PT cells that already overexpress VANGL1. To assess the treatment of recombinant Wnt5a on VANGL1 overexpressing cells, the 21PT + EV and 21PT + VANGL1-myc cells were placed in the upper chamber of a transwell system and allowed to invade through the pores in order to reach FBS (chemoattractant) that was present in the lower chamber. Recombinant Wnt5a protein was present in the upper and lower chambers at a concentration of 600ng/mL. Recombinant Wnt5a treatment had no effect on invasion of the 21PT + EV or the 21PT + VANGL1-myc (*Figure 3.18A, 3.18B*).

3.4 Objective 2: Test molecular controls of breast cancer progression. Specific aim 3: Determine the role of WNT5A and VANGL1 on breast cancer progression via shRNA knockdown using the 21T cell lines

3.4.1 WNT5A and VANGL1 mRNA levels were individually knocked down in 21MT-1 cells

To further assess the role of non-canonical Wnt pathway during breast cancer progression, WNT5A and VANGL1 expression was knocked down in the 21MT-1 cell

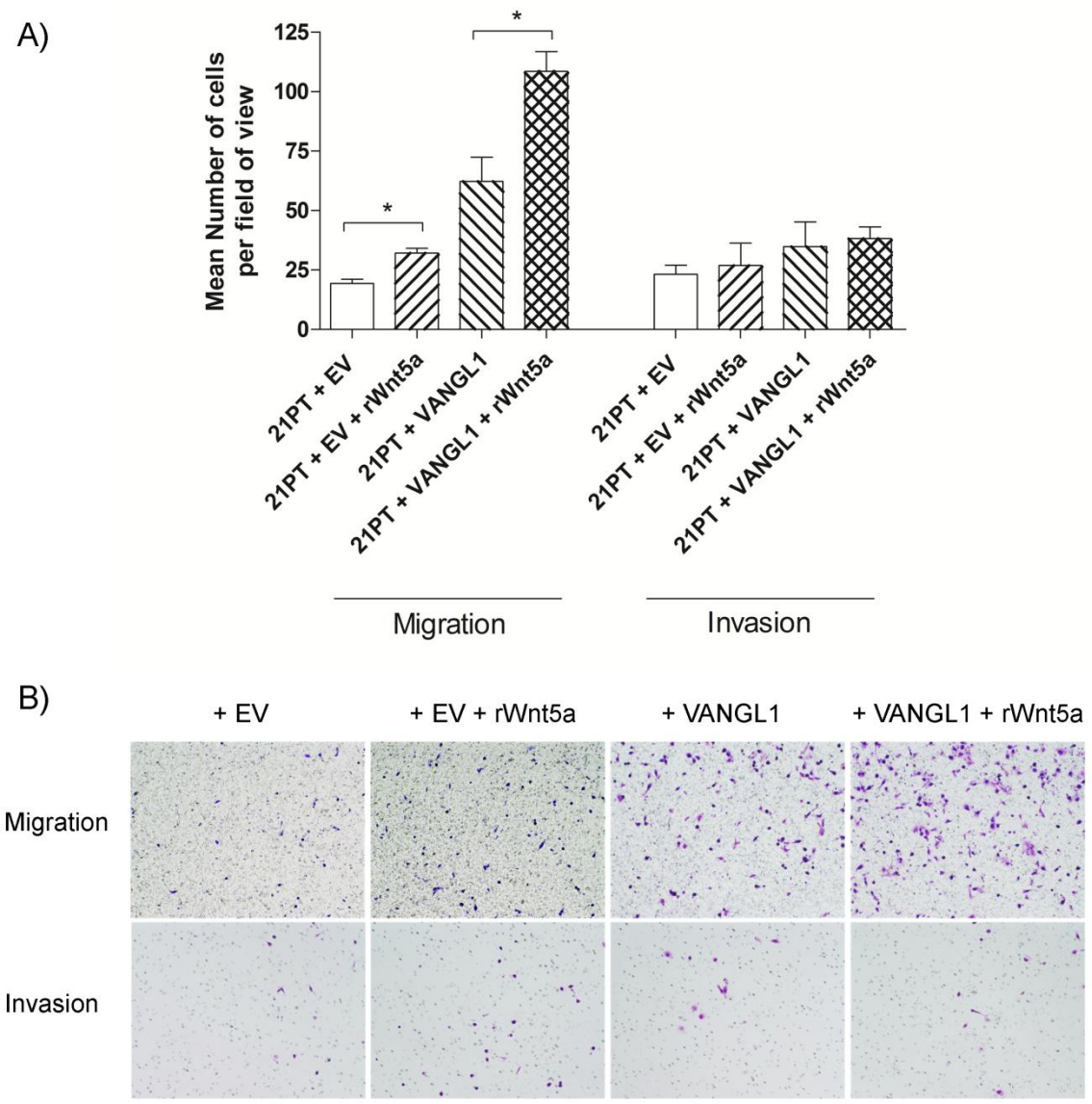

Figure 3.18 Recombinant Wnt5a treatment increases migration but not invasion in the 21PT + VANGL1-myc cell line. A) Transwell migration assay using 21PT + EV and 21PT + VANGL1-myc cells towards FBS for 5 hours with recombinant Wnt5a treatment. Wnt5a protein treatment increased the number of 21PT + EV and 21PT + VANGL1-myc cells that migrated to the underside of the transwell membranes compared to no Wnt5a treatment. B) Transwell invasion assay using 21PT + EV and 21PT + VANGL1-myc cells towards FBS for 20 hours with recombinant Wnt5a treatment. Wnt5a treatment had no effect on the number of 21PT + EV and 21PT + VANGL1-myc cells that migrated to the underside of the transwell membranes. C) Representative images used for counting the number of cells per field of view. To analyze the number of cells per field of view a one-way ANOVA was performed with Tukey's post hoc test and $p<0.05$ was considered statistically significant. *$p<0.05$.

line using shRNA against both genes separately. WNT5A mRNA knockdown was achieved using one of the three shRNAs and VANGL1 knockdown was achieved with all three shRNAs in the 21MT-1 cell line. WNT5A expression was decreased by 2.23-fold (SE 0.076) compared to an off target knockdown control ($p<0.05$) (*Figure 3.19A*). In the most efficient knockdown, VANGL1 expression was decreased by 11.1-fold (SE 0.0064) compared to an off target knockdown control ($p<0.01$) (*Figure 3.19B*).

3.4.2 WNT5A or VANGL1 knockdown had no effect on the 3D morphology or growth of 21MT-1 cells

To assess the effect of WNT5A and VANGL1 knockdown on 3D morphology and cell growth, the 21MT-1 + shWNT5A, 21MT-1 + shVANGL1, and 21MT-1 + shLUC cells were grown in the 3D morphology Matrigel assay for 12 days. The proportion of cell colonies exhibiting lumen formation, polarized colonies, and spherical colonies (vs. non-spherical colonies) were assessed. The number of nuclei per colony was also assessed. Compared to the off target knockdown (21MT-1 + shLUC), WNT5A knockdown did not have an effect on 3D morphology (lumen formation, polarized colonies, spherical colonies) or the number of nuclei per cell colony at day 12 (*Figure 3.20A, 3.20B, 3.20C*). Similarly, compared to the off target knockdown, VANGL1 knockdown did not have an effect on 3D morphology or the number of nuclei per cell colony at day 12 (*Figure 3.20A, 3.20B, 3.20C*).

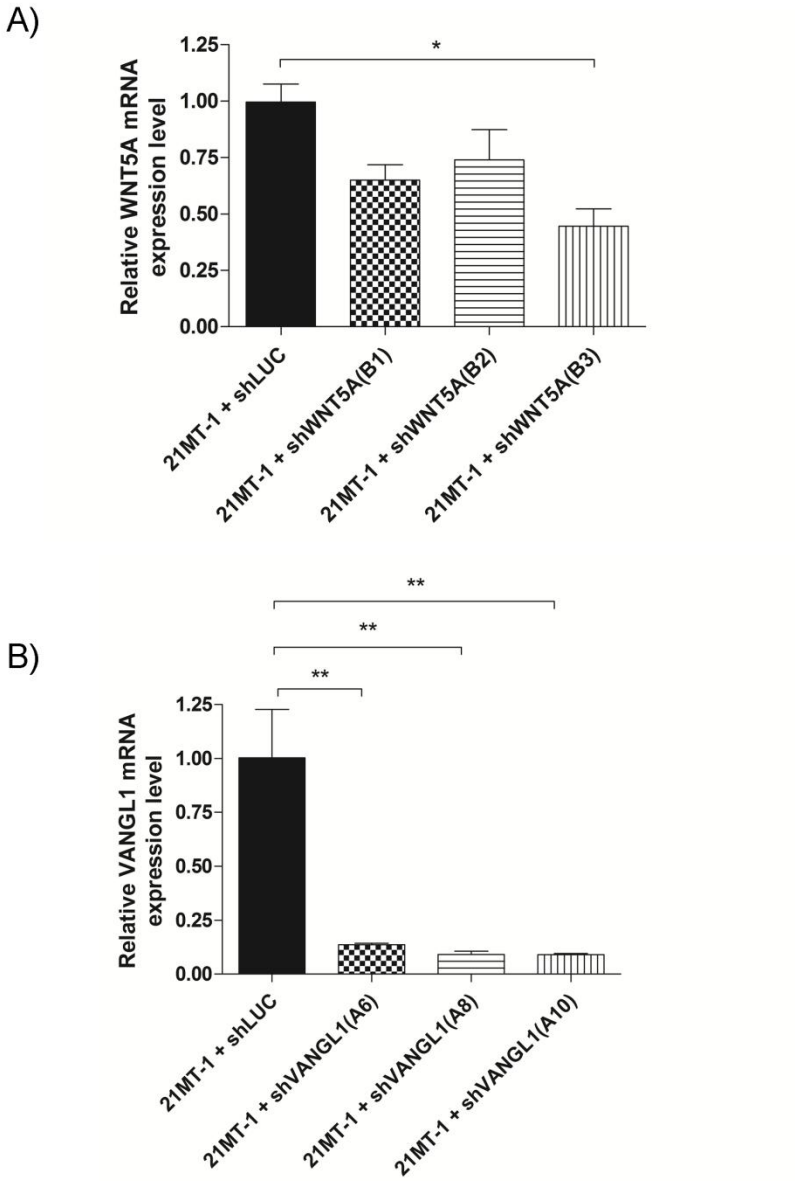

Figure 3.19 WNT5A and VANGL1 knockdown in 21MT-1 cells. A) Using a panel of three different shRNAs, WNT5A mRNA expression was knocked down in 21MT-1 cells. Only one shRNA effectively knocked down expression of WNT5A. B) Using a panel of three different shRNAs, VANGL1 mRNA expression was knocked down in 21MT-1 cells. All three shRNAs were effective in knocking down VANGL1 expression. To analyze mRNA expression a one-way ANOVA was performed with Tukey's post hoc test and $p<0.05$ was considered statistically significant. *$p<0.05$, **$p<0.01$.

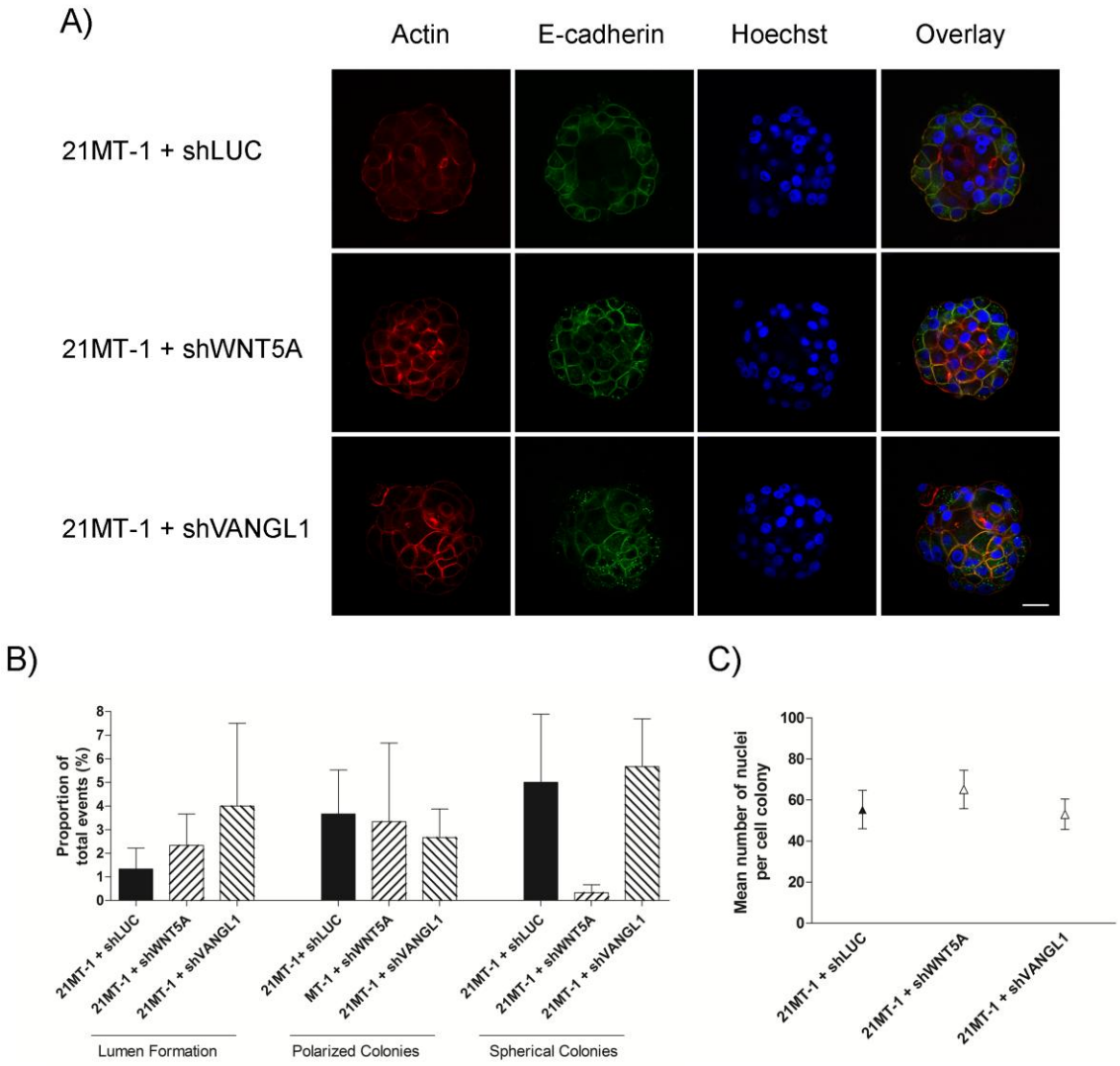

Figure 3.20 WNT5A and VANGL1 knockdown had no effect on the 3D morphology or growth of 21MT-1 cells. The 21MT-1 + shLUC, 21MT-1 + shWNT5A, and 21MT-1 + shVANGL1 cells were grown on top of 100% Matrigel in αHE + 2% FBS and 2% Matrigel for 12 days. Cell colonies were fixed, permeabilized, stained, and imaged using confocal microscopy. A) Representative cell colonies are shown at each day. Actin is shown in red, E-cadherin is shown in green, and the nuclear stain Hoechst is shown in blue. An overlay of all three channels is shown in the final set of panels. B) There was no effect of either WNT5A or VANGL1 knockdown on 3D morphology of 21MT-1 cells. C) There was no effect of either WNT5A or VANGL1 knockdown on the number of nuclei per cell colony. Colony morphology was analyzed using one-way ANOVA followed by Tukey's post hoc test and $p<0.05$ was considered statistically significant. Scale bar represent 30μm.

Chapter 4

4 Discussion

Worldwide, breast cancer continues to be a major health concern for women. In North America, although there has been a decreasing trend in the mortality rate over the last several decades, there will still be approximately 45 000 deaths due to metastatic breast cancer in 2012 (American Cancer Society 2012; Canadian Cancer Society's Steering Committee on Cancer Statistics 2012). From a clinical perspective, there is a need to understand what drives the progression of breast cancer from earlier non-invasive lesions to an invasive phenotype.

The 21T cell lines have been shown to represent a mammary tumor progression series and mimic specific stages of breast cancer in vitro and in vivo (Souter et al. 2010). Subsequent expression profiling has revealed significant differences in the non-canonical Wnt/PCP pathway members WNT5A and VANGL1 (Souter et al. 2010).

WNT5A, the prototypical Wnt ligand which activates non-canonical Wnt signalling, has been shown to act as both an oncogene and tumor suppressor in different studies (Olson and Gibo 1998; Liang et al. 2003; Kremenevskaja et al. 2005; Leris et al. 2005; Ying et al. 2007; Ying et al. 2008; Liu et al. 2008; Pukrop et al. 2006; Weeraratna et al. 2002; Kurayoshi et al. 2006). This dual effect of WNT5A may be due to the cellular context in which it is presented. For example, the effect of WNT5A may be due to the presence or absence of other Wnt pathway components (such as VANGL1).

This study was designed to determine the cellular context that is required for WNT5A to act as an oncogene as opposed to a tumor suppressor in breast cancer using the 21T cell lines as a model for breast cancer progression. Results demonstrate that

WNT5A can act as an oncogene that drives progression towards a more invasive phenotype in a cell line representing DCIS (21NT) but not in a cell line representing ADH (21PT). Results also indicate that WNT5A's effect in increasing invasion is partially due to a downstream effector of the PCP pathway, RHOA. Finally, results demonstrate that high VANGL1 expression alone is not sufficient to promote WNT5A-induced progression to an invasive phenotype.

4.1 The 21T cells grown in the "on-top" 3D morphology assay have distinct structural features and growth patterns

Objective 1 was to improve the existing in vitro breast cancer progression model to assess 3D morphology with the 21T cell lines. Here, the 21T cell lines were characterized using the "on-top" method and imaged using confocal microscopy. Consistent with the "embedded" method that was previously used in our lab (Souter et al. 2010), the 21T cells continue to have distinct 3D morphologies and growth patterns when used in the "on-top" assay after similar endpoints (i.e. 12 days). The use of the 21T cells in an embedded 3D in vitro system has proven useful in distinguishing the 21T cells (21PT vs. 21NT vs. 21MT-1) based on 3D morphology as well as identifying potential regulators of progression (Souter et al. 2010). Embedding the 21T cell lines in Matrigel is expensive and preparing the cells for imaging is time consuming. However, seeding cells on top of Matrigel instead of embedding them has the potential to use fewer materials (Matrigel) and processing them for imaging via immunofluorescence can be faster than H&E staining of paraffin embedded Matrigel plugs. In addition, imaging is facilitated by

having the cells grow in a single plane in the “on-top” assay. Thus, future work can take advantage of the “on-top” assay for imaging of the 21T cell lines.

4.2 PCP signaling promotes breast cancer progression in 21NT cells

To determine the role of PCP signalling in early breast cancer progression, WNT5A was overexpressed in 21PT and 21NT cells, representing ADH and DCIS respectively. WNT5A overexpression increased migration in both 21PT and 21NT cells, but only increased invasion in 21NT cells.

WNT5A overexpression increased RHOA mRNA levels in both the 21PT and 21NT cells. Subsequent knockdown of RHOA in WNT5A overexpressing 21PT and 21NT cells decreased WNT5A-induced migration to levels similar to parental cells, thus implicating the PCP pathway in enhancing cell migration. This is consistent with the known role of PCP signalling in regulating the actin cytoskeleton and increasing migration. However, RHOA knockdown only partially decreased WNT5A-induced invasion in 21NT cells (WNT5A overexpression did not increase invasion in 21PT cells).

An increase in migration alone is not sufficient for cancerous cells to acquire the ability to invade into the surrounding stroma. In this case, it appears that in 21NT cells some other gene(s) may be involved in allowing further progression to invasion. Furthermore, this work suggests that some aspect of WNT5A-induced invasion of 21NT cell occurs through a RHOA independent pathway. MMPs are related to the invasive phenotype, and induction of their expression may be a critical event in early breast cancer progression to invasion (Chang and Werb 2001). In human osteosarcoma cell lines, WNT5A has been shown to activate c-Src through the ROR2 co-receptor, which leads to

the expression of MMP-13 (Enomoto et al. 2009). WNT5A has also been shown to induce the expression of MMP-1 in prostate cancer cells through the AP-1 axis by activation of PKC-δ and JNK (Yamamoto et al. 2010). WNT5A signalling is also linked to the expression of MMP-2 in renal cell carcinoma cell lines (Wright et al. 2009). Laminin c2, a subunit of the basement membrane protein laminin-5 (Miyazaki 2006), has been identified as a gene regulated by WNT5A (Yamamoto et al. 2009). Laminin c2 contains a promoter region which binds JunD, an AP-1 element (Olsen et al. 2000). WNT5A has been shown to activate PKC and JNK, recruiting JunD to the AP-1 site of the laminin c2 promoter (Yamamoto et al. 2009). Abnormal laminin c2 expression has been detected at the invasive front of gastric and colon cancer, suggesting that laminin c2 is involved in invasion, although the mechanism remains unclear (Koshikawa et al. 1999; Pyke et al. 1995). Therefore, abnormal WNT5A signalling via the AP-1 axis may be involved in invasion through the expression of MMPs and laminin c2, in addition to increased cell migration resulting from a rearrangement of the actin cytoskeleton through the downstream effector RHOA.

In the present study, VANGL1 overexpression alone was capable of enhancing migration of 21PT cells, but had no effect on 21PT cell invasion, 3D morphology, or growth, similar to the effects of WNT5A overexpression. This is consistent with its known role as a core PCP component. However, VANGL1 has previously been shown to increase invasion in colorectal cancer by recruiting PKC-δ to the plasma membrane and enhancing AP-1 transcriptional activity (Kho et al. 2009).

High VANGL1 expression was initially hypothesized as the context in which WNT5A can act as a promoter of breast cancer progression. However, analysis of mRNA

levels in the 21T cell lines revealed that VANGL1 expression was similar in both 21PT and 21NT cells, and upon WNT5A overexpression in these cell lines, only the 21NT cells invaded more in a transwell invasion assay. In addition, in 21PT cells that overexpressed VANGL1, recombinant Wnt5a treatment did not increase invasion. Thus, results demonstrate that although high VANGL1 expression induces cell migration of 21PT cells, high VANGL1 alone is not sufficient to promote WNT5A-induced progression to an invasive phenotype.

It is conceivable that, in 21PT cells, WNT5A and VANGL1 do not increase invasion because of a missing component in the AP-1 axis that is downstream of VANGL1 or PKC-δ. Future studies will examine downstream components of the AP-1 axis in 21PT and 21NT cells to determine if this pathway is necessary for WNT5A- or VANGL1-induced invasion.

4.3 Genes that could determine the cellular context required for WNT5A to promote progression to invasion

There are 22 defined mitogen-activated protein kinase kinase kinases (MAP3Ks) and over 40 total mitogen-activated protein kinases (MAP2Ks and MAPKs) (Cuevas et al. 2007). This large network of MAPKs represents 8% of the human kinome. Downstream components of the MAPK signalling network, including JNK, p38, and extracellular signal-regulated kinase 5 (ERK5) are activated in a number of cancers, such as breast, prostate, squamous and hepatocellular carcinoma (Davidson et al. 2006; Hui et al. 2008; McCracken et al. 2008; Sticht et al. 2008; Montero et al. 2009; Zen et al. 2009; Wang et al. 2010; Wagner and Nebreda 2009).

Activation of these downstream MAPKs is controlled by upstream MAP3Ks that have also been shown to be dysregulated in cancer cells. For example, the MAP3K Tpl2 has been shown to be overexpressed in 40% of human breast cancers (Sourvinos et al. 1999). An activating mutation of Tpl2 was found in a patient with basal-like breast cancer and cells containing this Tpl2 mutation were increased in the metastatic tissue (Ding et al. 2010). Also, the MAP3Ks, MEKK3 and A-Raf, are overexpressed in non-small-cell lung cancer (Lee et al. 2010b).

Recently, using MDA-MB-231 cells in an orthotopic xenograft model to screen the function of seven MAP3Ks in controlling tumor metastasis, MAP3K2 (also known as MEKK2) was identified as a potential regulator of metastasis. Specifically, knocking down expression of MAP3K2 with shRNA inhibited metastasis of MDA-MD-231 tumors in SCID mice (Cronan et al. 2012). Inhibition of WNT signalling in MDA-MB-231 cells also decreased invasion in a β-catenin independent manner (Klemm et al. 2011).

MAP3K2 expression is 1.7 to 1.8 fold higher in 21NT cells than in 21PT cells (Souter et al. 2010). This differential expression of MAP3K2 in the 21NT and 21PT cell lines could be responsible for the differing effects of WNT5A on invasion and may provide the cellular context that allows WNT5A to induced progression to invasion (Figure 4.1). Future work will examine the role that MAP3K2 plays in response to WNT5A overexpression in the 21T cell lines.

4.4 WNT5A during canonical Wnt/β-catenin dependent signalling

There is conflicting evidence as to whether WNT5A antagonizes or agonizes β-catenin dependent signalling. An early observation of WNT5A was its ability to inhibit

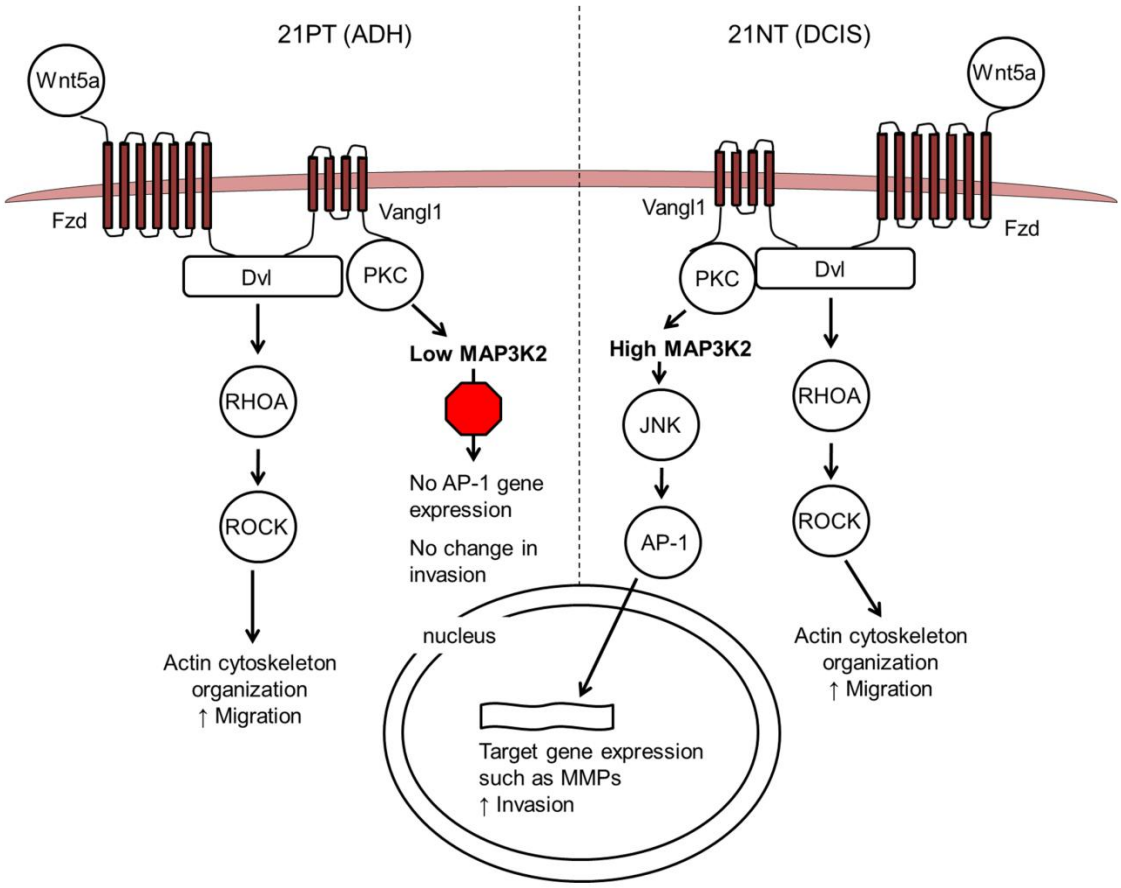

Figure 4.1 Speculative mechanism of differential WNT5A effect in the 21T cell lines. WNT5A overexpression increases migration in both 21PT (ADH) and 21NT (DCIS) through a RHOA dependent pathway. Additionally, due to high levels of MAP3K2 (Souter et al. 2010), WNT5A overexpression in 21NT cells increases invasion in an AP-1 dependent manner. This effect is not seen in 21PT cells due to low MAP3K2.

the canonical Wnt/β-catenin dependent pathway (Torres et al. 1996) by antagonizing the effect of Wnt1. Studies in WNT5A knockout mice also revealed that β-catenin signalling was enhanced (Topol et al. 2003; Sato et al. 2010). Several mechanisms can explain this possible inhibitory effect of WNT5A on β-catenin dependent signalling. For example, WNT5A has been shown to inhibit β-catenin dependent gene expression through the activation of Nemo-like kinase (NLK) whereby WNT5A activates CaMK through the activation of TGF-β-activated kinase (TAK) (Ishitani et al. 1999; Ishitani et al. 2003). It has also been shown that WNT5A can activate PKCα, leading to the phosphorylation of RORα. Phosphorylated RORα inhibits β-catenin dependent gene expression through the inhibition of the recruitment of co-activators to the promoter regions of target genes (Lee et al. 2010a). WNT5A has been shown to affect the stability of β-catenin by inducing the expression of an ubiquitin E3 ligase (Siah2), a protein that degrades β-catenin (Topol et al. 2003). Finally, WNT5A may inhibit β-catenin signalling at the level of the receptor. Canonical and non-canonical Wnts have been shown to use a common mechanism to activate completely different co- receptors (i.e. ROR1/2 and LRP5/6), while acting through similar Fzd receptors (Grumolato et al. 2010). Thus, WNT5A can prevent WNT3A binding to Fzd2, inhibiting signalling through LRP6 and β-catenin (Sato et al. 2010).

WNT5A has also been shown to stimulate β-catenin signalling in some cases. For example, overexpression of WNT5A and Fzd5 or Fzd4 in Xenopus embryos induced expression of Wnt/β-catenin target genes (He et al. 1997; Umbhauer et al. 2000). In addition, overexpression of Fzd4 and LRP5 enabled WNT5A to stabilize β-catenin protein and allow it entry into the nucleus, where it complexes with T-cell

factor/lymphoid enhancer factor transcription factors (Mikels and Nusse 2006). This suggests that receptor expression may be one particular cellular context that dictates the output of WNT5A. However, the stimulatory effects of WNT5A on the β-catenin signalling have only been shown under conditions where the receptors are overexpressed. It is unclear if WNT5A can have agonistic effects on the β-catenin pathway under normal physiological conditions. However, it may be necessary to consider WNT5A-induced activation of β-catenin signalling during pathological conditions where expression of canonical Wnt receptors is increased.

In the present study the stabilization of β-catenin and signalling through β-catenin dependent processes was not examined. It is conceivable that WNT5A overexpression may have an effect on β-catenin which in turn may effect cancer progression in the 21T cell lines. However, aberrant β-catenin signalling is primarily involved in proliferation, tumor growth, and tumor initiation, and since growth of the 21T cells was not affected by WNT5A overexpression, it seems unlikely that altered β-catenin function played a role in WNT5A-induced breast cancer progression in these cells.

4.5 Limitations and future work

The effect of WNT5A and VANGL1 knockdown was examined in the 21MT-1 cell line (representing invasive mammary carcinoma), but only growth and 3D morphology were measured, finding no effect. However, there was only a 2.23-fold decrease in WNT5A expression due to shRNA knockdown; whereas in the parental cell lines, WNT5A expression is much lower in the 21NT cells (109.1-fold). For future work with the 21MT-1 cells, in order to conclusively establish the importance of WNT5A expression to malignancy, the knockdown in WNT5A expression should preferably be to

a level similar to 21PT and 21NT cells. This could be accomplished by using shRNAs that target different regions of the WNT5A mRNA. Another limitation of the knockdown studies with the 21MT-1 cells is that they are lacking an effective measure of invasiveness. This is due to an intrinsic limitation of the 21MT-1 cells; 21MT-1 cells are too big to fit through 8.0μm and 12.0μm pores of the transwell membrane. The 21MT-1 cells have been shown to be more invasive than the 21PT and 21NT cells in a time lapse invasion assay in which the cells were embedded in Matrigel (Souter et al. 2010). Future studies should take advantage of this assay using 21MT-1 + shWNT5A and 21MT-1 + shVANGL1 cells in order to assess the effect of WNT5A and VANGL1 knockdown on invasiveness of this metastatic breast cancer cell line.

4.6 Summary

This study provides evidence that WNT5A can promote progression during an early stage of breast cancer. WNT5A overexpression increased invasion in a cell line representing DCIS (21NT), but not in a cell line representing ADH (21PT). It was hypothesized that this differential effect of WNT5A on invasion may be due to the presence or absence of other non-canonical Wnt/PCP pathway genes such as VANGL1. Overexpression of VANGL1 alone or with recombinant Wnt5a protein did not increase invasion of 21PT cells. VANGL1 mRNA levels were also found to be similar in both 21PT and 21NT cells. Thus VANGL1 was likely not responsible for WNT5A's differential effect on invasion.

Future studies should examine other genes that establish the cellular context that is required for WNT5A's invasive properties. One possible gene is MAP3K2. MAP3K2 is involved in the AP-1 axis and activates JNK, which is downstream of both WNT5A

and VANGL1. MAP3K2 is expressed in higher levels in the 21NT cells compared to the 21PT cells and has been shown to promote breast cancer metastasis in MBA-MD-231 derived tumors.

Understanding the role of WNT5A and PCP signalling during progression is complicated when considering progression is not only an epithelial driven process. However, this study sheds light on the role that WNT5A and PCP signalling plays on breast epithelial cells during the transition to an invasive phenotype. With this work and continued research in this area, it is hopeful that a more complete understanding of the cellular context that allows WNT5A to induce progression is elucidated.

References

Allinen M, Beroukhim R, Cai L et al (2004) Molecular characterization of the tumor microenvironment in breast cancer. Cancer Cell 6:17-32

Allred DC, Mohsin SK, Fuqua SA (2001) Histological and biological evolution of human premalignant breast disease. Endocr Relat Cancer 8:47-61

Allred DC, Wu Y, Mao S et al (2008) Ductal carcinoma in situ and the emergence of diversity during breast cancer evolution. Clin Cancer Res 14:370-378

Amari M, Suzuki A, Moriya T et al (1999) LOH analyses of premalignant and malignant lesions of human breast: frequent LOH in 8p, 16q, and 17q in atypical ductal hyperplasia. Oncol Rep 6:1277-1280

American Cancer Society (2012) Cancer Facts & Figues 2012. American Cancer Society

Anastas JN, Biechele TL, Robitaille M et al (2012) A protein complex of SCRIB, NOS1AP and VANGL1 regulates cell polarity and migration, and is associated with breast cancer progression. Oncogene 31:3696-3708

Arpino G, Laucirica R, Elledge RM (2005) Premalignant and in situ breast disease: biology and clinical implications. Ann Intern Med 143:446-457

Band V, Zajchowski D, Swisshelm K et al (1990) Tumor progression in four mammary epithelial cell lines derived from the same patient. Cancer Res 50:7351-7357

Barrow JR (2006) Wnt/PCP signaling: a veritable polar star in establishing patterns of polarity in embryonic tissues. Semin Cell Dev Biol 17:185-193

Boldt V, Stacher E, Halbwedl I et al (2010) Positioning of necrotic lobular intraepithelial neoplasias (LIN, grade 3) within the sequence of breast carcinoma progression. Genes Chromosomes Cancer 49:463-470

Briand P, Lykkesfeldt AE (2001) An in vitro model of human breast carcinogenesis: epigenetic aspects. Breast Cancer Res Treat 65:179-187

Buerger H, Mommers EC, Littmann R et al (2001) Ductal invasive G2 and G3 carcinomas of the breast are the end stages of at least two different lines of genetic evolution. J Pathol 194:165-170

Buerger H, Otterbach F, Simon R et al (1999) Comparative genomic hybridization of ductal carcinoma in situ of the breast-evidence of multiple genetic pathways. J Pathol 187:396-402

Canadian Cancer Society's Steering Committee on Cancer Statistics (2012) Canadian Cancer Statisitics 2012. Canadian Cancer Society

Cao D, Polyak K, Halushka MK et al (2008) Serial analysis of gene expression of lobular carcinoma in situ identifies down regulation of claudin 4 and overexpression of matrix metalloproteinase 9. Breast Cancer Res 10:R91

Chang C, Werb Z (2001) The many faces of metalloproteases: cell growth, invasion, angiogenesis and metastasis. Trends Cell Biol 11:S37-43

Chen H, Fok KL, Yu S et al (2011) CD147 is required for matrix metalloproteinases-2 production and germ cell migration during spermatogenesis. Mol Hum Reprod 17:405-414

Cronan MR, Nakamura K, Johnson NL et al (2012) Defining MAP3 kinases required for MDA-MB-231 cell tumor growth and metastasis. Oncogene 31:3889-3900

Cuevas BD, Abell AN, Johnson GL (2007) Role of mitogen-activated protein kinase kinase kinases in signal integration. Oncogene 26:3159-3171

Curtis C, Shah SP, Chin SF et al (2012) The genomic and transcriptomic architecture of 2,000 breast tumours reveals novel subgroups. Nature

Davidson B, Konstantinovsky S, Kleinberg L et al (2006) The mitogen-activated protein kinases (MAPK) p38 and JNK are markers of tumor progression in breast carcinoma. Gynecol Oncol 102:453-461

Debnath J, Mills KR, Collins NL et al (2002) The role of apoptosis in creating and maintaining luminal space within normal and oncogene-expressing mammary acini. Cell 111:29-40

Debnath J, Muthuswamy SK, Brugge JS (2003) Morphogenesis and oncogenesis of MCF-10A mammary epithelial acini grown in three-dimensional basement membrane cultures. Methods 30:256-268

Desmedt C, Sotiriou C (2006) Proliferation: the most prominent predictor of clinical outcome in breast cancer. Cell Cycle 5:2198-2202

Ding L, Ellis MJ, Li S et al (2010) Genome remodelling in a basal-like breast cancer metastasis and xenograft. Nature 464:999-1005

Dissanayake SK, Wade M, Johnson CE et al (2007) The Wnt5A/protein kinase C pathway mediates motility in melanoma cells via the inhibition of metastasis suppressors and initiation of an epithelial to mesenchymal transition. J Biol Chem 282:17259-17271

Ellis IO (2010) Intraductal proliferative lesions of the breast: morphology, associated risk and molecular biology. Mod Pathol 23 Suppl 2:S1-7

Enomoto M, Hayakawa S, Itsukushima S et al (2009) Autonomous regulation of osteosarcoma cell invasiveness by Wnt5a/Ror2 signaling. Oncogene 28:3197-3208

Eusebi V, Magalhaes F, Azzopardi JG (1992) Pleomorphic lobular carcinoma of the breast: an aggressive tumor showing apocrine differentiation. Hum Pathol 23:655-662

Ewald AJ, Brenot A, Duong M et al (2008) Collective epithelial migration and cell rearrangements drive mammary branching morphogenesis. Dev Cell 14:570-581

Fauquette W, Dong-Le Bourhis X, Delannoy-Courdent A et al (1997) Characterization of morphogenetic and invasive abilities of human mammary epithelial cells: correlation with variations of urokinase-type plasminogen activator activity and type-1 plasminogen activator inhibitor level. Biol Cell 89:453-465

Fitzgibbons PL, Henson DE, Hutter RV (1998) Benign breast changes and the risk for subsequent breast cancer: an update of the 1985 consensus statement. Cancer Committee of the College of American Pathologists. Arch Pathol Lab Med 122:1053-1055

Fournier MV, Martin KJ (2006) Transcriptome profiling in clinical breast cancer: from 3D culture models to prognostic signatures. J Cell Physiol 209:625-630

Goetz MP, Suman VJ, Ingle JN et al (2006) A two-gene expression ratio of homeobox 13 and interleukin-17B receptor for prediction of recurrence and survival in women receiving adjuvant tamoxifen. Clin Cancer Res 12:2080-2087

Goodrich LV (2008) The plane facts of PCP in the CNS. Neuron 60:9-16

Gou L, Wang W, Tong A et al (2011) Proteomic identification of RhoA as a potential biomarker for proliferation and metastasis in hepatocellular carcinoma. J Mol Med (Berl) 89:817-827

Grumolato L, Liu G, Mong P et al (2010) Canonical and noncanonical Wnts use a common mechanism to activate completely unrelated coreceptors. Genes Dev 24:2517-2530

He X, Saint-Jeannet JP, Wang Y et al (1997) A member of the Frizzled protein family mediating axis induction by Wnt-5A. Science 275:1652-1654

Hebner C, Weaver VM, Debnath J (2008) Modeling morphogenesis and oncogenesis in three-dimensional breast epithelial cultures. Annu Rev Pathol 3:313-339

Hu M, Yao J, Cai L et al (2005) Distinct epigenetic changes in the stromal cells of breast cancers. Nat Genet 37:899-905

Hu M, Yao J, Carroll DK et al (2008) Regulation of in situ to invasive breast carcinoma transition. Cancer Cell 13:394-406

Hui L, Zatloukal K, Scheuch H et al (2008) Proliferation of human HCC cells and chemically induced mouse liver cancers requires JNK1-dependent p21 downregulation. J Clin Invest 118:3943-3953

Ishitani T, Kishida S, Hyodo-Miura J et al (2003) The TAK1-NLK mitogen-activated protein kinase cascade functions in the Wnt-5a/Ca(2+) pathway to antagonize Wnt/beta-catenin signaling. Mol Cell Biol 23:131-139

Ishitani T, Ninomiya-Tsuji J, Nagai S et al (1999) The TAK1-NLK-MAPK-related pathway antagonizes signalling between beta-catenin and transcription factor TCF. Nature 399:798-802

Jerevall PL, Brommesson S, Strand C et al (2008) Exploring the two-gene ratio in breast cancer--independent roles for HOXB13 and IL17BR in prediction of clinical outcome. Breast Cancer Res Treat 107:225-234

Kamai T, Shirataki H, Nakanishi K et al (2010) Increased Rac1 activity and Pak1 overexpression are associated with lymphovascular invasion and lymph node metastasis of upper urinary tract cancer. BMC Cancer 10:164

Karner C, Wharton KA, Jr., Carroll TJ (2006) Planar cell polarity and vertebrate organogenesis. Semin Cell Dev Biol 17:194-203

Karnoub AE, Dash AB, Vo AP et al (2007) Mesenchymal stem cells within tumour stroma promote breast cancer metastasis. Nature 449:557-563

Katoh M (2005) WNT/PCP signaling pathway and human cancer (review). Oncol Rep 14:1583-1588

Kenny PA, Lee GY, Myers CA et al (2007) The morphologies of breast cancer cell lines in three-dimensional assays correlate with their profiles of gene expression. Mol Oncol 1:84-96

Kho AT, Zhao Q, Cai Z et al (2004) Conserved mechanisms across development and tumorigenesis revealed by a mouse development perspective of human cancers. Genes Dev 18:629-640

Kho DH, Bae JA, Lee JH et al (2009) KITENIN recruits Dishevelled/PKC delta to form a functional complex and controls the migration and invasiveness of colorectal cancer cells. Gut 58:509-519

Kikuchi A, Yamamoto H (2008) Tumor formation due to abnormalities in the beta-catenin-independent pathway of Wnt signaling. Cancer Sci 99:202-208

Kikuchi A, Yamamoto H, Sato A (2009) Selective activation mechanisms of Wnt signaling pathways. Trends Cell Biol 19:119-129

Kinoshita N, Iioka H, Miyakoshi A et al (2003) PKC delta is essential for Dishevelled function in a noncanonical Wnt pathway that regulates Xenopus convergent extension movements. Genes Dev 17:1663-1676

Klemm F, Bleckmann A, Siam L et al (2011) beta-catenin-independent WNT signaling in basal-like breast cancer and brain metastasis. Carcinogenesis 32:434-442

Kohn AD, Moon RT (2005) Wnt and calcium signaling: beta-catenin-independent pathways. Cell Calcium 38:439-446

Kojima Y, Acar A, Eaton EN et al (2010) Autocrine TGF-beta and stromal cell-derived factor-1 (SDF-1) signaling drives the evolution of tumor-promoting mammary stromal myofibroblasts. Proc Natl Acad Sci U S A 107:20009-20014

Koshikawa N, Moriyama K, Takamura H et al (1999) Overexpression of laminin gamma2 chain monomer in invading gastric carcinoma cells. Cancer Res 59:5596-5601

Kremenevskaja N, von Wasielewski R, Rao AS et al (2005) Wnt-5a has tumor suppressor activity in thyroid carcinoma. Oncogene 24:2144-2154

Kunju LP, Kleer CG (2007) Significance of flat epithelial atypia on mammotome core needle biopsy: Should it be excised? Hum Pathol 38:35-41

Kurayoshi M, Oue N, Yamamoto H et al (2006) Expression of Wnt-5a is correlated with aggressiveness of gastric cancer by stimulating cell migration and invasion. Cancer Res 66:10439-10448

Kusama R, Fujimori M, Matsuyama I et al (2000) Clinicopathological characteristics of atypical cystic duct (ACD) of the breast: assessment of ACD as a precancerous lesion. Pathol Int 50:793-800

Lakhani SR, Collins N, Stratton MR et al (1995) Atypical ductal hyperplasia of the breast: clonal proliferation with loss of heterozygosity on chromosomes 16q and 17p. J Clin Pathol 48:611-615

Lee GY, Kenny PA, Lee EH et al (2007) Three-dimensional culture models of normal and malignant breast epithelial cells. Nat Methods 4:359-365

Lee JH, Cho ES, Kim MY et al (2005) Suppression of progression and metastasis of established colon tumors in mice by intravenous delivery of short interfering RNA targeting KITENIN, a metastasis-enhancing protein. Cancer Res 65:8993-9003

Lee JH, Park SR, Chay KO et al (2004) KAI1 COOH-terminal interacting tetraspanin (KITENIN), a member of the tetraspanin family, interacts with KAI1, a tumor metastasis suppressor, and enhances metastasis of cancer. Cancer Res 64:4235-4243

Lee JK, Bae JA, Sun EG et al (2009) KITENIN increases invasion and migration of mouse squamous cancer cells and promotes pulmonary metastasis in a mouse squamous tumor model. FEBS Lett 583:711-717

Lee JM, Kim IS, Kim H et al (2010a) RORalpha attenuates Wnt/beta-catenin signaling by PKCalpha-dependent phosphorylation in colon cancer. Mol Cell 37:183-195

Lee W, Jiang Z, Liu J et al (2010b) The mutation spectrum revealed by paired genome sequences from a lung cancer patient. Nature 465:473-477

Leris AC, Roberts TR, Jiang WG et al (2005) WNT5A expression in human breast cancer. Anticancer Res 25:731-734

Lerwill MF (2008) Flat epithelial atypia of the breast. Arch Pathol Lab Med 132:615-621

Liang H, Chen Q, Coles AH et al (2003) Wnt5a inhibits B cell proliferation and functions as a tumor suppressor in hematopoietic tissue. Cancer Cell 4:349-360

Liu XH, Pan MH, Lu ZF et al (2008) Expression of Wnt-5a and its clinicopathological significance in hepatocellular carcinoma. Dig Liver Dis 40:560-567

Logan CY, Nusse R (2004) The Wnt signaling pathway in development and disease. Annu Rev Cell Dev Biol 20:781-810

Lu YJ, Osin P, Lakhani SR et al (1998) Comparative genomic hybridization analysis of lobular carcinoma in situ and atypical lobular hyperplasia and potential roles for gains and losses of genetic material in breast neoplasia. Cancer Res 58:4721-4727

Ma XJ, Dahiya S, Richardson E et al (2009) Gene expression profiling of the tumor microenvironment during breast cancer progression. Breast Cancer Res 11:R7

Ma XJ, Salunga R, Tuggle JT et al (2003) Gene expression profiles of human breast cancer progression. Proc Natl Acad Sci U S A 100:5974-5979

MacDonald BT, Tamai K, He X (2009) Wnt/beta-catenin signaling: components, mechanisms, and diseases. Dev Cell 17:9-26

MacMillan CD, Chambers AF, Tuck AB (2012) Progression of early breast cancer to an invasive phenotype. In: Ahmad A (ed) Breast Cancer Metastasis and Drug Resistance: Progress and Prospects. Springer

Maekawa M, Ishizaki T, Boku S et al (1999) Signaling from Rho to the actin cytoskeleton through protein kinases ROCK and LIM-kinase. Science 285:895-898

Malmberg KJ (2004) Effective immunotherapy against cancer: a question of overcoming immune suppression and immune escape? Cancer Immunol Immunother 53:879-892

Marshall LM, Hunter DJ, Connolly JL et al (1997) Risk of breast cancer associated with atypical hyperplasia of lobular and ductal types. Cancer Epidemiol Biomarkers Prev 6:297-301

Martel M, Barron-Rodriguez P, Tolgay Ocal I et al (2007) Flat DIN 1 (flat epithelial atypia) on core needle biopsy: 63 cases identified retrospectively among 1,751 core biopsies performed over an 8-year period (1992-1999). Virchows Arch 451:883-891

Martin KJ, Patrick DR, Bissell MJ et al (2008) Prognostic breast cancer signature identified from 3D culture model accurately predicts clinical outcome across independent datasets. PLoS One 3:e2994

Mastracci TL, Shadeo A, Colby SM et al (2006) Genomic alterations in lobular neoplasia: a microarray comparative genomic hybridization signature for early neoplastic proliferationin the breast. Genes Chromosomes Cancer 45:1007-1017

McCracken SR, Ramsay A, Heer R et al (2008) Aberrant expression of extracellular signal-regulated kinase 5 in human prostate cancer. Oncogene 27:2978-2988

Medina A, Reintsch W, Steinbeisser H (2000) Xenopus frizzled 7 can act in canonical and non-canonical Wnt signaling pathways: implications on early patterning and morphogenesis. Mech Dev 92:227-237

Merle P, de la Monte S, Kim M et al (2004) Functional consequences of frizzled-7 receptor overexpression in human hepatocellular carcinoma. Gastroenterology 127:1110-1122

Middleton LP, Palacios DM, Bryant BR et al (2000) Pleomorphic lobular carcinoma: morphology, immunohistochemistry, and molecular analysis. Am J Surg Pathol 24:1650-1656

Mikels AJ, Nusse R (2006) Purified Wnt5a protein activates or inhibits beta-catenin-TCF signaling depending on receptor context. PLoS Biol 4:e115

Miller FR, Santner SJ, Tait L et al (2000) MCF10DCIS.com xenograft model of human comedo ductal carcinoma in situ. J Natl Cancer Inst 92:1185-1186

Miyazaki K (2006) Laminin-5 (laminin-332): Unique biological activity and role in tumor growth and invasion. Cancer Sci 97:91-98

Moffat J, Grueneberg DA, Yang X et al (2006) A lentiviral RNAi library for human and mouse genes applied to an arrayed viral high-content screen. Cell 124:1283-1298

Mohinta S, Wu H, Chaurasia P et al (2007) Wnt pathway and breast cancer. Front Biosci 12:4020-4033

Moinfar F, Man YG, Bratthauer GL et al (2000) Genetic abnormalities in mammary ductal intraepithelial neoplasia-flat type ("clinging ductal carcinoma in situ"): a simulator of normal mammary epithelium. Cancer 88:2072-2081

Montero JC, Ocana A, Abad M et al (2009) Expression of Erk5 in early stage breast cancer and association with disease free survival identifies this kinase as a potential therapeutic target. PLoS One 4:e5565

Morandi L, Marucci G, Foschini MP et al (2006) Genetic similarities and differences between lobular in situ neoplasia (LN) and invasive lobular carcinoma of the breast. Virchows Arch 449:14-23

Nubler-Jung K, Bonitz R, Sonnenschein M (1987) Cell polarity during wound healing in an insect epidermis. Development 100:163-170

O'Connell P, Pekkel V, Fuqua SA et al (1998) Analysis of loss of heterozygosity in 399 premalignant breast lesions at 15 genetic loci. J Natl Cancer Inst 90:697-703

Olsen J, Lefebvre O, Fritsch C et al (2000) Involvement of activator protein 1 complexes in the epithelium-specific activation of the laminin gamma2-chain gene promoter by hepatocyte growth factor (scatter factor). Biochem J 347:407-417

Olson DJ, Gibo DM (1998) Antisense wnt-5a mimics wnt-1-mediated C57MG mammary epithelial cell transformation. Exp Cell Res 241:134-141

Olson MF, Sahai E (2009) The actin cytoskeleton in cancer cell motility. Clin Exp Metastasis 26:273-287

Orimo A, Gupta PB, Sgroi DC et al (2005) Stromal fibroblasts present in invasive human breast carcinomas promote tumor growth and angiogenesis through elevated SDF-1/CXCL12 secretion. Cell 121:335-348

Oyama T, Iijima K, Takei H et al (2000) Atypical cystic lobule of the breast: an early stage of low-grade ductal carcinoma in-situ. Breast Cancer 7:326-331

Page DL, Dupont WD (1993) Anatomic indicators (histologic and cytologic) of increased breast cancer risk. Breast Cancer Res Treat 28:157-166

Page DL, Dupont WD, Rogers LW et al (1985) Atypical hyperplastic lesions of the female breast. A long-term follow-up study. Cancer 55:2698-2708

Page DL, Rogers LW (1992) Combined histologic and cytologic criteria for the diagnosis of mammary atypical ductal hyperplasia. Hum Pathol 23:1095-1097

Paik S, Shak S, Tang G et al (2004) A multigene assay to predict recurrence of tamoxifen-treated, node-negative breast cancer. N Engl J Med 351:2817-2826

Palmer TD, Ashby WJ, Lewis JD et al (2011) Targeting tumor cell motility to prevent metastasis. Adv Drug Deliv Rev 63:568-581

Pan SH, Chao YC, Hung PF et al (2011) The ability of LCRMP-1 to promote cancer invasion by enhancing filopodia formation is antagonized by CRMP-1. J Clin Invest 121:3189-3205

Pinder SE, Ellis IO (2003) The diagnosis and management of pre-invasive breast disease: ductal carcinoma in situ (DCIS) and atypical ductal hyperplasia (ADH)--current definitions and classification. Breast Cancer Res 5:254-257

Polyak K, Hu M (2005) Do myoepithelial cells hold the key for breast tumor progression? J Mammary Gland Biol Neoplasia 10:231-247

Porter D, Lahti-Domenici J, Keshaviah A et al (2003) Molecular markers in ductal carcinoma in situ of the breast. Mol Cancer Res 1:362-375

Pukrop T, Klemm F, Hagemann T et al (2006) Wnt 5a signaling is critical for macrophage-induced invasion of breast cancer cell lines. Proc Natl Acad Sci U S A 103:5454-5459

Pyke C, Salo S, Ralfkiaer E et al (1995) Laminin-5 is a marker of invading cancer cells in some human carcinomas and is coexpressed with the receptor for urokinase plasminogen activator in budding cancer cells in colon adenocarcinomas. Cancer Res 55:4132-4139

Riento K, Ridley AJ (2003) Rocks: multifunctional kinases in cell behaviour. Nat Rev Mol Cell Biol 4:446-456

Rizki A, Weaver VM, Lee SY et al (2008) A human breast cell model of preinvasive to invasive transition. Cancer Res 68:1378-1387

Sato A, Yamamoto H, Sakane H et al (2010) Wnt5a regulates distinct signalling pathways by binding to Frizzled2. EMBO J 29:41-54

Schlessinger K, Hall A, Tolwinski N (2009) Wnt signaling pathways meet Rho GTPases. Genes Dev 23:265-277

Schnitt SJ (2003) The diagnosis and management of pre-invasive breast disease: flat epithelial atypia--classification, pathologic features and clinical significance. Breast Cancer Res 5:263-268

Semenov MV, Habas R, Macdonald BT et al (2007) SnapShot: Noncanonical Wnt Signaling Pathways. Cell 131:1378

Sgroi DC (2010) Preinvasive breast cancer. Annu Rev Pathol 5:193-221

Shaw KR, Wrobel CN, Brugge JS (2004) Use of three-dimensional basement membrane cultures to model oncogene-induced changes in mammary epithelial morphogenesis. J Mammary Gland Biol Neoplasia 9:297-310

Shieh DB, Godleski J, Herndon JE, 2nd et al (1999) Cell motility as a prognostic factor in Stage I nonsmall cell lung carcinoma: the role of gelsolin expression. Cancer 85:47-57

Simons M, Mlodzik M (2008) Planar cell polarity signaling: from fly development to human disease. Annu Rev Genet 42:517-540

Simpson PT, Gale T, Reis-Filho JS et al (2005) Columnar cell lesions of the breast: the missing link in breast cancer progression? A morphological and molecular analysis. Am J Surg Pathol 29:734-746

Simpson PT, Reis-Filho JS, Lambros MB et al (2008) Molecular profiling pleomorphic lobular carcinomas of the breast: evidence for a common molecular genetic pathway with classic lobular carcinomas. J Pathol 215:231-244

Sotiriou C, Wirapati P, Loi S et al (2006) Gene expression profiling in breast cancer: understanding the molecular basis of histologic grade to improve prognosis. J Natl Cancer Inst 98:262-272

Sourvinos G, Tsatsanis C, Spandidos DA (1999) Overexpression of the Tpl-2/Cot oncogene in human breast cancer. Oncogene 18:4968-4973

Souter LH, Andrews JD, Zhang G et al (2010) Human 21T breast epithelial cell lines mimic breast cancer progression in vivo and in vitro and show stage-specific gene expression patterns. Lab Invest 90:1247-1258

Stampfer MR, Yaswen P (2000) Culture models of human mammary epithelial cell transformation. J Mammary Gland Biol Neoplasia 5:365-378

Sticht C, Freier K, Knopfle K et al (2008) Activation of MAP kinase signaling through ERK5 but not ERK1 expression is associated with lymph node metastases in oral squamous cell carcinoma (OSCC). Neoplasia 10:462-470

Strutt H, Strutt D (2005) Long-range coordination of planar polarity in Drosophila. Bioessays 27:1218-1227

Sung KE, Yang N, Pehlke C et al (2011) Transition to invasion in breast cancer: a microfluidic in vitro model enables examination of spatial and temporal effects. Integr Biol (Camb) 3:439-450

Takemaru KI, Ohmitsu M, Li FQ (2008) An oncogenic hub: beta-catenin as a molecular target for cancer therapeutics. Handb Exp Pharmacol:261-284

Talmadge JE, Fidler IJ (2010) AACR centennial series: the biology of cancer metastasis: historical perspective. Cancer Res 70:5649-5669

Tanegashima K, Zhao H, Dawid IB (2008) WGEF activates Rho in the Wnt-PCP pathway and controls convergent extension in Xenopus gastrulation. EMBO J 27:606-617

Tavassoli FA, Norris HJ (1990) A comparison of the results of long-term follow-up for atypical intraductal hyperplasia and intraductal hyperplasia of the breast. Cancer 65:518-529

Tomar A, Schlaepfer DD (2009) Focal adhesion kinase: switching between GAPs and GEFs in the regulation of cell motility. Curr Opin Cell Biol 21:676-683

Topol L, Jiang X, Choi H et al (2003) Wnt-5a inhibits the canonical Wnt pathway by promoting GSK-3-independent beta-catenin degradation. J Cell Biol 162:899-908

Torres MA, Yang-Snyder JA, Purcell SM et al (1996) Activities of the Wnt-1 class of secreted signaling factors are antagonized by the Wnt-5A class and by a dominant negative cadherin in early Xenopus development. J Cell Biol 133:1123-1137

Tree DR, Ma D, Axelrod JD (2002) A three-tiered mechanism for regulation of planar cell polarity. Semin Cell Dev Biol 13:217-224

Ueno K, Hiura M, Suehiro Y et al (2008) Frizzled-7 as a potential therapeutic target in colorectal cancer. Neoplasia 10:697-705

Umbhauer M, Djiane A, Goisset C et al (2000) The C-terminal cytoplasmic Lys-thr-X-X-X-Trp motif in frizzled receptors mediates Wnt/beta-catenin signalling. EMBO J 19:4944-4954

van de Vijver MJ, He YD, van't Veer LJ et al (2002) A gene-expression signature as a predictor of survival in breast cancer. N Engl J Med 347:1999-2009

Veeman MT, Axelrod JD, Moon RT (2003) A second canon. Functions and mechanisms of beta-catenin-independent Wnt signaling. Dev Cell 5:367-377

Venkitaraman R (2010) Lobular neoplasia of the breast. Breast J 16:519-528

Vincan E, Swain RK, Brabletz T et al (2007) Frizzled7 dictates embryonic morphogenesis: implications for colorectal cancer progression. Front Biosci 12:4558-4567

Wagner EF, Nebreda AR (2009) Signal integration by JNK and p38 MAPK pathways in cancer development. Nat Rev Cancer 9:537-549

Walch A, Seidl S, Hermannstadter C et al (2008) Combined analysis of Rac1, IQGAP1, Tiam1 and E-cadherin expression in gastric cancer. Mod Pathol 21:544-552

Walzer T, Vivier E (2011) G-protein-coupled receptors in control of natural killer cell migration. Trends Immunol 32:486-492

Wang F, Weaver VM, Petersen OW et al (1998) Reciprocal interactions between beta1-integrin and epidermal growth factor receptor in three-dimensional basement membrane breast cultures: a different perspective in epithelial biology. Proc Natl Acad Sci U S A 95:14821-14826

Wang X, Chao L, Li X et al (2010) Elevated expression of phosphorylated c-Jun NH2-terminal kinase in basal-like and "triple-negative" breast cancers. Hum Pathol 41:401-406

Wang Y (2009) Wnt/Planar cell polarity signaling: a new paradigm for cancer therapy. Mol Cancer Ther 8:2103-2109

Wang Y, Steinbeisser H (2009) Molecular basis of morphogenesis during vertebrate gastrulation. Cell Mol Life Sci 66:2263-2273

Wang Y, Zang QS, Liu Z et al (2011) Regulation of VEGF-induced endothelial cell migration by mitochondrial reactive oxygen species. Am J Physiol Cell Physiol 301:C695-704

Weaver VM, Howlett AR, Langton-Webster B et al (1995) The development of a functionally relevant cell culture model of progressive human breast cancer. Semin Cancer Biol 6:175-184

Weaver VM, Petersen OW, Wang F et al (1997) Reversion of the malignant phenotype of human breast cells in three-dimensional culture and in vivo by integrin blocking antibodies. J Cell Biol 137:231-245

Weeraratna AT, Jiang Y, Hostetter G et al (2002) Wnt5a signaling directly affects cell motility and invasion of metastatic melanoma. Cancer Cell 1:279-288

Wei Q, Zhao Y, Yang ZQ et al (2008) Dishevelled family proteins are expressed in non-small cell lung cancer and function differentially on tumor progression. Lung Cancer 62:181-192

Weidner N, Semple JP (1992) Pleomorphic variant of invasive lobular carcinoma of the breast. Hum Pathol 23:1167-1171

Wellings SR, Jensen HM (1973) On the origin and progression of ductal carcinoma in the human breast. J Natl Cancer Inst 50:1111-1118

Wellings SR, Jensen HM, Marcum RG (1975) An atlas of subgross pathology of the human breast with special reference to possible precancerous lesions. J Natl Cancer Inst 55:231-273

Wong GT, Gavin BJ, McMahon AP (1994) Differential transformation of mammary epithelial cells by Wnt genes. Mol Cell Biol 14:6278-6286

Wright TM, Brannon AR, Gordan JD et al (2009) Ror2, a developmentally regulated kinase, promotes tumor growth potential in renal cell carcinoma. Oncogene 28:2513-2523

Wu G, Huang X, Hua Y et al (2011) Roles of planar cell polarity pathways in the development of neural [correction of neutral] tube defects. J Biomed Sci 18:66

Yagyu R, Hamamoto R, Furukawa Y et al (2002) Isolation and characterization of a novel human gene, VANGL1, as a therapeutic target for hepatocellular carcinoma. Int J Oncol 20:1173-1178

Yamamoto H, Kitadai Y, Oue N et al (2009) Laminin gamma2 mediates Wnt5a-induced invasion of gastric cancer cells. Gastroenterology 137:242-252, 252 e241-246

Yamamoto H, Oue N, Sato A et al (2010) Wnt5a signaling is involved in the aggressiveness of prostate cancer and expression of metalloproteinase. Oncogene 29:2036-2046

Yao J, Weremowicz S, Feng B et al (2006) Combined cDNA array comparative genomic hybridization and serial analysis of gene expression analysis of breast tumor progression. Cancer Res 66:4065-4078

Ying J, Li H, Chen YW et al (2007) WNT5A is epigenetically silenced in hematologic malignancies and inhibits leukemia cell growth as a tumor suppressor. Blood 110:4130-4132

Ying J, Li H, Yu J et al (2008) WNT5A exhibits tumor-suppressive activity through antagonizing the Wnt/beta-catenin signaling, and is frequently methylated in colorectal cancer. Clin Cancer Res 14:55-61

Zallen JA (2007) Planar polarity and tissue morphogenesis. Cell 129:1051-1063

Zen K, Yasui K, Nakajima T et al (2009) ERK5 is a target for gene amplification at 17p11 and promotes cell growth in hepatocellular carcinoma by regulating mitotic entry. Genes Chromosomes Cancer 48:109-120

Zhu Y, Tian Y, Du J et al (2012) Dvl2-dependent activation of Daam1 and RhoA regulates Wnt5a-induced breast cancer cell migration. PLoS One 7:e37823

Zijlstra A, Lewis J, Degryse B et al (2008) The inhibition of tumor cell intravasation and subsequent metastasis via regulation of in vivo tumor cell motility by the tetraspanin CD151. Cancer Cell 13:221-234

Curriculum Vitae

Name: **Connor MacMillan**

Post-secondary Education and Degrees:

University of Guelph
Guelph, Ontario, Canada
2006-2010 BSc (Hons) Biomedical Science with Distinction

University of Western Ontario
London, Ontario, Canada
2010-2013 MSc, Department of Pathology

Honours and Awards:

University of Guelph Entrance Scholarship, 2006-2007
Harold Livergant Scholarship, 2006-2010
Queen Elizabeth II Aiming for the Top Scholarship, 2006-2010
Deans' Scholarship, 2007-2008, 2008-2009, 2009-2010
Richard and Sophia Hungerford Travel Scholarship, 2008-2009
Undergraduate Student Research Award, 2008-2009
Hagen Undergraduate Scholarship, 2009-2010
Tony and Anne Arrell Scholarship, 2009-2010
Alexander Graham Bell Canada Graduate Scholarship, 2010-2011
Ontario Graduate Scholarship, 2010-2011, 2011-2012
Western Graduate Research Scholarship, 2010-2011, 2011-2012
Schulich Scholarship for Medical Research, 2010-2011
American Society for Cell Biology Travel Award, 2011-2012
Translational Breast Cancer Research Studentship, 2011-2012

Related Work Experience

Undergraduate Student Researcher
Department of Molecular and Cellular Biology, University of Guelph, Guelph, Ontario
2009-2010

Graduate Student Researcher
London Regional Cancer Program, London Health Sciences Centre, London, Ontario
2010-2012

Publications:

MacMillan CD, Chambers AF, Tuck AB (2012). Progression of early breast cancer to an invasive phenotype. In: A Ahmad (ed) Breast Cancer Metastasis and Drug Resistance: Progress and Prospects. Springer